STOCHASTIC MODELING AND PROGNOSTIC ANALYSIS OF COMPLEX SYSTEMS USING CONDITION-BASED REAL-TIME SENSOR SIGNALS

A Thesis
Presented to
The Academic Faculty

by

Linkan Bian

In Partial Fulfillment
of the Requirements for the Degree
Doctor of Philosophy in the
H. Milton Stewart School of Industrial and Systems Engineering

Georgia Institute of Technology
May 2013

STOCHASTIC MODELING AND PROGNOSTIC ANALYSIS OF COMPLEX SYSTEMS USING CONDITION-BASED REAL-TIME SENSOR SIGNALS

Approved by:

Professor Nagi Gebraeel, Advisor
H. Milton Stewart School of Industrial and
Systems Engineering
Georgia Institute of Technology

Professor Paul Kvam
H. Milton Stewart School of Industrial and
Systems Engineering
Georgia Institute of Technology

Professor Jianjun Shi
H. Milton Stewart School of Industrial and
Systems Engineering
Georgia Institute of Technology

Professor Chelsea C. White III
H. Milton Stewart School of Industrial and
Systems Engineering
Georgia Institute of Technology

Professor Elsayed Elsayed
Department of Industrial and Systems
Engineering
Rutgers University

Date Approved: 8 March 2013

To my parents, my wife, and my son on the way.

ACKNOWLEDGEMENTS

I would like to thank all the people who have taught me, helped me, and inspired me during my doctoral study.

Especially, I would like to express my deepest gratitude to my advisor, Professor Nagi Gebraeel. He has guided me through my five-year doctoral study with incredible patience, and provided me with tremendous support and encouragement. I am not only inspired by his passion and talents on academic research, but also influenced by his professional ethics and life attitudes, from which I will benefit for my lifetime.

I am extremely grateful to Professor Jianjun Shi. I have worked under his guidance for all the years of my doctoral study as a Ph.D. student of System Informatics and Control (SIAC). He has supported me with great mentorship on academics life. I have benefited so much from his broad knowledge and deep insights that I consider myself very fortunate.

I would like to thank Professor Elsayed Elsayed for his valuable mentorship and later his great support for my research and career. I want to acknowledge my sincere gratitude to Professor Chelsea White III, who not only has served on my dissertation committee, but also gave me so much help and guidance on my career. My thanks also go to Professor Paul Kvam for serving on my dissertation committee and providing so many insightful suggestions.

I also want to thank my colleagues in Systems Monitoring and Prognostics Lab at Georgia Institute of Technology: Dr. Alaa Elwany, Dr. Rensheng Zhou, Mr. Xiaolei Fang, Ms. Li Hao, and Mr. Murat Yildirim. It is such an honor to work with these talented people and gain their friendship.

Last but not least, I would like to thank my parents and my wife. I cannot ask more from my parents, who have given me unconditional and unlimited love and support despite of the ups and downs of my life. I also owe tremendously to my wife, Dr. Yun Xue, who supports and loves me with her full heart, in good times and in hard times.

TABLE OF CONTENTS

LIST OF TABLES

LIST OF FIGURES

SUMMARY

This dissertation presents a stochastic framework for modeling the degradation processes of components in complex engineering systems using sensor based signals. Chapters 1 and 2 discuses the challenges and the existing literature in monitoring and predicting the performance of complex engineering systems.

Chapter 3 presents the degradation model with the absorbing failure threshold for a single unit and the RLD estimation using the first-passage-time approach. Subsequently, we develop the estimate of the RLD using the first-passage-time approach for two cases: information prior distributions and non-informative prior distributions. A case study is presented using real-world data from rolling elements bearing applications.

Chapter 4 presents a stochastic methodology for modeling degradation signals from components functioning under dynamically-evolving environmental conditions. We utilize in-situ sensor signals related to the degradation process, as well as the environmental conditions, to predict and continuously update, in real-time, the distribution of a component's residual lifetime. Two distinct models are presented. The first considers future environmental profiles that evolve in a deterministic manner while the second assumes the environment evolves as a continuous-time Markov chain.

Chapters 5 and 6 generalize the failure-dependent models and develop a general model that examines the interactions among the degradation processes of interconnected components/subsystems. In particular, we model how the degradation level of one component affects the degradation rates of other components in the system. Hereafter, we refer to this type of component-to-component interaction caused by their stochastic dependence as degradation-rate-interaction (DRI). Chapter 5 focuses on the scenario in which these changes occur in a discrete manner, whereas, Chapter 6 focuses on the scenario, in which DRIs occur in a continuous manner. We demonstrate that incorporating the effects of component interactions significantly improves the prediction accuracy of RLDs.

Finally, we outline the conclusion remarks and a future work plan in Chapter 7.

CHAPTER I

INTRODUCTION

The use of real-time sensor data for continuously monitoring critical engineering components in complex systems (wind turbine systems, aircraft navigation systems, smart grids, nuclear reactor cooling systems, etc.) holds significant promise for not only assessing the current health of components, but for dynamically predicting the future remaining lifetime of components in complex engineering systems. Today, advances in sensor technologies, especially those related to sensor miniaturization and improved energy consumption, have enabled the health and performance monitoring of complex engineering systems, as well as the environmental conditions in which they operate. These condition-based sensor data include vibration data, acoustic data, oil analysis data, temperature, pressure, moisture, humidity, weather or environment data, etc.

Condition-based sensor data acquired from functioning units are usually correlated with the underlying physics-of-failure and known as degradation signals (cf. [47]). In this context, a component or system is considered to have failed once its degradation signal crosses a predetermined failure threshold (assuming a single mode of failure). These degradation-based signals serve as a proxy for physical degradation and can be used to predict the residual lifetime distributions of the engineering systems and their constituent components. Predicting such distributions entails accurately understanding the future evolution of degradation signals from the constituent components of a complex system. This is generally very challenging because the environmental/operational conditions and the interactions among the constituent components cause enormous uncertainty in the patterns of degradation signals.

In this dissertation, we focus on developing a stochastic degradation framework that utilizes real-time sensory information to improve the prediction accuracy of residual life distributions (RLDs) for components in complex engineering systems. Accurately predicting the RLDs of an engineering system is generally a difficult problem because of the following challenges :

1. The RLD of a unit depends not only on reliability data that reflect population characteristics but also the real-time condition of an operating unit. This requires the integration of traditional reliability analysis and condition-based degradation signals.

2. In industrial applications, engineering systems are often subject to variable operating/environmental conditions, the effect of which, if not properly considered, may greatly reduce the accuracy

of RLD estimations.

3. The reliability of a complex system depends on the RLDs of its constituent components and the interactions among them. The research area of component interactions has not been well explored.

1.1   Research Challenges

1.1.1   Challenges With Traditional Reliability Models and Conventional Condition Monitoring Techniques

Most conventional reliability formalisms treat failures as a random process rather than a process of evolution across a continuum of degradation states. Reliability models focus on evaluating failure measures for a population of components, primarily, by collecting and analyzing failure data (cf. [12], [37], [32], [39], [60], [71], [84], and [139]). The uncertainty associated with degradation and failure processes-even for identical components functioning under similar operating conditions-is usually characterized by parametric and empirical failure distributions. These distributions are used to evaluate component reliability. This is achieved using time- and state-dependent reliability techniques, covariate models, static/dynamic models, and physics-of-failure models. System reliability is evaluated using reliability measures of its constituents (components). A system is defined as a given configuration of components whose proper functioning over a stated interval of time determines whether the system will perform as designed. However, these approaches provide little ongoing reliability information of a particular unit/system that is currently functioning in the field. Besides, failure behavior of each unit depends on the changes in work the operational age or time that the unit has survived, operating environment, and failure interaction between components.

On the other end of the spectrum, conventional condition monitoring (CM) techniques focus on collecting sensory information from a functioning device in order to determine its state of health (cf. [113], [122], [129], [131], and [143]). Condition monitoring is very useful when direct observations of physical degradation processes, such as fatigue, wear, corrosion, etc, are not possible. Condition-based sensory signals, such as vibration, temperature, acoustic emissions, etc, often exhibit characteristics patterns that are correlated with the underlying physical transitions that occur during degradation. Some applications include condition monitoring of bearings, machine, engines,
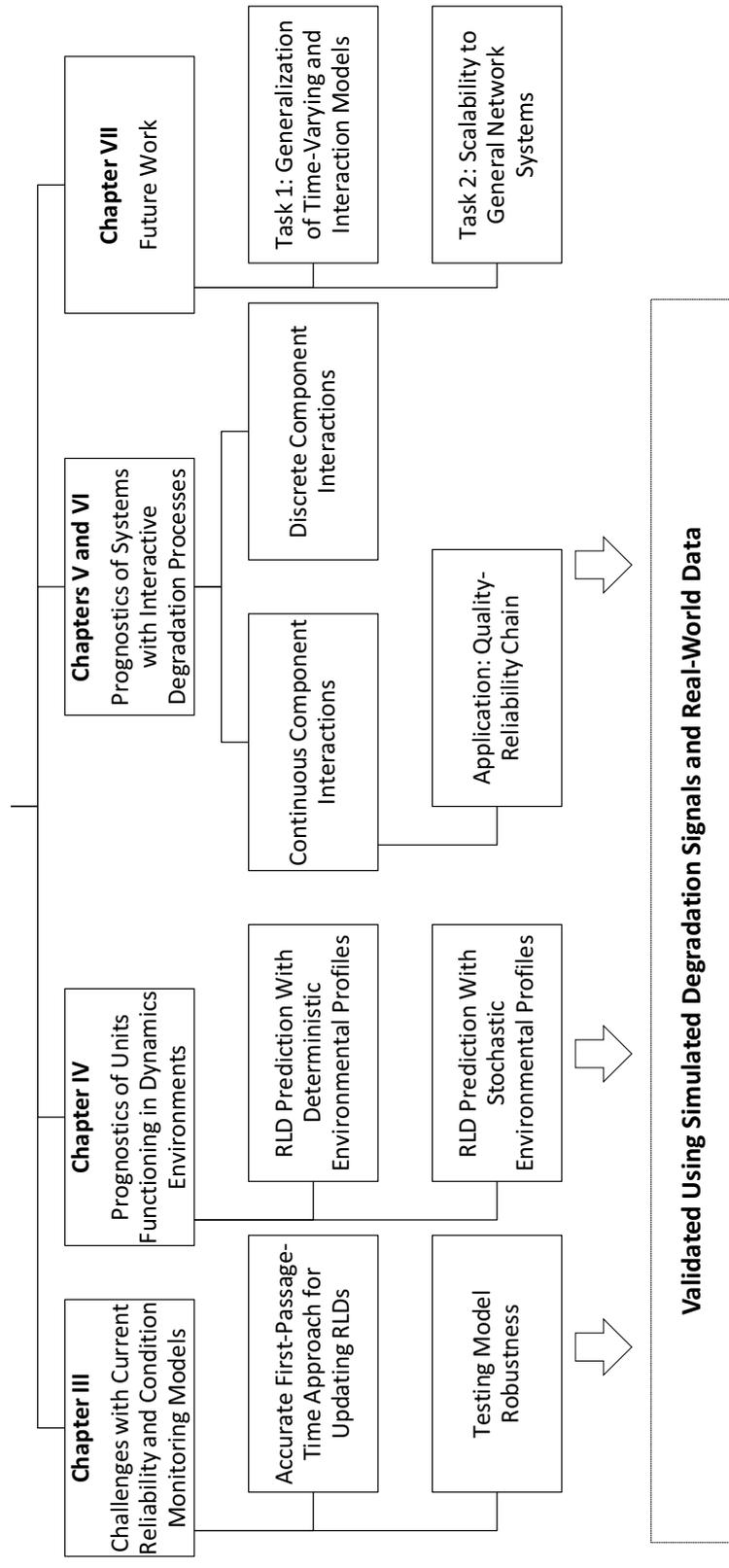
Figure 1.0.1: Organization of this dissertation.

cardiac pacemakers, blood glucose, and body temperature among others. Unfortunately, CM techniques focus on the degradation characteristics of individual components with little or no emphasis on the characteristics of the component's population. This leaves out a critical source of information when trying to predict failures using CM techniques.

As noted by [89], failure prediction that incorporates condition-based data and lifetime data tend to provide more accurate reliability estimation. The limited literature that combines the reliability formalisms with condition monitoring methods includes [47], [46], [48], and other relevant prognostic papers. However, in these papers, the residual life distribution is estimated using an approximation of the actual distribution.

1.1.2 Challenges With the Effects of Operational/Environmental Conditions

The use of real-time sensor data for continuously monitoring critical engineering components in complex systems holds significant promise for predicting the future remaining life of components dynamically. One aspect of dynamic reliability assessment that is often overlooked is the impact of the component's physical or operating environment on its useful lifetime. For example, increasing the load and speed of rotating machinery may accelerate the degradation of its constituent components, such as roller bearings. Similarly, large variations in the ambient operating temperature may adversely effect electronic components. The uncertainties associated with component degradation processes coupled with the effects of time-varying environmental and operation conditions pose significant challenges to the accurate assessment of the useful lifetime distribution of critical components. Therefore, the development of stochastic models that can incorporate the effect of environmental or operating conditions has become an important issue to reliability modelers and engineers alike.

As noted by [24], the vast majority of conventional failure models assume that prevailing environmental conditions are temporally invariant, or have no effect on deterioration and failure processes. However, generally speaking, harsh environments tend to accelerate the degradation mechanisms that occur prior to failure as compared to milder environments. The limited number of failure models that do consider environmental effects generally belong to one of two groups: (1) hazard rate models that treat environmental conditions as model covariates (cf. [57] and [75]), and (2)

5

stochastic wear and/or shock models in which the wear and/or shock intensities are modulated by the environment (cf. [37] and [62]). Even these models have key limitations that impact their applicability. First, the failure rate functions of the first group are only useful for making inferences about a large population of components but not about specific components. Moreover, failure rates cannot be observed or measured for individual components (cf. [118]). The second group of models are useful for deriving analytical lifetime distributions (or their transforms) and assessing, probabilistically, the time-to-failure. The limitation of these models is that they treat failure as a random event and do not provide information about the evolution of the physical degradation process that occurs prior to failure (cf. [125]).

1.1.3 Challenges With the Effects of Component Interactions

Predicting the lifetime of a complex system requires an accurate evaluation of the degradation states of its constituent components, and a sufficient understanding of how these states evolve in the future. These challenges become more complicated when the components of a system are interdependent. There are different forms of dependencies as noted in [35]: economic dependence, structural dependence, and stochastic dependence. (a) Economic dependence implies that either costs can be saved when several components are jointly maintained instead of separately. (b) Structural dependence applies if components structurally form a part, so that maintenance of a failed component implies maintenance of other components as well. (c) Stochastic dependence occurs if the state of a component influences the lifetime distribution of other components. This paper focuses on stochastic dependence, which refers to situations where the failure or degradation of one component influences the lifetime of other components in the system. In particular, we assume when a component degrades (say due to wear, or plastic deformation), it affects the performance of other components in the system by accelerating their degradation processes. Wind turbines are an example of a typical mechanical system where, for example, the degradation of hydrodynamic bearings may result in increasing the looseness of primary transmission shafts, which in turn may increase the vibration levels in the gearbox. Such a scenario will definitely alter and most probably accelerate the degradation of the constituent gears. In networked systems such as power grids, the aging of generators or transformers in a subnetwork may result in increased demands on other

6

units in the network. This results in increasing their loading profiles, and in turn accelerates their degradation processes. Similar arguments can be made for various applications domains such as mechanical systems (cf. [39, 88]), smart grids (cf. [59, 130]), water distribution systems (cf. [115]), and other multi-component systems.

To date, many reliability models that consider component lifetime distributions in multi-component systems assume that component lifetimes are independent (cf. [22, 40]). Although such an assumption may help in obtaining mathematically tractable models, these models remain unrealistic and inappropriate for applications where stochastic dependence is indeed present (cf. [14, 119]). The limited literature that considers stochastic dependence can be divided into two groups. The first group focuses on how the failure of one component affects the failure rates of other components in a given system (cf. [68, 92, 95]). In the second group, stochastic dependence among component lifetimes is characterized by correlated multivariate lifetime distributions, the parameters of which change as the failures of components occur (cf. [44, 79, 87]). Both of these two approaches focus on modeling the distribution of component lifetime or time-to-failure. It would be difficult to utilize these methods to characterize the degradation processes of components and the interactions between before component failure occurs.

1.2 Proposed Research

This dissertation proposes a stochastic degradation framework that utilizes the real-time observations of sensory signals and the degradation characteristics associated with the entire population of similar components to estimate the RLDs. We will investigate how to accurately estimate the RLD of a single component using a first-passage-time approach, how to model various effects of environmental conditions on the degradation signals, and how to characterize the interactions among the degradation signals of constituent components in a multi-component system.

1.2.1 Estimating the RLD of a Component Using a First-Passage-Time Approach

Very few research efforts such as [46], [47], and [133] have utilized real-time degradation signals to update the residual life distributions (RLDs) of a single component. In this context, the RLDs represented the time distribution until the observed degradation signal crossed a predetermined failure threshold. Our proposed model in Chapter 3 is an extension of [46] and [47], in which the

authors used an approximation method to predict the RLD and pointed out that the prediction accuracy would be improved if the first-passage-time of degradation process was utilized to estimate the failure time.

Our methodology begins with the development of a degradation model, in which the degradation signal is characterized by a stochastic process, and the failure threshold is the absorbing barrier of this stochastic process. Since degradation signals are monitored at discrete epochs in most applications, our model accounts for the engineering fact that the failure time is greater than the latest observation epoch of degradation. That is, we exclude the degradation signals that cross the failure threshold between discrete observation epochs from our space of degradation signals. Furthermore, our degradation model consists of deterministic coefficients that capture degradation attributes common to all units of a population and stochastic coefficients that capture the unit-to-unit variability, such as the rate of degradation. The estimates of these coefficients can be obtained using a sample of historical degradation signals or from expert knowledge. Next, we focus on a unit/component that has been operating in the field, whose degradation signal is used to update the prior distributions of the stochastic coefficients in a Bayesian manner. The updated model is then used to revise the component's residual life distribution (RLD) with a first-passage time approach. We will demonstrate through a real-world case study that this approach provides accurate prediction of the residual life and is relatively robust with respect to different levels of signal-to-noise ratios when compared to existing models.

1.2.2 Characterizing the Effects of Environmental Conditions on The Degradation Signal of a Single Component

We develop a stochastic methodology for modeling degradation signals from components functioning under dynamically-evolving environmental conditions. We utilize in-situ sensor signals related to the degradation process, as well as the environmental conditions, to predict and continuously update, in real-time, the distribution of a component's residual lifetime. Our models assume that the real-time rate at which a system's degradation signal increases (or decreases) is affected by the severity of the current environmental or operational conditions. In addition, we account for the reality that transitions in the environmental and operational conditions may induce upward or downward jumps in the amplitude of the degradation signal, depending on the nature of the changes.

To estimate residual life distributions (RLDs), we consider two cases, both of which take into consideration the future characteristics of the environmental conditions. In the first case, we assume the component operates in a dynamic environment that transitions between distinct states and follows a deterministic profile, (i.e., there is no uncertainty about how the environment transitions in the future). This case is appropriate when the component experiences conditions that might occur in a cyclic manner. As an example of such a scenario, consider the rotational speed and thrust profiles that a jet engine experiences during the take-off, cruising, and landing cycles. The second case also assumes dynamic environmental or operating conditions but allows for the future environmental profile to be uncertain. Specifically, the transition times and dwell times in each distinct environmental state are stochastic and characterized using a continuous-time Markov chain model. This case may be appropriate for systems that are exposed to uncertain environments, such as weather conditions. For example, the velocity of wind as it relates to the productivity of wind turbines, or temperature and humidity changes as they relate to electronic components in aircraft avionics systems. For both cases, we propose a stochastic model for characterizing the degradation signal of the component and use this model to predict the residual lifetime by estimating the distribution of the first-passage time of the signal to a critical degradation threshold.

1.2.3 Characterizing the Component Interactions Among the Degradation Signals from Multi-Component Systems

While the existing models address the challenges associated with component dependencies by studying the effects that a component's failure has on the remaining functioning components, our approach addresses this problem at a much more fundamental level. Instead of focusing on the effects of failure, we focus on modeling the effects of ongoing degradation processes that take place prior to failure. In particular, we are interested in studying how the degradation level of one component affects the degradation rate of other components in the system. We assume that sensor data obtained from a functioning component can be synthesized into degradation-base signals, which are directly correlated with the severity of the components' physical degradation state. Consequently, interactions among components will be manifested in the behavior of their respective degradation signals. In other words, degradation interaction may cause a noticeable change in the rate by which

the amplitude of a component's degradation signal (hereafter referred to as degradation rate) increases or decreases over time.

We propose a stochastic degradation framework that models the inherent degradation processes of components as well as the effects of degradation interactions among interdependent components. Two types of component interactions are considered: (1) We will first consider degradation interactions that occur on a continuous basis, referred to as continuous interaction. In other words, the degradation rate of each component is continuously being influenced by the amplitudes of the degradation signals of other components. Thus, changes in the degradation rates are much more subtle and occur continuously over time. (2) The second type of interactions, which occur at discrete levels of degradation, are referred to as discrete interactions. In other words, changes in the degradation rate of a component occur when other components reach pre-specified levels of degradation, i.e., when their degradation signals reach specific amplitudes or amplitude ranges. This proposed stochastic framework will be used to estimate the residual life distributions (RLDs) of constituent components in a given system. The RLDs will be updated based on real-time senor signals in a Bayesian manner. This updating scheme allows us to incorporate information about the latest degradation states of the components that are being monitored.

1.3 Dissertation Organization

The organization of this dissertation is illustrated in Figure 1.0.1. Chapter 2 surveys the relevant literature on reliability estimating, degradation modeling, lifetime estimation under time-varying operational conditions, system reliability with and without component dependence.

Chapter 3 presents the degradation model with the absorbing failure threshold for a single unit and the RLD estimation using the first-passage-time approach. We start by presenting a base-case model, where the evolution of the degradation signal is model using a random coefficient linear model with residual terms follow a Brownian motion process. Subsequently, we develop the estimate of the RLD using the first-passage-time approach for two cases: information prior distributions and non-informative prior distributions. A case study is presented using real-world data from rolling elements bearing applications. A paper based on this work can be found in [19].

Chapter 4 presents a stochastic methodology for modeling degradation signals from components functioning under dynamically-evolving environmental conditions. We utilize in-situ sensor signals related to the degradation process, as well as the environmental conditions, to predict and continuously update, in real-time, the distribution of a component's residual lifetime. Two distinct models are presented. The first considers future environmental profiles that evolve in a deterministic manner while the second assumes the environment evolves as a continuous-time Markov chain. For the first model, we compare our method with two benchmark models and demonstrate that our approach significantly improves the prediction accuracy of RLDs by incorporating the signals jumps in the future. For the second model, we conduct comprehensive simulation studies to evaluate the performance of our method for various values of model parameters. Papers based on this work can be found in [17, 18, 20].

Chapters 5 and 6 generalize the failure-dependent models and develop a general model that examines the interactions among the degradation processes of interconnected components/subsystems. In particular, we model how the degradation level of one component affects the degradation rates of other components in the system. Hereafter, we refer to this type of component-to-component interaction caused by their stochastic dependence as degradation-rate-interaction (DRI).

Chapter 5 focuses on the scenario in which these changes occur in a discrete manner. In particular, changes in the degradation rate of a component occur when other stochastically dependent components reach pre-specified degradation levels, i.e., when their degradation signals reach specific amplitudes or amplitude ranges. From a practical perspective, discrete-type DRIs can take place in applications where, for example, different levels of wear or plastic deformation result in categorically different effects on the degradation processes of other components. Our approach rests on the idea that degradation signals from interdependent components can be divided into amplitude ranges that correspond to discrete degradation states. When a component transitions from one state to a more severe state, it triggers a DRI, which results in increasing the degradation rates of other dependent components. Consequently, the times at which DRIs take place correspond to change-points in the degradation rates of the components of the system. Using this approach, we develop a stochastic degradation modeling framework where the evolution of degradation signals is modeled as a continuous-time stochastic process, and in which degradation interactions are modeled

as change-points in the growth rate of the signals. A change-point detection algorithm is utilized to identify the times that correspond to degradation interactions. Historical degradation signals are used to estimate the model parameters and their prior distributions. However, the main benefit of this approach lies in the ability to utilize *in-situ* degradation signals from the components of fielded systems to update the model parameters in a Bayesian manner, and predict their residual life distributions. A paper based on this work can be found in [16].

Chapter 6 focuses on the scenario, in which DRIs occur in a continuous manner. Specifically, changes in the degradation rate of a component is continuously affected by the amplitudes of degradation signals of other components. To model such dynamics among the degradation signals of components in a given system, we utilize the approach of SDE systems, the coefficient matrix of which characterizes the inter-dependency among system components. One major advantage of using an SDE approach is that we can exploit the mathematical tools of Ito's formulae and express the component RLDs in closed-form expressions. Once the degradation model is established, we utilize the real-time degradation signals from the components of a system functioning in the field to update the model parameters and the component/system residual life distributions in a Bayesian manner. To validate our methodology, we conduct a series of simulation studies for testing the prediction accuracy with various of model parameters. The results are compared with a benchmark model, which does not consider component interactions. We demonstrate that incorporating the effects of component interactions significantly improves the prediction accuracy of RLDs. A paper based on this work can be found in [15].

Finally, we outline the conclusion remarks and a future work plan in Chapter 7.

CHAPTER II

LITERATURE REVIEW

In this chapter, we survey the literature that is related to our research areas. That is, reliability estimation, degradation modeling, lifetime estimation under time-varying environments, and reliability models for multi-component systems.

2.1 Reliability Estimation and Degradation Modeling

Most existing degradation models focus on estimating the lifetime distribution of a population of similar units. [84] proposed a regression model with random effects to characterize the degradation trend of a population of components. The authors developed a two-stage approach for the parameter estimation. Monte Carlo simulation was used to obtain point estimates and confidence intervals for reliability assessment. Along this line, [104] modeled degradation using nonlinear regression models with random coefficients. Different from [84], the authors utilized a full Bayesian approach for the statistic inference and verified their method using fatigue crack growth data. These models are based on the assumption of independent and identically distributed (iid) Gaussian noise. That is, these regression models with random effects assume that the underlying degradation process is determined by a monotonic function with iid error.

To model the degradation process, which is not necessarily monotonic and exhibits temporal variability, researchers developed degradation models with stochastic processes, such as the Wiener process, the Gamma process and discrete Markov processes. A major advantage of modeling degradation processes with Wiener processes is that by [31] the distribution of the failure time has a closed-form expression, known as the inverse Gaussian distribution. Based on this property, [37] used the Wiener process with a time-varying drift to model the degradation signals from accelerated life tests under variable stress. The authors developed a timescale transformation to convert the non-stationary Wiener process to a stationary Wiener process, and proved that the resulting failure times followed an inverse Gaussian distribution. This transformation was applied by [137], in which the authors modeled the degradation of self-regulating heat cables subject to high-stress reliability testing. Other applications of Wiener processes can be found in [1], [75], [80], [96], and [102]. In addition, variations of the Wiener process, such as the integrated Wiener process and the geometric Brownian motion, have also been utilized in degradation models based on the characteristics of data. For example, [124] used an integrated Wiener process to model the degradation process in burn-in

tests for highly reliable products. The authors compared the proposed method with conventional procedures and showed that their method is more sensitive and efficient in detecting defects. [99] and [100] investigated the use of geometric Brownian motion in modeling degradation and developed the expression of failure time distribution. In their later work, [100] introduced environmental variables to capture different operating conditions.

Besides Wiener processes, Gamma processes and discrete Markov processes have appeared in many applications of degradation models. The major advantage of modeling a degradation process with a Gamma process is that the computation of the crossing time to a pre-specified threshold is straightforward because of the monotonic property of Gamma processes. [118] summarized failure models in dynamic environments and investigated the use Gamma processes in such environments. [70] incorporated the Gamma process with random effects to model unit-to-unit differences in the degradation signals among a population of similar components. The authors developed estimates of model parameters and failure time distribution with the aid of numerical methods. The proposed method is verified with the crack-growth data. [38] investigated a repairable system which was assumed to be maintained and repaired upon each failure. The authors modeled the degradation processes of individual components with independent Gamma processes. Based on this model, the author computed the mean function, which represents the expected number of failures up to a certain time, and discussed the corresponding maintenance policy. Other applications of Gamma processes can be found in [99], [100], [101], and [123]. Additionally, discrete Markov processes also show promising applications in modeling degradation processes. [62] considered the reliability of a single-unit system whose cumulative damage over time was a degradation process, which depended on an external environment process. The external process was characterized as a discrete Markov process with continuous time. [63] extended [62] by incorporating both environment observations and degradation measures in their stochastic failure model to numerically compute the failure time distributions. These two papers assume discrete Markov processes in which the system state sojourn time follows an exponential distribution. [66] generalized [62] and [63] by loosing the assumption of Markov processes to Semi-Markov processes.

In addition to the reliability literature above, a large amount of papers on joint modeling of longitudinal and survival data in biostatistics have applied similar approaches. For example, [34],

[41], and [138] examined linear regression models with random effects for studying AIDS data. These models consider repeated measurements of a time-dependent covariate, which is related to the disease risk. Furthermore, [74] and [136] considered a linear model with a stationary Wiener process. The trend of the linear model varies over time in order to capture evolving biological fluctuations. Additionally, [74] modeled AIDS data using a bivariate Wiener process. To study the treatment effects, the authors presented a generalized linear regression model, which included baseline conditions and covariates. They derived an explicit formula of the residual life for prediction purposes. Recently, [76] incorporated the Markov property into a regression model and presented a new model for the survival analysis called Markov Threshold Regression, in which the degradation processes followed a stochastic process and failure occurred when the process first reached a failure state.

Very few papers such as [46], [47], and [133] have utilized real-time degradation signals to update the residual life distributions (RLDs) of a single component. In this context, the RLDs represented the time distribution until the observed degradation signal crossed a predetermined failure threshold. Our proposed model in Chapter 3 is an extension of [46] and [47], in which the authors used an approximation method to predict the RLD and pointed out that the prediction accuracy would be improved if the first-passage-time of degradation process was utilized to estimate the failure time. Another paper along this line is [133], which utilized Wiener processes with random effects to compute the residual life distribution. The most significant difference between our work and [133] is that we consider the failure threshold as an absorbing barrier of the degradation process whereas in [133] the failure threshold was considered as a crossing boundary. Our model implies an important inherent constraint that the failure time is always greater than the latest observation epoch. Since all the degradation observations occur at discrete time epochs in both papers, our model ensures that the degradation process will not cross the failure threshold between two discrete observation epochs. By contrast, the model in [133] included degradation processes which crossed the failure threshold between the observation times of degradation signals. Finally, we restrict our choices of the prior distribution for the degradation rate among those which take only positive values (such as Gamma, Weibull, lognormal, etc.) because the rate of degradation is never negative in

reality. In [133], the author assumes a normal distribution for the drift rate. As a result, the degradation processes of [133] may drift away from the failure threshold, which is unrealistic for modeling the degradation process that causes the failure of a component.

2.2 *Lifetime Estimation Under Time-Varying Environmental/Operational Conditions*

Residual life estimation for components operating under time-invariant environmental conditions has been studied extensively in the literature. [84] and [104] considered regression models with random effects to characterize the degradation trend of a population of components. These regression models assume that the underlying degradation processes are determined by a trend function with independent and identically distributed Gaussian noise. To model degradation processes that exhibit temporal variability, researchers have characterized the evolution of degradation using stochastic processes, e.g., the Wiener process, the gamma process, etc. A major advantage of modeling degradation processes using a Wiener process is that the failure time distribution exists in closed-form as the inverse Gaussian distribution (cf. [31]). [47] and [133] utilized the Wiener process to model real-time degradation signals and computed the residual life distribution (RLD) of a single component. Besides, the gamma process has been utilized to model degradation processes that are almost surely monotone. [125] provided a comprehensive review of the use of the gamma process in maintenance modeling. However, none of the models described here considered the effects of the component's operating environment.

The literature pertaining to modeling the degradation of components operating under time-varying environments can be divided into two groups. The first group of papers are based on the proportional hazard model (PHM) that was first introduced by [30]. Due to its generality and flexibility, the PHM has been widely utilized to relate the hazard function to environmental conditions (cf. [57, 7, 80]). By contrast, the second group of papers focuses on modeling the degradation process or its manifestations. These processes are usually characterized using Brownian motion, general Markov processes, or random coefficients models to characterize degradation measures or signals (cf. [37], [48], and [62]). [116] has provided a comprehensive review of recent papers that estimate the RLD of components operating in time-varying environments.

In the first group of models that use PHMs to incorporate the effects of environmental conditions, some researchers considered the environmental condition to be deterministic and modeled its effects as a time-varying covariate with a pre-specified functional form. For example, [93] focused on a reliability model operating in a deterministic environment in which the hazard rate was a quadratic time-dependent function of the environment. Along these lines, [45] investigated dynamic operational conditions in which the hazard function is piecewise exponential. More generally, [103] analyzed a repairable systems's failure behavior using additive hazard models. Other extensions and applications of PHMs in deterministic environments can be found in [75], [126], [119], [82], and [145]. These models assume that the evolution of the covariate (environmental) condition is known – an assumption that can be rather restrictive. To account for scenarios in which the future environment is assumed to evolve stochastically, some PHMs assume the environmental covariate is driven by a Markov process. For example, [7] presented a PHM with a Markovian covariate and applied an approximation method to estimate the failure time distribution and represented the resulting expression in a complex integral form. Computational issues associated with this problem were further investigated by [6] who proposed a general numerical method to approximate the failure time distribution. Similar approximation techniques were applied in [49], in which the authors used a hidden Markov model to characterize the unobservable degradation status. Recently, [147] discussed condition-based inspection policies for systems subject to random shocks. The amplitude of these shocks are driven by a Markov process that characterizes the environmental conditions.

The second group of literature focuses on modeling the degradation process or its manifestations, i.e., degradation signals ([47]). These processes are usually characterized using stochastic processes such as the Wiener process, the gamma processes or general Lévy processes to model degradation measures and signals. A major advantage of this approach is that the covariates can be directly related to the environmental/operational conditions. For example, [37] applied Brownian motion with a stress-dependent drift to accelerated life test experiments and developed the failure time distribution. The authors proposed a time-scale transformation that converts non-stationary Brownian motion to a stationary Wiener process to obtain a closed-form expression for the RLD. The same transformation was applied in [137]. [48] extended the model in [37] to include the effects of shocks on the signal amplitude at environment transition epochs. These types of models

consider scenarios in which the environmental profile is deterministic and have been widely used in accelerated life testing (see [81] and [123]) and biomedical engineering (see [118], [75], and [73]).

Researchers have also developed failure models for components operating in random environments. Two types of environmental effects on the degradation process have been considered: (1) random shocks that increase or decrease the degradation instantaneously, and (2) changes in the degradation rate. The first model to consider a system subject to random shocks was proposed by [40] who assumed shocks arrive according to a Poisson process. This model was later extended by [2] and [42] to optimal inspection and maintenance problems. Similarly, [78] examined the lifetime distribution of a system under dynamic stress. The system stress was also modeled as a Poisson process whose time-varying rate parameter is driven by a shot-noise process. More generally, [56] investigated the failure of a system under environmental conditions that evolves as a Markov renewal shock process. A common theme among these works is that the environment is primarily modeled as a shock process, but the impact of the environment on the degradation rate is not considered. Other researchers have investigated the effects of environmental conditions on the degradation rate using general Markov processes, whose properties and applications were discussed in [28]. [29] presented a model in which the environment is modeled as a Markov process and the degradation evolves according to an increasing Lévy process. The resulting degradation process was expressed as an additive functional of the environment. [62] examined a similar problem wherein the system degrades linearly at a rate that depends on the state of the random environment. He derived double Laplace transform expressions for the distribution of the first passage time to a fixed threshold. [64] extended the model in [62] to include homogeneous Poisson shocks, each of which induces a random amount of damage to the component. In [65], a model with Markov-modulated degradation rates and Poisson shock intensities was studied. Both transient and asymptotic reliability indices were obtained therein. However, these papers did not account for the possibility of shocks that may occur at environment transition epochs.

The models presented in Chapter 4 belong to the second group of models that focus on characterizing the degradation process, or an associated signal of degradation, in dynamic environments. Our work is unique and distinguished from existing models in at least two aspects. First, unlike degradation models that focus on estimating the lifetime of a population of components (cf. [37]), our

primary aim is to estimate the RLD of an individual, fielded component by incorporating its unique degradation signal. As a result, the estimated RLD exploits not only prior information, but also the future environmental profile. Second, unlike typical random shock models (cf. [64]), our approach accounts for the reality that environment transitions may induce upward or downward jumps in the amplitude of the degradation signal, depending on the nature of the changes. In other words, our method accounts for the scenario when shocks in degradation signals occur at environment transition epochs, instead of randomly. As a result, shock models presented in [64, 65] can be considered as special cases of our proposed degradation model with randomly evolving environmental profiles.

2.3 Reliability Estimation for Systems

The lifetime distributions of systems with independent components have been studied extensively. We classify these approaches into two categories: qualitative methods and quantitative methods. The qualitative methods include Fault Tree Analysis (FTA), Failure Mode and Effects Criticality Analysis (FMEA and FMECA), and other techniques. These methods have straightforward engineering interpretations, a review of which can be found in [23] and [77]. On the other hand, quantitative models assume that the state of the system can be represented as a function of the state of its components (cf. [22, 10, 54, 53, 142]). Within this category of models, some researchers have utilized dynamic Markov models and semi-Markov models to characterize the evolution of system states (cf. [3, 52, 90, 142, 27]). With the aid of the mathematical tools of Markov processes, the transitions of the states of the system can be estimated in closed-form expressions. A comprehensive review of many modeling techniques of multi-state reliability can be found in [83]. A major advantage of models with independent components is that they result in mathematically tractable expressions of system reliability. This feature has been utilized by many researchers to evaluate the reliability of large and complex system via various methods, some of which are summarized in [55]. These methods include minimal cut sets approximation ([58]), probability network ([67]), Monte Carlo simulation ([9]), and other approaches. However, it has been pointed out that the independence assumption among components may not be realistic in many industrial applications and may lead to errors in estimating the lifetimes of components/systems (cf. [120, 88]).

With regard to the dependence among components, we limit our discussion to the statistical dependence of component lifetimes instead of the economical dependence in maintenance activities, as described in [121]. [68] partitioned the models that account for component interactions into two groups: (1) shock models and (2) load-share models. Shock models focus on investigating the joint multivariate distributions of component lifetimes as failures occur. The Marshall-Olkin multivariate exponential distribution, presented by [86], is a typical example of this approach. However, [52] argued that this approach is not realistic when the system failures are affected by their use and the amount of load they experience. To model the component interaction in this scenario, researchers developed load-share models, in which the failure of one component changes the failure rates of surviving components. The majority of current research in system reliability with component interactions focus on investigating and generalizing load-share models. The pioneering paper by [44] characterizes the lifetime of a two-component system using a bivariate exponential distribution, which was extended by [107], [112], [119] and others.

Different from the classification by [68], [91] provided another classification for multi-component models with component dependence from the perspective of maintenance activities, which identifies three types of failure interactions for a two-component system: Type I interaction assumes that the failure of one component induces failure of other components, i.e., there are two types of failure modes, natural and induced (cf. [109, 114]); Type II interaction considers two components, where the failure of the first component can possibly induce failure of the second component, however, failure of the second only induces shocks (typically modeled as a non-homogeneous Poisson process) in the first (cf. [11, 146]); Type III interaction assumes that the failure of one component affects the failure rate of the others. Other research efforts in this class of literature include [4], [110], [36], and [119]. One major limitation of this class of approaches is that they are restricted to the scenario, in which only the failure event triggers component interactions. This assumption might not be realistic for characterizing the interactions among the degradation processes of system component and estimating their residual life distributions.

Unlike the previous models, many research efforts are dedicated to examining inter-dependent multivariate degradation data that are observed before failure occurs. [132] provided a probability framework for modeling the reliability of a system with inter-dependent components by assuming a

multivariate normal distribution of component degradation processes. The interdependency among components are captured by the covariance matrix of multivariate degradation measures. This model was extended in [79], which considered the effects of common environments on dependency among components. Different from this research line, which modeled component dependency using the covariance of degradation measure, our approach focuses on the amplitude of one component affects the degradation rates of other components. Other methods that investigated the modeling of inter-dependent degradation processes can be classified into two subgroups: **Multi-Dimensional Time Series Models** provide an intuitive tool to fit multivariate degradation data (cf. [85], [141]). The dependency among components are captured by a transition matrix. However, this approach relies on using Kalman filters to predict the future transitions of component degradation processes. Kalman Filters are known to perform poorly with high dimensional data, as noted by [50]. **Techniques that utilize Copulas** have also been applied to model multiple competing risks in reliability. The advantage of the copula method is that, the degradation process of each component can be modeled independently using various stochastic processes, such as the Wiener process (cf. [134]), the Gamma process (cf. [148], [98]), and the shock process (cf. [134]). The interdependency among individual degradation processes is subsequently modeled by a given copula function. [108] provided an insightful summary for using various types of copulas. Although the method of copula has the flexibility of synthesizing individual degradation processes, the correlation between individual processes are completely defined by the given copula function, instead of the actual physical conditions of individual components.

The model presented in Chapter 5 generalizes the failure-dependent models, which only investigate the dependence on the failure events in multi-component systems. Specifically, we examine the interactions among the degradation processes of inter-connected components. Our work is unique and distinguished from existing models in that no previous papers have investigated the RLDs of the system and its components with interactive degradation processes to the best of our knowledge. Moreover, we will prove that our proposed degradation framework include the three types of failure interactions, proposed by [91], as special cases. In addition, unlike conventional reliability models that focus on estimating lifetime distributions of a population of similar systems, our primary aim is to estimate the RLD of a fielded system by incorporating its unique degradation signals. That is,

by observing the evolution of degradation signals, the RLDs of the system and its components can be updated in real time; therefore, the estimated RLDs exploit not only prior information, but also the real-time interactions among inter-connected components.

Chapter 6 models the degradation signals of system components using a system of stochastic differential equations (SDEs), the coefficient matrix of which captures the interactions among the component degradation signals. By solving this SDE system, we can estimate the future evolution of degradation signals as well as their interactions, and eventually estimate the component residual life distributions. Although the SDE model is widely used in various applications including economics, finance, and actuarial science, its application to model independent degradation processes in reliability are few. [140] proposed an SDE model to capture the correlation between degradation characteristics with random stresses. The authors developed the estimation of component lifetime distributions by assuming a full rank coefficient matrix, which may not be practical in many real world applications. We propose a more general SDE model by relaxing the condition of the coefficient matrix, and derive a closed-form expression for the residual life distributions of components. In addition, unlike conventional reliability approaches that focus on estimating lifetime distributions of a population of similar systems, our primary objective is to estimate the RLDs of components in a fielded system by incorporating its unique degradation signals. That is, by observing the evolution of degradation signals, component interactions are determined by the actual physical conditions of components, such as component degradation and replacement. Hence, the RLDs of components can be updated in real time; therefore, the estimated RLDs exploit not only prior information, but also the real-time interactions among interconnected components.

CHAPTER III

ESTIMATING THE RLD OF A COMPONENT USING A FIRST-PASSAGE-TIME APPROACH

This chapter generalizes the models by [46] and [47], in which the authors used an approximation method to predict the RLD and pointed out that the prediction accuracy would be improved if the first-passage-time of degradation process was utilized to estimate the failure time. A recent paper in this area is [133], which utilized Wiener processes with random effects to compute the residual life distribution. The most significant difference between our work and [133] is that we consider the failure threshold as an absorbing barrier of the degradation process whereas in [133] the failure threshold was considered as a crossing boundary. Our model implies an important inherent constraint that the failure time is always greater than the latest observation epoch. Since all the degradation observations occur at discrete time epochs in both papers, our model ensures that the degradation process will not cross the failure threshold between two discrete observation epochs. By contrast, the model in [133] included degradation processes which crossed the failure threshold between the observation times of degradation signals. Last but not least, we restrict our choices of the prior distribution for the degradation rate among those which take only positive values (such as Gamma, Weibull, lognormal, etc.) because the rate of degradation is never negative in reality. In [133], the author assumes a normal distribution for the drift rate. As a result, the degradation processes of [133] may drift away from the failure threshold, which implies the component would never fail.

The model development, evaluation, and validation are discussed in the following sections. Sections 3.1 and 3.2 discusses the degradation modeling framework with a detailed development of a base case linear degradation model and the corresponding estimation of the RLD. In Section 3.3, we evaluate the performance of our degradation model using simulated degradation signals. In Section 3.4, the model is validated using real-world vibration-based degradation signals from a rotating machinery application.

3.1 Degradation Modeling

Unique to our work, we model the degradation signal as a stochastic process $\{S(t), t > 0\}$ with an absorbing barrier D, where D is the failure threshold and $S(t)$ is the amplitude/level of the degradation signal at time t. The failure threshold D is assumed to be a constant and can be determined using engineering knowledge or defined based on industrial standards, such as ISO 2732 for machinery

vibration. We model the failure threshold D as an absorbing barrier of the degradation signal $S(t)$. As a result, the degradation signal $S(t)$ exists only before $S(t)$ reaches the failure threshold D for the first time. Since the degradation signals are monitored at discrete epochs in most applications, a degradation model without the absorbing barrier may include the degradation signals that cross the failure threshold between discrete observation epochs when estimating model parameters using signal observations. Different from these type of models such as [133], our model focuses on the stochastic processes that remain below the failure threshold by the latest observation epoch.

Before the failure, we assume that the degradation signal $S(t)$ is represented as follows:

$$S(t) = H(t; \kappa, \theta) + B(t) \qquad (3.1.1)$$

where $H(\cdot)$ represents the parametric functional form of the model (for example, linear, exponential, polynomial and others), θ is a deterministic coefficient (parameter) that captures degradation characteristics common across all units of a population, and κ is a stochastic parameter that captures unit-to-unit variability in the degradation rate. In addition, signal transients due to randomness in the degradation process itself are captured by $B(t)$, which is assumed to be a Brownian motion with $B(t) \sim \mathcal{N}(0, \sigma^2 t)$. To model the random effects across units, we assume that the coefficient κ and the error variance σ^2 are random variables with the probability density function denoted by $\pi(\kappa, \sigma^2)$.

The primary objective of this work is to provide a framework for online updating the RLD of the component based on discrete observations of the signal process $S(t)$ using a first-passage-time approach. We utilize real-time degradation signals observed from components that are operating in the field to update the coefficients of the degradation model in a Bayesian manner. The updated degradation model is in turn used to compute an updated RLD for the each component based on its latest degradation state. Specifically, *in-situ* degradation signals communicated from a fielded component are used to update the distribution of κ and σ^2. The updated model is then used to estimate the corresponding RLD of the component. Subsequent signal observations are used to revise the model and continuously update the RLD. Suppose that the degradation signal is monitored at times $t_0, t_1, \ldots, t_k$ such that $0 = t_0 < t_1 < \ldots < t_k$, and let $s(t_i)$ denote the observed signal at observation time t_i. We store the set of observations in a vector $s_k \in \mathbb{R}^{k+1}$, where $s_k = (s(0), s(t_1), \ldots, s(t_k))'$. The component's lifetime corresponds to the first time the degradation signal $\{S(t) : t \geq 0\}$ crosses

the failure threshold D. Given the model parameters κ and σ^2, the distribution of a component's lifetime, denoted by T_D, is written as :

$$\mathbb{P}(T_D > t | \kappa, \sigma^2) = \mathbb{P}(\max_{0 < r < t} S(r) < D | \kappa, \sigma^2) = \mathbb{P}(\max_{0 < v < t} H(v; \kappa, \theta) + B(v) < D | \kappa, \sigma^2) \tag{3.1.2}$$

Therefore, the unconditional distribution of T_D can be expressed as:

$$\mathbb{P}(T_D > t) = \iint_{\kappa, \sigma^2} \mathbb{P}(\max_{0 < r < t} H(r; \kappa, \theta) + B(r) < D | \kappa, \sigma^2) \pi(\kappa, \sigma^2) \, \mathrm{d}\kappa \mathrm{d}\sigma^2 \tag{3.1.3}$$

Furthermore, let R_k denote the remaining time needed for the signal to first reach the threshold D. Our aim is to estimate the distribution of R_k namely

$$\mathbb{P}(R_k \leq t - t_k | \boldsymbol{s_k}), \quad t > t_k.$$

Based on our model, the latest observation epoch t_k implies an inherent condition that the stochastic process $S(t)$ does not cross its absorbing barrier by time t_k. More formally, we denote the condition that $S(t)$ does not cross the failure threshold D during the time interval $[t_0, t_k]$ by $A_{[t_0, t_k]}$. Next, let $v(\kappa, \sigma^2 | \boldsymbol{s_k}, A_{[t_0, t_k]})$ be the posterior distribution of (κ, σ^2). We compute $v(\kappa, \sigma^2 | \boldsymbol{s_k}, A_{[t_0, t_k]})$ as follows :

$$v(\kappa, \sigma^2 | \boldsymbol{s_k}, A_{[t_0, t_k]}) = \frac{\pi(\kappa, \sigma^2) f(\kappa, \sigma^2) | \boldsymbol{s_k}, A_{[t_0, t_k]}}{\iint_{\kappa, \sigma^2} \pi(\kappa, \sigma^2) f(\kappa, \sigma^2 | \boldsymbol{s_k}, A_{[t_0, t_k]}) \, \mathrm{d}\kappa \mathrm{d}\sigma^2} \tag{3.1.4}$$

where $\pi(\kappa, \sigma^2)$ is the prior distribution of (κ, σ^2), and $f(\kappa, \sigma^2 | \boldsymbol{s_k}, A_{[t_0, t_k]})$ is the likelihood function. The likelihood function does not only depends on the monitored signals $\boldsymbol{s_k} = (s(0), s(t_1), \ldots, s(t_k))'$ but also $A_{[t_0, t_k]}$. As a result, our estimates of (κ, σ^2) are only based on the degradation signals of surviving components whose amplitudes are completely below the failure threshold. In other words, we exclude from our consideration the stochastic processes that cross the failure threshold between observation epochs. Next, we define R_k as the residual life of the component evaluated at time t_k. The updated RLD of the component can be estimated using the following expression:

$$\mathbb{P}(R_k > t | \boldsymbol{s_k}, A_{[t_0, t_k]}) = \iint_{(\kappa, \sigma^2)} v(\kappa, \sigma^2 | \boldsymbol{s_k}, A_{[t_0, t_k]}) \mathbb{P}(R_k > t | \kappa, \sigma^2) \, \mathrm{d}\kappa \mathrm{d}\sigma^2$$

To demonstrate our framework, we consider a base case degradation model with an exponential functional form for $H(\cdot)$ in Section 3.2. We will discuss a Bayesian updating framework for updating the stochastic parameters of the degradation model using real-time degradation signals. We will

27

examine two scenarios : (1) a first case where a sample of historical degradation signals are available and used to estimate the distribution of the stochastic coefficients of the model and (2) a second case where there is no historical data or expert knowledge available.

3.2 Linear Degradation Model : a Base Case Model

In this section, we demonstrate our proposed framework in Section 3.1 by assuming that the functional $H(\cdot)$ takes a linear form $H(t; \kappa, \theta) = \kappa t$. As a result, the degradation signal with failure threshold D is modeled as :

$$S(t) = \kappa t + B(t) \tag{3.2.1}$$

where $B(t)$ is assumed to evolve as a Brownian motion with mean 0 and variance $\sigma^2 t$. κ and σ^2 have a prior distribution with the probability density function $\pi(\kappa, \sigma^2)$. Given κ and σ^2, the degradation signal evolves as a Brownian motion with positive drift κ. The resulting distribution of lifetime T_D given κ and σ^2 follows an inverse-Gaussian distribution :

$$\mathbb{P}(T_D > t | \kappa, \sigma^2) = 1 - IG(t; \mu_0, \lambda_0), \tag{3.2.2}$$

and the unconditional distribution of T_D is given as:

$$\mathbb{P}(T_D > t) = \iint_{(\kappa, \sigma^2)} (1 - IG(t; \mu_0, \lambda_0)) \pi(\kappa, \sigma^2) \, d\kappa \, d\sigma^2 \tag{3.2.3}$$

where $IG(.; \mu, \lambda)$ is the cdf of the inverse Gaussian distribution with parameters μ, λ and

$$\mu_0 = \frac{D}{\kappa}, \quad \lambda_0 = \frac{D^2}{\sigma^2} \tag{3.2.4}$$

At time t_k, the posterior distribution of (κ, σ^2) given the signals $s_k = (s(t_0), \ldots, s(t_k))$ is expressed as

$$\nu(\kappa, \sigma^2 | s_k, A_{[t_0, t_k]}) = \frac{\pi(\kappa, \sigma^2) f(\kappa, \sigma^2 | s_k, A_{[t_0, t_k]})}{\int_{\kappa, \sigma^2} \pi(\kappa, \sigma^2) f(\kappa, \sigma^2 | s_k, A_{[t_0, t_k]}) \, d\kappa d\sigma^2} \tag{3.2.5}$$

where $\pi(\kappa, \sigma^2)$ is the prior distribution of (κ, σ^2), and $f(\kappa, \sigma^2 | s_k, A_{[t_0, t_k]})$ is the likelihood function. The next theorem gives the expression of the likelihood function.

28

Theorem 3.2.1. *For the degradation model, as described by Equation (3.2.1), the likelihood function* $f(\kappa, \sigma^2 | \mathbf{s}_k, A_{[t_0, t_k]})$ *given the observations of degradation signals* $\mathbf{s}_k$ *is expressed as follows*

$$f(\kappa, \sigma^2 | \mathbf{s}_k, A_{[t_0, t_k]})$$

$$= \left(\frac{1}{\sqrt{2\pi\sigma^2 \Delta t}} \right)^k \prod_{j=1}^{k} \phi \left(\frac{s(t_j) - s(t_{j-1}) - \kappa\Delta t}{\sqrt{\sigma^2 \Delta t}} \right) \left[1 - \exp \left(-2\frac{(D - s(t_{j-1}))(D - s(t_j))}{\sigma^2 \Delta t} \right) \right] \quad (3.2.6)$$

Proof. We denote by $\tilde{f}(\mathbf{s}_k, A_{[t_0, t_k]} | \kappa, \sigma^2)$ the joint probability density function of $(\mathbf{s}_k, A_{[t_0, t_k]})$ given parameters (κ, σ^2). In this case,

$$\tilde{f}(\mathbf{s}_k, A_{[t_0, t_k]} | \kappa, \sigma^2) = f(\kappa, \sigma^2 | \mathbf{s}_k, A_{[t_0, t_k]}).$$

Let $y_i = s(t_i) - s(t_{i-1}), i = 1, 2, \ldots,$ and $A_{[t_i, t_j]}$ represents the event that the degradation signal does not cross the failure threshold, D, within the interval $[t_i, t_j]$. We decompose the expression of $\tilde{f}(\kappa, \sigma^2 | \mathbf{s}_k, A_{[t_0, t_k]})$ to the product of likelihood functions with only one observation given the prior information. That is, $\tilde{f}(y_i, A_{t_{i-1}, t_i} | \mathbf{s}_{i-1}, A_{[t_0, t_{i-1}]})$.

$$\tilde{f}(\kappa, \sigma^2 | \mathbf{s}_k, A_{[t_0, t_k]})$$

$$= \tilde{f}(y_1, A_{[t_0, t_1]} | \kappa, \sigma^2) \tilde{f}(y_2, A_{[t_1, t_2]} | \mathbf{s}_1, A_{[t_0, t_1]}, \kappa, \sigma^2) \ldots \tilde{f}(y_k, A_{[t_{k-1}, t_k]} | \mathbf{s}_{k-1}, A_{[t_0, t_{k-1}]}, \kappa, \sigma^2)$$

$$= \prod_{i=1}^{k} \tilde{f}(y_i, A_{[t_{i-1}, t_i]} | \mathbf{s}_{i-1}, A_{[t_0, t_{i-1}]}, \kappa, \sigma^2)$$

By the Markov property,

$$\tilde{f}(y_i, A_{[t_{i-1}, t_i]} | \mathbf{s}_{i-1}, A_{[t_0, t_{i-1}]}, \kappa, \sigma^2) = \tilde{f}(y_i, A_{[t_{i-1}, t_i]} | s(t_{j-1}), \kappa, \sigma^2)$$

Thus,

$$\tilde{f}(\kappa, \sigma^2 | \mathbf{s}_k, A_{t_0, t_k})$$

$$= \prod_{i=1}^{k} \tilde{f}(y_i, A_{[t_{i-1}, t_i]} | s(t_{j-1}), \kappa, \sigma^2)$$

$$= \left(\frac{1}{\sqrt{2\pi\sigma^2 \Delta t}} \right)^k \prod_{j=1}^{k} \phi \left(\frac{y_j - \kappa\Delta t}{\sqrt{\sigma^2 \Delta t}} \right) \left[1 - \exp \left(-2\frac{(D - s(t_{j-1}))(D - s(t_j))}{\sigma^2 \Delta t} \right) \right]$$

since

$$\tilde{f}(y_j, A_{[t_{j-1}, t_j]} | s(t_{j-1}), \kappa, \sigma^2) = \frac{1}{\sqrt{2\pi\sigma^2 \Delta t}} \phi \left(\frac{y_j - \kappa\Delta t}{\sqrt{\sigma^2 \Delta t}} \right) \left[1 - \exp \left(-2\frac{(D - s(t_{j-1}))(D - s(t_j))}{\sigma^2 (\Delta t)} \right) \right]$$

by [31], where $\phi(.)$ represents the pdf of standard normal distribution. $\square$

The next step is to use the posterior distribution of $\pi(\kappa, \sigma^2)$ to compute an updated distribution of the component's residual lifetime at time t_k. The updated distribution of the residual lifetime R_k is given as follows:

$$\mathbb{P}(R_k > t | s_k, A_{[t_0, t_k]}) = \iint_{(\kappa, \sigma^2)} \nu(\kappa, \sigma^2 | s_k, A_{[t_0, t_k]}) \mathbb{P}(R_k > t | s_k, \kappa, \sigma^2) \, \mathrm{d}\kappa \mathrm{d}\sigma^2 \qquad (3.2.7)$$

where $\mathbb{P}(R_k > t | s_k, \kappa, \sigma^2) = (1 - IG(t; \mu_k, \lambda_k))$ with $\mu_k = \frac{D - s(t_k)}{\kappa}$ and $\lambda_k = \frac{(D - s(t_k))^2}{\sigma^2}$.

Remark 3.2.1. *An important distinction needs to be made here regarding the random variable R_k and the standard residual life distribution. Assume for the moment that the distribution of T_D is known in advance. Then the residual life distribution is defined by $\mathbb{P}(T_D > t + t_k | T_D > t_k)$, for $t \geq 0$. However, for real applications computing the residual life distribution in this way is problematic because (1) the true distribution of T_D is not typically known in advance, and (2) it does not exploit available information about the* current *condition of the component – information that can drastically affect the estimate of the remaining useful lifetime of the component.*

The calculation of expression (3.2.7) depends on our choice of the prior distribution $\pi(\kappa, \sigma^2)$. We consider two scenarios for $\pi(\kappa, \sigma^2)$. The first case considers applications where historical degradation data is available. The choice of prior distributions for the model parameters depends on the historical dataset. Examples of such distributions include the Gamma distribution, the lognormal distribution, the Weibull distribution and so on. We provide an illustrative example when the prior distribution of κ follows a Gamma distribution and that of σ^2 follows an inverse-Gamma distribution. We consider this pair of distributions because they provide the best fit for degradation data that will be used later in our case study in Section 3.4. The second case considers situations where historical degradation data is unavailable. For this case, we assume that κ and σ^2 follow a non-informative prior distribution.

3.2.1   Case 1: Informative Prior Distribution

This case focuses on applications which have historical degradation data, such as a sample of degradation signals. The historical degradation data can be used to estimate the prior distribution of κ and σ^2. Unlike most of the existing literature that uses normal distributions, we assume that κ follows a Gamma distribution with parameters (k_1, θ_1). The Gamma distribution is a more reasonable

choice for characterizing the degradation rate κ, since it ensures that the probability of negative degradation rate is zero. That is, $\mathbb{P}(\kappa < 0) = 0$. On the other hand, we assume that σ^2 follows an inverse-Gamma distribution with parameters (k_2, θ_2). The choice of an inverse-Gamma distribution for σ^2 is to ensure conjugacy with the likelihood function $f(\kappa, \sigma^2 | s_k, A_{[t_0, t_k]})$. Assuming that κ and σ^2 are independent, we express the prior distribution of (κ, σ^2) as follows:

$$\pi(\kappa, \sigma^2) = \left(\kappa^{k_1-1} \frac{\exp(-\kappa/\theta_1)}{\Gamma(k_1)\theta_1^{k_1}} \right) \left((\sigma^2)^{-(k_2+1)} \exp(-\theta_2/\sigma^2) \frac{\theta_2^{k_2}}{\Gamma(k_2)} \right) \tag{3.2.8}$$

Given that we observed a sequence of degradation signals s_k from a fielded component, the posterior distribution of (κ, σ^2) can be obtained by substituting (3.2.8) in expression (3.2.5):

$$\nu(\kappa, \sigma^2 | s_k, A_{[t_0, t_k]})$$

$$= \frac{h_k(\kappa, \sigma^2)\kappa^{k_1-1}(\sigma^2)^{-(k_2+1+k/2)} \exp(-\frac{\kappa}{\theta_1} - \frac{1}{\sigma^2}(\theta_2 + \frac{\sum_{j=1}^{k}(s(t_j)-s(t_{j-1}))^2}{2\Delta t}))}{\int_{(\kappa,\sigma^2)} h_k(\kappa, \sigma^2)\kappa^{k_1-1}(\sigma^2)^{-(k_2+1+k/2)} \exp(-\frac{\kappa}{\theta_1} - \frac{1}{\sigma^2}(\theta_2 + \frac{\sum_{j=1}^{k}(s(t_j)-s(t_{j-1}))^2}{2\Delta t})) \, d\kappa d\sigma^2} \tag{3.2.9}$$

where

$$h_k(\kappa, \sigma^2) = \prod_{j=1}^{k} \left[1 - \exp(-2\frac{(D - s(t_{j-1}))(D - s(t_j))}{\sigma^2 \Delta t}) \right] \exp\left(\frac{\kappa s(t_k)}{\sigma^2} - \frac{\kappa^2 t_k}{2\sigma^2} \right)$$

By substituting (3.2.9) in expression (3.2.7), the updated RLD of the fielded component that is being monitored can be written as:

$$\mathbb{P}(R_k > t | s_k, A_{[t_0, t_k]})$$

$$= \frac{\int_{(\kappa,\sigma^2)}(1 - IG(t; \mu_k, \lambda_k))h_k(\kappa, \sigma^2)\kappa^{k_1-1}(\sigma^2)^{-(k_2+1+k/2)} \exp(-\frac{\kappa}{\theta_1})\exp(-\frac{1}{\sigma^2}(\theta_2 + \frac{\sum_{j=1}^{k}(s(t_j)-s(t_{j-1}))^2}{2\Delta t})) \, d\kappa d\sigma^2}{\int_{(\kappa,\sigma^2)} h_k(\kappa, \sigma^2)\kappa^{k_1-1}(\sigma^2)^{-(k_2+1+k/2)} \exp(-\frac{\kappa}{\theta_1})\exp(-\frac{1}{\sigma^2}(\theta_2 + \frac{\sum_{j=1}^{k}(s(t_j)-s(t_{j-1}))^2}{2\Delta t})) \, d\kappa d\sigma^2}$$

$$= \frac{\mathbb{E}_{(\kappa,\tilde{\sigma}^2)}[h_k(\kappa, \tilde{\sigma}^2)(1 - IG(t; \mu_k, \tilde{\lambda}_k))]}{\mathbb{E}_{(\kappa,\tilde{\sigma}^2)}[h_k(\kappa, \tilde{\sigma}^2)]} \tag{3.2.10}$$

where $\tilde{\sigma}^2 \sim \text{inv-}\Gamma(k_3, \theta_3)$ with $k_3 = k_2 + k/2$ and $\theta_3 = \theta_2 + \frac{\sum_{j=1}^{k}(s(t_j)-s(t_{j-1}))^2}{2\Delta t}$; and $\tilde{\lambda}_k = \frac{(D-s(t_k))^2}{\tilde{\sigma}^2}$. To compute expression (3.2.10), we propose a Monte-Carlo simulation approach to estimate the involved expectations. The sequence of steps involved in this procedure is outlined below :

1. Select a sufficiently large number of realizations M, say $M = 5,000$;

2. Simulate M realizations of κ and $\tilde{\sigma}^2$ from the distributions : $\tilde{\sigma}^2 \sim \text{inv-}\Gamma(k_3, \theta_3)$ and $\kappa \sim \Gamma(k_1, \theta_1)$;

3. Denote by κ_i and $\tilde{\sigma}_i^2$ the ith realization of κ and $\tilde{\sigma}^2$ and compute

$$h_k(\kappa_i, \tilde{\sigma}_i^2)(1 - IG(t; \mu_k, \tilde{\lambda}_k)) \text{ and } h(\kappa_i, \tilde{\sigma}_i^2);$$

4. Estimate (3.2.10) using the following expression :

$$\frac{\sum_{i=1}^{M} h_k(\kappa_i, \tilde{\sigma}_i^2)(1 - IG(t; \mu_k, \tilde{\lambda}_k))/M}{\sum_{i=1}^{M} h_k(\kappa_i, \tilde{\sigma}_i^2)/M}.$$

Furthermore, we utilize expression (3.2.10) to obtain the mean and the confidence intervals of R_k. The mean estimate of R_k is expressed as :

$$\mathbb{E}(R_k | s_k, A_{[t_0, t_k]}) = \frac{\mathbb{E}_{(\kappa, \tilde{\sigma}^2)}[h_k(\kappa, \tilde{\sigma}^2)\mu_k]}{\mathbb{E}_{(\kappa, \tilde{\sigma}^2)}[h_k(\kappa, \tilde{\sigma}^2)]} \tag{3.2.11}$$

For any $0 < \alpha < 1$, assume that t_α satisfies

$$\mathbb{P}(R_k > t_\alpha | s_k, A_{[t_0, t_k]}) = \alpha$$

we can also use formula (3.2.10) to compute the $t_{\alpha/2}$ and $t_{1-\alpha/2}$ numerically. The $100\%(1 - \alpha)$ confidence interval is computed as $(t_{1-\alpha/2}, t_{\alpha/2})$.

3.2.2 Case 2: Non-informative Prior Distribution

The second case considers applications where no historical data or expert knowledge is available. Thus, it is not possible to estimate and obtain an informative prior distribution for κ and σ^2. We assume that (κ, σ^2) follow a non-informative prior distribution:

$$\pi(\kappa, \sigma^2) = \frac{1}{\sigma^2} \mathbf{1}_{\{\sigma^2 > 0\}} \tag{3.2.12}$$

The posterior distribution of (κ, σ^2) given that we observed a sequence of degradation signals s_k from a fielded component can be obtained by substituting (3.2.12) in expression (3.2.5):

$$\nu(\kappa, \sigma^2 | s_k, A_{[t_0, t_k]})$$

$$= \frac{g_k(\sigma^2)\left[(\sigma^2)^{-\frac{k+1}{2}} \exp\left(-\frac{\sum_{j=1}^{k}((s(t_j)-s(t_{j-1}))-\bar{y})^2}{2\sigma^2 \Delta t}\right)\right]\left[\frac{1}{\sqrt{\sigma^2}} \exp\left(-\frac{k(\kappa\Delta t-\bar{y})^2}{2\sigma^2 \Delta t}\right)\right]}{\int_{(\kappa, \sigma^2)} g_k(\sigma^2)\left[(\sigma^2)^{-\frac{k+1}{2}} \exp\left(-\frac{\sum_{j=1}^{k}((s(t_j)-s(t_{j-1}))-\bar{y})^2}{2\sigma^2 \Delta t}\right)\right]\left[\frac{1}{\sqrt{\sigma^2}} \exp\left(-\frac{k(\kappa\Delta t-\bar{y})^2}{2\sigma^2 \Delta t}\right)\right] \, \mathrm{d}\kappa \mathrm{d}\sigma^2} \tag{3.2.13}$$

where

$$g_k(\sigma^2) = \prod_{j=1}^{k} \left[1 - \exp(-2\frac{(D - s(t_{j-1}))(D - s(t_j))}{\sigma^2 \Delta t}) \right] \quad \text{and} \quad \bar{y} = \frac{\sum_{i=1}^{k}(s(t_i) - s(t_{i-1}))}{k}$$

By substituting (3.2.13) in expression (3.2.7), the updated RLD of the fielded component that is being monitored can be written as:

$$\mathbb{P}(R_k > t | s_k, A_{[t_0, t_k]})$$

$$= \frac{\int_{(\kappa,\sigma^2)} (1 - IG(t; \mu_k, \lambda_k)) g_k(\sigma^2) \left[(\sigma^2)^{-\frac{k+1}{2}} \exp\left(-\frac{\sum_{j=1}^{k}((s(t_j)-s(t_{j-1}))-\bar{y})^2}{2\sigma^2\Delta t} \right) \right] \left[\frac{1}{\sqrt{\sigma^2}} \exp\left(-\frac{k(\kappa\Delta t-\bar{y})^2}{2\sigma^2\Delta t} \right) \right] \, d\kappa d\sigma^2}{\int_{(\kappa,\sigma^2)} g_k(\sigma^2) \left[(\sigma^2)^{-\frac{k+1}{2}} \exp\left(-\frac{\sum_{j=1}^{k}((s(t_j)-s(t_{j-1}))-\bar{y})^2}{2\sigma^2\Delta t} \right) \right] \left[\frac{1}{\sqrt{\sigma^2}} \exp\left(-\frac{k(\kappa\Delta t-\bar{y})^2}{2\sigma^2\Delta t} \right) \right] \, d\kappa d\sigma^2}$$

$$= \frac{\mathbb{E}_{(\tilde{\kappa},\tilde{\sigma}^2)}[g_k(\tilde{\kappa}, \tilde{\sigma}^2)(1 - IG(t; \tilde{\mu}_k, \tilde{\lambda}_k))]}{\mathbb{E}_{(\tilde{\sigma}^2)}[g_k(\tilde{\sigma}^2)]} \tag{3.2.14}$$

where $\tilde{\mu}_k = \frac{D-s(t_k)}{\tilde{\kappa}}$, $\tilde{\lambda}_k = \frac{(D-s(t_k))^2}{\tilde{\sigma}^2}$, $\tilde{\sigma}^2 \sim \text{inv-}\Gamma(k_4, \theta_4)$ and $\tilde{\kappa}|\tilde{\sigma}^2 \sim \mathcal{N}(k_5, \theta_5)$ with

$$k_4 = \frac{k-1}{2}, \quad \theta_4 = \frac{\sum_{j=1}^{k}((s(t_j)-s(t_{j-1}))-\bar{y})^2}{2\Delta t}, \quad k_5 = \frac{\bar{y}}{\Delta t}, \quad \theta_5 = \frac{\sigma^2}{k\Delta t};$$

Expression (3.2.14) can be estimated using the same simulation technique we proposed in Section 3.2.1. Similarly, the mean estimate of the component's residual lifetime is expressed as follows :

$$\mathbb{E}(R_k | s_k, A_{[t_0, t_k]}) = \frac{\mathbb{E}_{(\tilde{\kappa},\tilde{\sigma}^2)}[g_k(\tilde{\kappa}, \tilde{\sigma}^2)\tilde{\mu}_k]}{\mathbb{E}_{(\tilde{\sigma}^2)}[g_k(\tilde{\sigma}^2)]} \tag{3.2.15}$$

For any $0 < \alpha < 1$, assume that t_α satisfies

$$\mathbb{P}(R_k > t_\alpha | s_k, A_{[t_0, t_k]}) = \alpha$$

we can also use formula (3.2.10) to compute the $t_{\alpha/2}$ and $t_{1-\alpha/2}$ numerically. The $100\%(1 - \alpha)$ confidence interval is computed as $(t_{1-\alpha/2}, t_{\alpha/2})$.

The performance of our base case degradation model will be evaluated for the informative and non-informative cases using two separate studies. The first is a study involving simulated degradation signals while the second uses vibration-based degradation signals from a real-world rotating machinery application.

3.3 Analyzing Degradation Models Using Simulated Data

The objective of using simulated degradation signals is to study the effect of signal characteristics on the performance of our degradation modeling framework. Specifically, we investigate the effect of signal-to-noise ratio on the performance of the base case exponential degradation model under the informative and the non-informative assumptions for the prior distribution of κ and σ^2. For each scenario, we evaluate the accuracy of predicting the residual lifetime and investigate the effect of two levels of signal-to-noise ratios. Two groups of degradation signals, Groups H and L, are simulated using equation (3.2.1): $S(t_i) = \kappa t_i + B(t_i)$. Each group of signals corresponds to a specific signal-to-noise ratio. Degradation signals in Group H have a relatively high signal-to-noise ratio, whereas signals in Group L have a lower ratio. For each group, degradation signals are simulated using random values of κ and σ^2 that are generated from pre-specified distributions (shown below).

- Degradation signals in Group H are simulated using the following distribution for κ and σ^2:
  $\kappa \sim \Gamma(100, 0.01)$ and $\sigma^2 \sim$ inv-$\Gamma(102, 101)$, thus,

$$\mathbb{E}[\kappa] = 1, \text{var}[\kappa] = 0.01, \mathbb{E}[\sigma^2] = 1, \text{var}[\sigma^2] = 0.01, \frac{\mathbb{E}[\kappa]}{\sqrt{\mathbb{E}[\sigma^2]}} = 1 \qquad (3.3.1)$$

- Degradation signals in Group L are simulated using the following distribution for κ and σ^2:
  $\kappa \sim \Gamma(100, 0.01)$ and $\sigma^2 \sim$ inv-$\Gamma(10^4, 10^6)$, thus,

$$\mathbb{E}[\kappa] = 1, \text{var}[\kappa] = 0.01, \mathbb{E}[\sigma^2] = 100, \text{var}[\sigma^2] = 1, \frac{\mathbb{E}[\kappa]}{\sqrt{\mathbb{E}[\sigma^2]}} = 0.1 \qquad (3.3.2)$$

where $\frac{\mathbb{E}[\kappa]}{\sqrt{\mathbb{E}[\sigma^2]}}$ represents the signal-to-noise ratio.

For each signal group, we generate two types of degradation signals, "historical" and "validation". "Historical" degradation signals simulate the existence of a historical database and are used to estimate the prior distribution of (κ, σ^2) for Case 1, using informative prior. A total of 200 "historical" degradation signals are simulated until they reach a predetermined failure threshold: 100 signals using the settings of Group H and another 100 using the settings of Group L. Without loss of generality, we define a failure threshold, $D = 500$. Figure 3.3.1 shows an example of the degradation signals in each group. Note that the 200 "historical" degradation signals will only be used to estimate the prior distribution for Case 1 and will not be used for Case 2, non-informative prior distribution.

34
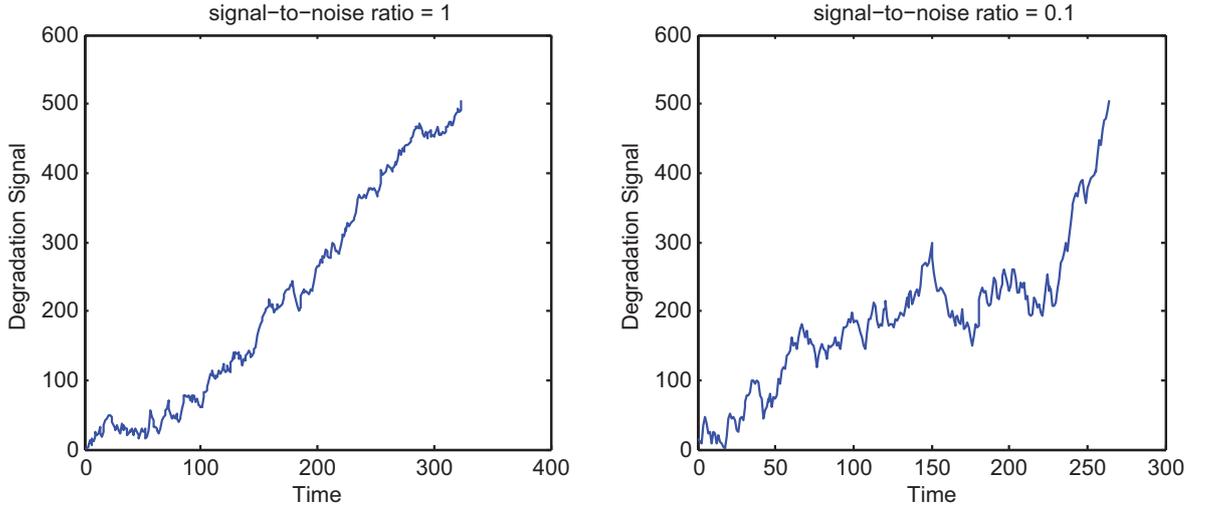
Figure 3.3.1: Evolution of degradation signals with the Brownian motion residual term.

The second type of degradation signals is referred to as the "validation" degradation signals. These signals are used to simulate real-time signals being communicated (for example, via embedded sensors) from components that are operating in the field. They are generated in a similar manner as their historical counterparts, i.e., using the same prior distributions for κ and σ^2 as specified above. Assuming that the signal is being generated from a fielded component, each time a signal observation is made, it is used to compute the posterior distribution of (κ, σ^2) (using expressions (3.2.9) and (3.2.13)), and update the corresponding RLD (using expressions (3.2.10) and (3.2.14)) A total of 200 "validation" degradation signals are simulated until they reach a predetermined failure threshold (up to and including the time of failure). One hundred degradation signals are simulated using the settings of Group H and another 100 using settings of Group L. For the simulation experiments, let L_i denote the lifetime of the ith simulated path, and let $\hat{L}_i$ be the estimated lifetime (using our updating procedure). Then the prediction error (%) for the ith degradation signal is given by

$$\delta_i = \frac{|L_i - \hat{L}_i|}{L_i} \times 100. \tag{3.3.3}$$

3.3.1 Model Performance Using Informative Prior Distribution

The "historical" degradation signals that have been generated earlier are used to estimate the parameters of the degradation model. We use the two-stage method proposed by [84] to estimate the prior distribution, $\pi(\kappa, \sigma^2)$. First, we let $S_i(t)$ represent the degradation signal from component i for $i = 1, \ldots, 100$. The corresponding degradation model is expressed as $S_i(t) = \kappa_i t + B_i(t)$, where κ_i represents the degradation signal of component i, and $B_i(t)$ the residual term of the degradation signal from component i. We then define the term $r_{i,m}$ as follows:

$$r_{i,m} = \frac{s_i(t_m) - s_i(t_{m-1})}{\Delta t} = \kappa_i + \frac{B_i(t_m) - B_i(t_{m-1})}{\Delta t}$$

For the degradation signal from component i, $r_{i,m}$'s are clearly i.i.d. with distribution, $\mathcal{N}(\kappa_i, \sigma_i^2/\Delta t)$. Let $(\hat{\kappa}_i, \hat{\sigma}_i^2)$ denote the maximum likelihood estimate of (κ_i, σ_i^2). For $i = 1, \ldots, 100$, we fit the resulting estimates, $\hat{\kappa}_i$ and $\hat{\sigma}_i^2$ to a Gamma and an inverse-Gamma distribution, respectively. This process is performed for the two types of signal groups, Group H and Group L. The estimated distributions are shown below.

- For group H,

$$\hat{\kappa} \sim \Gamma(187.78, 7.91 \times 10^{-3}), \quad \hat{\sigma}^2 \sim \Gamma^{-1}(153.25, 167.48) \tag{3.3.4}$$

- For group L,

$$\hat{\kappa} \sim \Gamma(204.80, 7.3 \times 10^{-3}), \quad \hat{\sigma}^2 \sim \Gamma^{-1}(1.41 \times 10^4, 1.59 \times 10^6) \tag{3.3.5}$$

Next, we use the "validation" degradation signals to emulate signals being communicated from (hypothetical) fielded components. Each time a signal is observed, it is used to update $\pi(\kappa, \sigma^2)$ and compute a corresponding RLD. To evaluate the performance of our model, we calculate an expected residual lifetime, $\mathbb{E}[R_k]$, using Equation (3.2.11), and then a corresponding prediction error using equation (3.3.3). Figure 3.3.2 presents the prediction error for each signal group, Group H with signal-to-noise ratio $=1$, and Group L with signal-to-noise ratio $=0.1$. The x-axis represents the degradation percentiles, where $1, 2, \ldots, 9$ refers to the $10^{th}, 20^{th}, \ldots, 90^{th}$ percentile of lifetimes; and the y-axis represents the prediction error evaluated at the corresponding degradation percentile.

Figure 3.3.2 demonstrates the performance of our model under degradation signals with different levels of signal-to-noise ratio. In fact, one noticeable difference between the two plots is that the

36
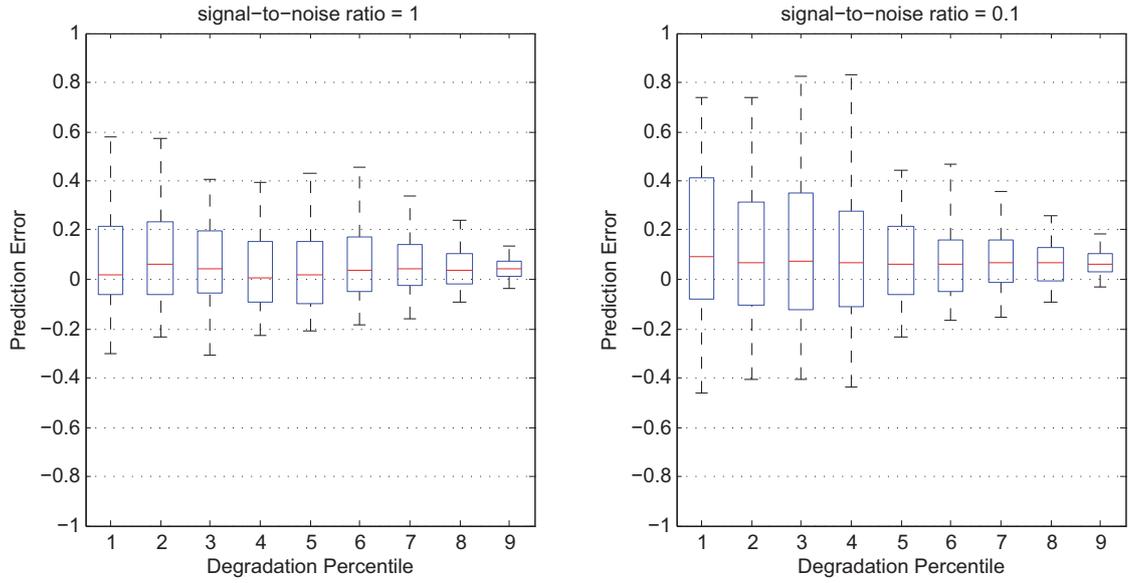
Figure 3.3.2: Prediction error of simulated signals using the informative prior distribution.

variance of the prediction error is relatively larger for signals with lower signal-to-noise ratio. However, in both cases, we notice that the variance of the prediction error decreases significantly with degradation percentiles. We believe that this is due to updating the RLDs at progressive degradation percentiles, which improves the prediction accuracy. Since we estimated the prior distribution from the historical data set, there might be a slight bias in the mean of the prediction error due to the difference between the estimated and the true values.

3.3.2 Model Performance Using Non-informative Prior Distribution

A similar approach is employed in evaluating the performance of the exponential degradation model under this setting. Since the stochastic model parameters are assumed to follow a non-informative prior distribution, we ignore the "historical" degradation signals because they are not used for any estimation process. Only the 200 "validation" degradation signals (100 signals for each signal group) are used to evaluate the performance of the model. Each signal observation is used to update the prior distribution of (κ, σ^2). An updated residual life distribution is evaluated and an expected residual lifetime, $\mathbb{E}[R_k]$, is calculated using equation (3.2.15).

Figure 3.3.3 presents box plots of the prediction error for each type of signal group. The plots show larger spread in the prediction error at earlier degradation percentiles (compared to Figure 3.3.2). This is most probably a result of using a non-informative prior distribution for (κ, σ^2).
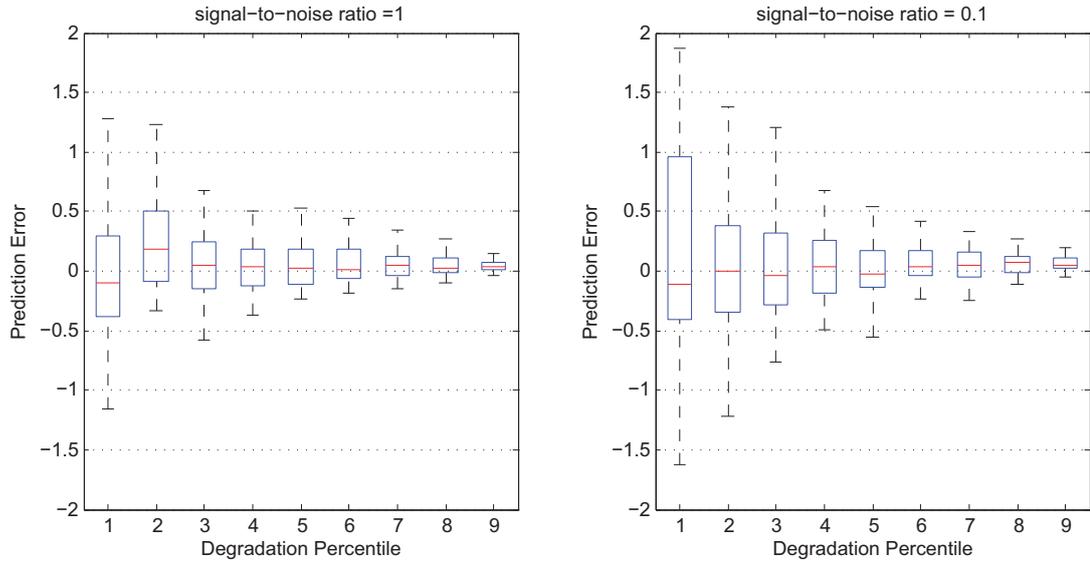
Figure 3.3.3: Prediction error of simulated signals using the non-informative prior distribuiton.

However, we notice that as more degradation signals are observed, a higher prediction accuracy can be attained. This is evident by observing that the width of the box plot becomes smaller as more degradation percentiles increase and more degradation signals are observed. Although the prediction accuracy of the degradation model when using a non-informative prior distribution is slightly less than the informative case, it is still comparable. In other words, the RLD of a partially degraded component can be predicted reasonably accurately even when prior/expert knowledge is unavailable.

3.4 Case Study: Implementation of Bearing Data

In this section, we present a case study with the implementation of ball bearings. We first discuss the vibration analysis that develops the degradation signals using the raw data from the accelerometers. Subsequently, we propose a procedure that examines the model assumption and estimates the parameters. Eventually, we compare our model with the benchmark model proposed in [47].

3.4.1 Experimental Setup

This case study considers a rotating machinery application. Vibration-based degradation signals are used to predict and update the RLD of partially degraded rolling element bearings using our

proposed first-passage time approach. Bearings are a crucial component of any rotating machinery. Bearing degradation typically begins with the formation of subsurface micro-cracks inside the raceway material. The crack propagates towards the surface of the raceway. Once cracks reach the surface, they dislodge pieces of the raceway material causing small pits on the surface, also known as spalls. Spalling increases the friction between the rolling elements (usually steel balls) and bearing raceways, which is typically accompanied by increased temperature. More importantly, spall formation and propagation along the surface of the raceway results in increased levels of vibration. The passage of the rolling elements over these spalls creates repetitive impacts that result in the excitation of fault-specific vibration frequencies related to the bearing defect. These defective frequencies are usually a function of the bearing's rotational speed, number of rolling elements, bearing dimensions, and geometry as discussed in [51].

An experimental setup is used to perform accelerated degradation tests on a sample of thrust ball bearings. We ran each test bearing under constant operating conditions, a load of 200 lbs and a rotational speed of 2200 rpm. Accelerometers attached to the testing chamber are used to monitor and acquire vibration signals. The time-domain signals, acquired every 2 minutes, are processed into the corresponding vibration frequency spectrum (using a FFT) with the aid of Labview software. The average of the amplitudes of the bearing's defective frequency (ball-passing frequency) and its first six harmonics were used to develop a vibration-based degradation signal. Furthermore, we define bearing failure based on the root mean square (RMS) value of the overall vibration acceleration. According to industrial standards for machinery vibration, ISO 2372, 2.0-2.2 Gs (G is a measure of acceleration) represents a "vibration-based danger level" for applications involving general-purpose mid-size machinery (our setup falls in this category of machines). This level was used to identify a corresponding failure threshold for our vibration-based degradation signal. Based on the signal observations, the failure threshold was identified as 0.025 V_{rms} (Root Mean Square Volts). The same degradation signals were used in [47] and [46].

3.4.2 Model Selection

We conducted two groups of tests: a set of 25 experiments for generating a historical data set, designated as ID 1 to 25 and a set of 25 online validation experiments, designated as ID 26 to 50

(as shown in Table 3.4.1). In particular, we use the degradation signals of bearings 1-25 to examine the assumption of our degradation model and estimate the prior distributions of κ and σ^2. We first examine the model assumption that the degradation signal from each bearing evolves as Brownian motion with a positive drift. To achieve this, we use the fact that Brownian motion has independent and identical normal increments. That is, for the degradation signals of each bearing, $s(t_i) - s(t_{i-1})$'s are independent random variables that follow $\mathcal{N}(\kappa(t_i - t_{i-1}), \sigma^2(t_i - t_{i-1}))$. We apply the Shapiro-Wilk test to $s(t_i) - s(t_{i-1})$'s for each bearing and present the resulting p-values in Table 3.4.2. We observe that the resulting p-values range from 0.68 to 0.99. Hence, we do not reject the model assumption of Brownian motion.

Table 3.4.1: Lifetimes of bearing 26 to 50 with unit=2 minutes.

Bearing	Lifetime	Bearing	Lifetime
26	216	39	99
27	98	40	136
28	165	41	83
29	152	42	156
30	227	43	190
31	77	44	195
32	154	45	133
33	148	46	116
34	128	47	98
35	217	48	197
36	128	49	116
37	277	50	141
38	100		

Subsequently, we apply the two-stage method, as in Section 3.3.1, to estimate κ and σ^2 for each bearing and use the estimated the values of κ and σ^2 to select the prior distributions. We investigate the goodness-of-fit for the Gamma distribution, the Weibull distribution, and the lognormal distribution for the purpose of illustration. We apply the Anderson-Darling test to the estimated values of

Table 3.4.2: P-Values of the Shapiro-Wilk test for the model assumption.

Bearing	P-Value	Bearing	P-Value
1	0.81	14	0.93
2	0.69	15	0.76
3	0.92	16	0.89
4	0.76	17	0.73
5	0.77	18	0.79
6	0.74	19	0.86
7	0.84	20	0.69
8	0.87	21	0.91
9	0.73	22	0.89
10	0.68	23	0.84
11	0.94	24	0.67
12	0.91	25	0.79
13	0.99		

κ and σ^2 from each bearing. Table 3.4.3 lists the resulting p-values for each choice of prior distributions. We observe that the lognormal distribution and the Weibull distribution are not suitable for $(\hat{\sigma}^2)^{-1}$, since the corresponding p-values are very small. Hence, we select the Gamma distribution as the prior distribution of $(\sigma^2)^{-1}$. Equivalently, we choose the inverse Gamma distribution as the prior distribution of σ^2. For the prior distribution of κ, we do not have strong evidence to reject the lognormal distribution and the Weibull distribution, although the p-value of the Gamma distribution is the highest. Hence, we will estimate and compare the RLD for these three prior distributions of κ. Since the Gamma distribution and the inverse Gamma distribution have fitted the estimated values of κ (p-value = 0.71) and $(\sigma^2)^{-1}$ (p-value = 0.83), respectively. Investigation of other prior distributions, such as the log-logistic distribution and the two-parameter exponential distribution, is not necessary. However, other choices of prior distributions should be considered if none of the Gamma, Weibull, and lognormal distributions can fit the estimated values of κ and σ^2.

Table 3.4.3: P-Values of the Anderson-Darling test for prior distributions.

	Gamma	Lognormal	Weibull
$\hat{\kappa}$	0.71	0.37	0.45
$(\hat{\sigma}^2)^{-1}$	0.83	0.02	0.01

Next, we validate our proposed approach using the degradation signals from the second group of tests, bearing 26-50. We estimate the RLD using three possible prior distributions of κ: the Gamma distribution, the Weibull distribution, and the lognormal distribution. Table 3.4.4 and Table 3.4.5 respectively present the estimates of the RLD at the 50th and 90th percentiles of each bearing's lifetime. The results are presented in the form of mean estimates and 95% confidence intervals. We compute the prediction error using equation (3.3.3) as described in Section 3.3.1. The prediction error is presented in Table 3.4.6. We observe that the Gamma prior distribution results in the highest prediction accuracy, since its mean estimate of the lifetime is closest to the actual lifetime for almost every bearing (as shown in Table 3.4.4 and Table 3.4.5).

Table 3.4.4: Prediction of the residual life at the 50th percentile of lifetimes.

	Gamma		Lognormal		Weibull	
Bearing	Mean	95% CI	Mean	95% CI	Mean	95% CI
26	235.56	(213.42, 285.97)	244.38	(214.28, 303.04)	237.78	(214.09 , 281.06)
27	90.22	(81.74, 109.53)	84.91	(75.14, 105.29)	85.28	(77.86, 100.80)
28	174.80	(158.37, 212.21)	182.72	(161.71, 226.57)	188.36	(161.98, 222.65)
29	170.96	(148.84, 207.55)	200.94	(177.84, 249.17)	173.25	(158.18, 204.78)
30	202.95	(187.73, 240.50)	199.33	(176.41, 247.17)	196.82	(179.70, 232.64)
31	83.10	(75.87, 98.47)	93.34	(82.61, 115.74)	90.26	(75.41, 106.68)
32	132.20	(122.29, 156.66)	110.88	(98.13, 137.49)	123.66	(112.90, 156.16)
33	136.16	(125.95, 161.35)	131.42	(116.31, 162.97)	134.03	(122.37, 158.42)
34	140.80	(128.24, 166.85)	160.72	(142.24, 199.29)	150.86	(137.74, 178.32)
35	189.26	(175.07, 224.27)	180.16	(159.45, 223.40)	190.67	(174.08, 225.37)
36	150.72	(137.91, 178.60)	171.01	(151.34, 212.05)	164.25	(149.96, 194.14)
37	253.76	(232.19, 300.71)	239.46	(211.93, 296.94)	237.78	(217.09, 281.05)
38	83.00	(75.95, 99.19)	69.20	(61.24, 85.81)	74.04	(67.60, 87.52)
39	112.77	(98.17, 133.63)	130.88	(115.83, 162.29)	121.87	(111.27, 144.05)
40	148.64	(134.22, 176.14)	165.70	(146.64, 205.46)	154.52	(134.07, 182.64)
41	71.23	(65.18, 84.41)	65.92	(58.34, 85.74)	67.39	(61.53, 87.66)
42	143.24	(131.06, 169.74)	130.14	(115.17, 161.37)	137.34	(125.39, 162.34)
43	167.70	(153.45, 198.72)	164.78	(145.83, 204.33)	171.89	(156.93, 203.17)
44	208.15	(190.46, 246.66)	221.41	(192.95, 274.55)	214.12	(195.49, 253.09)
45	144.28	(130.12, 170.97)	162.79	(144.07, 201.86)	158.11	(142.35, 186.89)
46	102.60	(93.88, 121.58)	97.64	(86.41, 121.07)	99.47	(90.81, 117.57)
47	107.40	(95.59, 127.27)	119.16	(105.46, 147.76)	112.69	(102.89, 133.20)
48	214.22	(194.01, 253.85)	228.71	(195.41, 283.60)	217.44	(198.52, 257.01)
49	101.64	(93.00, 120.44)	109.90	(97.26, 136.27)	104.26	(95.18, 123.23)
50	127.03	(116.23, 150.53)	119.44	(105.71, 148.11)	122.72	(112.04, 145.05)

Table 3.4.5: Prediction of the residual life at the 90th percentile of lifetimes.

	Gamma		Lognormal		Weibull	
Bearing	Mean	95% CI	Mean	95% CI	Mean	95% CI
26	224.64	(213.65, 243.36)	235.35	(222.53, 252.53)	229.13	(217.73, 247.46)
27	95.31	(89.49, 104.97)	91.96	(85.73, 98.67)	93.90	(88.05, 101.41)
28	159.95	(151.55, 174.14)	174.09	(164.08, 186.79)	162.52	(153.86, 175.52)
29	160.74	(150.31, 174.99)	170.58	(160.73, 183.02)	159.28	(150.75, 172.02)
30	218.49	(207.75, 236.78)	207.93	(196.37, 223.11)	214.06	(203.28, 231.18)
31	80.78	(75.54, 89.42)	84.94	(79.03, 91.13)	84.78	(79.30, 91.5)
32	142.30	(134.61, 155.26)	146.75	(138.00, 157.46)	136.30	(128.70, 147.19)
33	145.04	(137.24, 158.19)	141.37	(132.87, 151.68)	143.50	(135.61, 154.98)
34	139.20	(129.63, 151.94)	153.09	(144.05, 164.26)	145.02	(137.07, 156.62)
35	215.07	(204.46, 233.11)	194.27	(183.33, 208.44)	208.86	(198.29, 225.56)
36	135.68	(128.25, 148.17)	145.20	(136.52, 155.80)	139.67	(131.94, 150.84)
37	278.69	(265.54, 301.19)	268.39	(254.04, 287.97)	254.37	(241.93, 274.71)
38	94.50	(88.72, 104.11)	87.68	(81.65, 94.08)	91.64	(85.88, 98.97)
39	103.69	(97.54 , 113.95)	105.75	(98.89, 113.47)	103.65	(97.40, 111.94)
40	134.16	(126.79, 146.55)	151.28	(142.32, 162.32)	143.40	(135.52, 154.87)
41	79.06	(73.90, 87.59)	74.17	(68.76 , 79.58)	77.01	(71.85, 83.16)
42	157.81	(149.50, 171.85)	147.65	(138.86, 158.43)	153.55	(145.25, 165.83)
43	181.93	(172.65, 197.65)	171.91	(162.00, 184.46)	177.73	(168.43, 191.94)
44	193.29	(183.56, 209.81)	203.56	(192.20, 218.42)	197.60	(187.49, 213.40)
45	138.32	(130.79, 151.00)	144.92	(136.25, 155.49)	141.09	(133.30, 152.37)
46	113.65	(107.10, 124.60)	108.26	(101.28, 116.15)	117.39	(110.57, 126.77)
47	95.35	(89.54, 105.02)	104.46	(97.66, 112.08)	99.17	(93.10, 107.10)
48	201.81	(191.73, 218.93)	215.68	(203.76, 231.42)	206.46	(195.99, 222.98)
49	111.91	(105.43, 122.74)	105.36	(98.51, 113.04)	103.74	(97.48, 112.04)
50	141.01	(133.37, 153.87)	147.58	(138.79, 158.34)	142.89	(135.03, 154.32)

Table 3.4.6: Average prediction error at the 50th and 90th percentiles of lifetimes.

	Gamma	Weibull	Lognormal
50th percentile	18.25%	20.75%	23.56%
90th percentile	3.01%	4.71%	6.21%
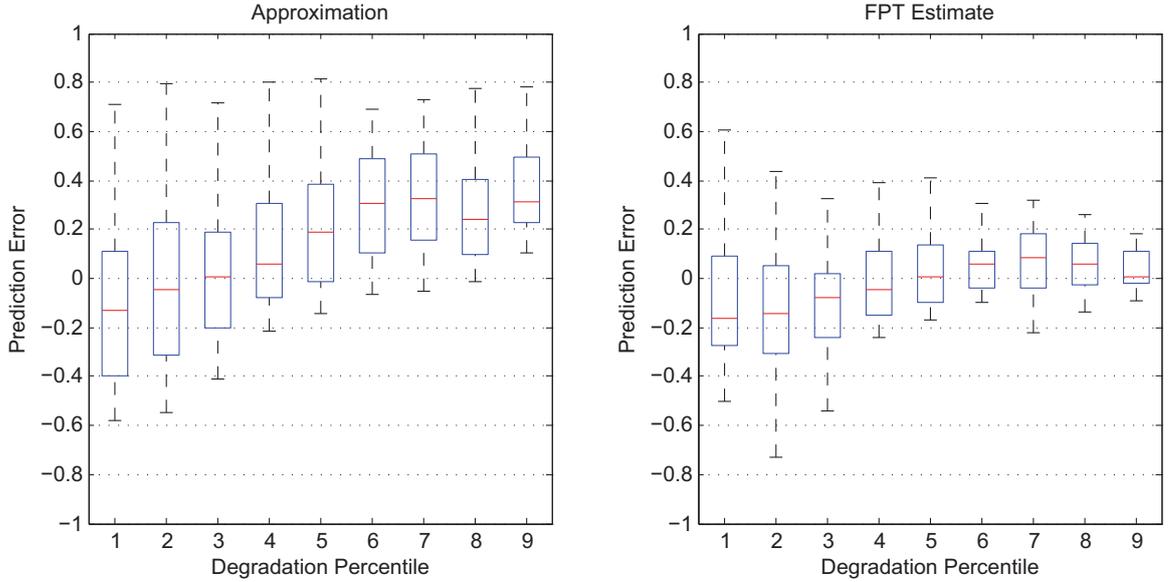
Figure 3.4.1: Prediction Error of Bearings 26 to 50.

3.4.3 Benchmark Model

Based on our previous analysis, the degradation model where κ and σ^2 follow the Gamma distribution and the inverse Gamma distribution respectively results in the highest accuracy of prediction. Next, we compare the performance of this model with a benchmark degradation model, the degradation model presented in [47], where the RLD at time t_k is evaluated using the following expression,

$$\mathbb{P}(R_k < t | s(t_k)) = \mathbb{P}(S(t_k + t) > D | s(t_k)) \tag{3.4.1}$$

Note that expression (3.4.1) does not necessarily represent the distribution of the first time that the degradation signal crosses the failure threshold. Consequently, the RLD calculated using this expression is an approximation. The approximation works well for degradation signals whose signal-to-noise ratio is high, thus, it is limited only to applications that exhibit degradation signals that have a high signal-to-noise ratio. Similar approximations have been widely presented in existing literature, such as [84].

The benchmark model is applied to the validation bearings, bearings 26 to 50. We calculate prediction error in a similar manner to that presented in the simulation study. The results are presented in the left plot of Figure 3.4.1. The prediction error calculated using our FPT approach are also shown in the right plot of Figure 3.4.1. We note that our FPT approach provides a reasonably accurate prediction of the residual life compared to the benchmark model. The benchmark method performs relatively poorly due to the fact that the signal-to-noise ratio for the bearing degradation signals is low, $\frac{\mathbb{E}(\kappa)}{\sigma} = 0.09$.

CHAPTER IV

DEGRADATION MODELING FOR REAL-TIME ESTIMATION OF RESIDUAL LIFETIMES IN DYNAMIC ENVIRONMENTS

In this chapter, we develop a stochastic methodology for modeling degradation signals from components functioning under dynamically-evolving environmental conditions. We utilize in-situ sensor signals related to the degradation process, as well as the environmental conditions, to predict and continuously update, in real-time, the distribution of a component's residual lifetime. Our models assume that the real-time rate at which a system's degradation signal increases (or decreases) is affected by the severity of the current environmental or operational conditions. In addition, we account for the reality that transitions in the environmental and operational conditions may induce upward or downward jumps in the amplitude of the degradation signal, depending on the nature of the changes. To estimate residual life distributions (RLDs), we consider two cases, both of which take into consideration the future characteristics of the environmental conditions. In the first case, we assume the component operates in a dynamic environment that transitions between distinct states and follows a deterministic profile, (i.e., there is no uncertainty about how the environment transitions in the future). This case is appropriate when the component experiences conditions that might occur in a cyclic manner. As an example of such a scenario, consider the rotational speed and thrust profiles that a jet engine experiences during the take-off, cruising, and landing cycles. The second case also assumes dynamic environmental or operating conditions but allows for the future environmental profile to be uncertain. Specifically, the transition times and dwell times in each distinct environmental state are stochastic and characterized using a continuous-time Markov chain model. This case may be appropriate for systems that are exposed to uncertain environments, such as weather conditions. For example, the velocity of wind as it relates to the productivity of wind turbines, or temperature and humidity changes as they relate to electronic components in aircraft avionics systems. For both cases, we propose a stochastic model for characterizing the degradation signal of the component and use this model to predict the residual lifetime by estimating the distribution of the first-passage time of the signal to a critical degradation threshold. Our approach is unique in that it unites historical data of a population of similar components with real-time sensor data that updates the residual life distribution dynamically.

The remainder of this chapter is organized as follows. Section 4.1 describes the first of our models which assumes the environment or operating conditions evolve dynamically, but in a deterministic manner. Section 4.2 extends the model of Section 4.1 by allowing the environment to

evolve in an uncertain manner. In Section 4.3, we describe a number of simulation studies to compare the results of our models with other existing in the current literature. We also illustrate the effectiveness of our models via a case study using real empirical data.

4.1 Degradation in a Deterministic, Dynamic Environment

In this section, we present the first of two degradation models and a procedure for estimating the residual life distribution (RLD) of the component in real time via Bayesian updating. Here, we assume that the environment is temporally dynamic but deterministic. This model forms the foundation of the model of Section 4.2, which considers a dynamic, randomly-varying environment. We begin with an elucidation of the notation and a few preliminaries.

For each $t \geq 0$, let $S(t)$ be the degradation signal at time t and let $S(0)$ be the initial signal observation. It is assumed that a population of identical components begins with the same initial degradation signal. At any time $t \geq 0$, the component's environment can occupy one of the states in a set $\mathcal{S} = \{1, 2, \ldots, m\}$, $m < \infty$. Deciding the appropriate number of environment states m, and a meaningful ordering of the states in $\mathcal{S}$, are important aspects of our modeling framework discussed in the following subsection. Let $\psi : [0, \infty) \to \mathcal{S}$ be an $\mathcal{S}$-valued *deterministic*, piecewise constant function so that $\psi(t)$ is the state of the environment at time t. That is, the environment visits the states in $\mathcal{S}$ in a deterministic way. Denote by $r(\psi(t))$ the component's rate of degradation at time t, i.e., whenever $\psi(t) = j \in \mathcal{S}$, the component degrades at rate $r(j)$. The rate function $r : \mathcal{S} \to \mathbb{R}$ is not restricted to the positive half-line (i.e., there are environment states for which the degradation signal exhibits a decreasing trend). Finally, we account for the reality that in typical applications, the degradation signal exhibits jumps at environment transition epochs. Therefore, we define a mapping $J : \mathcal{S} \to \mathbb{R}$ so that $J(\psi(v))$ is a function of the jump (either upward or downward) that occurs at time v. Specifically, for these models, the jump magnitude is a deterministic quantity that depends on the environment state just before and just after the jump epoch. The mapping J can assume a variety of forms; however, in this research we assume that the jump magnitude is proportional to the current state of the environment.

With these definitions and notation, the model of the degradation signal is

$$S(t) = S(0) + \int_0^t r(\psi(v))\mathrm{d}v + J(\psi(v)) + \sigma W(t), \qquad (4.1.1)$$

49

where $\{W(t) : t \geq 0\}$ is a standard Brownian motion (BM) process and σ ($\sigma > 0$) is its diffusion parameter. That is, for each $t \geq 0$, $\sigma W(t) \sim \mathcal{N}(0, \sigma^2 t)$ where $\mathcal{N}(a, b)$ denotes a normal random variable with mean a and variance b. This term models degradation effects that cannot be attributed to the environment process. The component's time to failure corresponds to the first time the degradation signal $\{S(t) : t \geq 0\}$ crosses a fixed, deterministic threshold D, i.e., the failure time, T_D, is the first passage time,

$$T_D = \inf\{t > 0 : S(t) \geq D\}.$$

Figure 4.1.1 depicts a sample path of the degradation signal $\{S(t) : t \geq 0\}$ and illustrates the effect of the deterministic environment on its evolution.
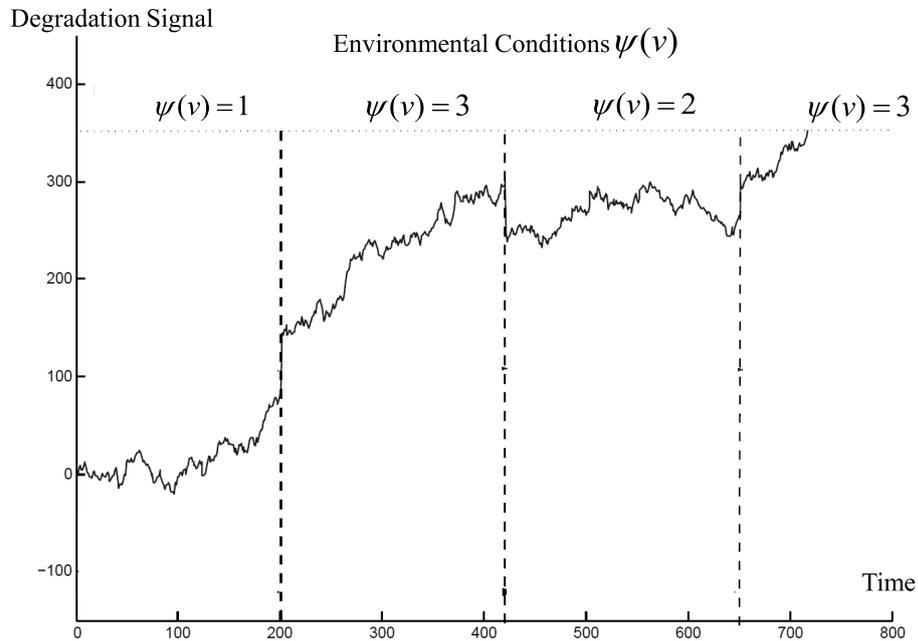
Figure 4.1.1: A sample path of degradation signals.

The primary objective of this work is to provide a framework for dynamically updating the remaining life distribution of the component based on discrete observations of the signal process $S(t)$ over time. Specifically, given a sequence of $k + 1$ realized signal observations, $\{s(t_i) : i = 0, 1, 2, \ldots, k\}$, let R_k denote the remaining time needed for the signal to first reach the threshold D, given the set of signal observations up to time t_k. Our aim is to estimate the distribution of R_k,

namely

$$\mathbb{P}(R_k \leq t - t_k \,|\, s(t_1), s(t_2), \ldots, s(t_k)), \quad t > t_k.$$

The novelty of our approach is the updating of the residual life distribution using real-time sensor data to dynamically estimate parameters of the signal model $S(t)$ within a Bayesian framework. This distinguishes our hybrid stochastic model from other failure models that either do not update parameter estimates in real time, or do not consider the evolution of the environment and its effects on the component. Next, we show how to use the signal and environment observations to dynamically estimate the residual life distribution of the component as it degrades over time.

4.1.1 Bayesian Updating of the Signal

In this subsection, we describe our Bayesian approach for updating the degradation model using prior information estimated from historical data in conjunction with real-time degradation signal observations obtained from a fielded component. For many applications, a historical database of degradation signals and environmental conditions is available for the estimation of prior information. However, even identical components can exhibit significant differences due to variations in the components' quality, etc. By combining both historical and real-time data, we are able to account for these inherent differences. The real-time updating of the degradation signal $S(t)$ hinges upon the updating of the degradation rate function r, the mapping J, and the drift parameter σ. Let us denote the joint prior distribution of (r, J, σ) by $\pi_s(r, J, \sigma)$ where we suppress the dependence of r and J on the environment state $\psi(t)$ for notational convenience. By monitoring in real time the degradation signal of a fielded component (via sensors), along with the current state of the environment, we will update the prior distribution π_s.

Suppose the degradation signal is monitored at times $t_0, t_1, \ldots, t_k$ such that $0 = t_0 < t_1 < \cdots < t_k$, and let $s(t_i)$ denote the observed signal at observation time t_i (the ith observation epoch). The set of observations will represented by a vector $s_k \in \mathbb{R}^{k+1}$, where $s_k = (s(0), s(t_1), \ldots, s(t_k))'$. Additionally, we must observe the magnitude of jumps occurring at environment transition epochs. Therefore, in addition to the vector s_k, we observe the ordered pairs, $\{(v_j, \psi(v_j^+)) \,:\, j = 1, 2, \ldots, n(t_k)\}$, where v_j is the time of the nth environment transition, $\psi(v_j^+))$ is the state of the environment just after the jth environment transition where for some $\epsilon > 0$, $v_j^+ = \lim_{\epsilon \downarrow 0} v_j + \epsilon$, and $n(t_k)$ is the cumulative number

51

of environment transitions up to time t_k. Using this convention, the environment maintains state u_i over the interval $[v_{i-1}, v_i)$, $i = 1, 2, \ldots n(t_k)$.

Next, we denote the likelihood function of the degradation signal by $f_s(s_k|r, J, \sigma)$. In the basic Bayesian framework, the posterior distribution of (r, J, σ) is computed by

$$\nu_s(r, J, \sigma|s_k) = \pi_s(r, J, \sigma)f_s(s_k|r, J, \sigma). \tag{4.1.2}$$

4.1.2 Estimating the Residual Life Distribution With Discrete Environmental States

When the future environmental profile is deterministic, the distribution of the residual life can be obtained using boundary crossing probabilities for a standard Brownian motion (BM) process. In particular, we consider a boundary that is piecewise linear over an interval $[0, T]$. We decompose the degradation signal into its deterministic and stochastic components, respectively so that

$$S(t) = \zeta(t) + \sigma W(t),$$

where $\zeta(t) \equiv s(0) + \int_0^t r(\psi(v))\mathrm{d}v + J(\psi(v))$ is the deterministic portion of the signal, and $\sigma W(t)$ is the stochastic component. The probability that the signal is below the threshold D at time t is given by

$$\mathbb{P}(S(t) < D) = \mathbb{P}(\sigma W(t) < D - \zeta(t)),$$

where, by virtue of our modeling framework, the function $D - \zeta(t)$ is linear in t. For convenience, we denote this function by $d(t) = D - \zeta(t)$, where the slope of $\zeta(t)$ is $r(\psi(t))$. The probability that the degradation signal does not exceed D on $[0, T]$ is equivalent to the complementary probability that a standard BM process crosses a linear boundary whose slope depends explicitly on the current environment state.

Boundary crossing probabilities for BM processes have been well-studied in the literature (cf. [117, 128]). For instance, if the function $d(t)$ is linear on $[0, T]$, [117] derived the (conditional) probability that a BM process crosses the linear boundary in this interval. This result was extended to piecewise linear functions without jump discontinuities on $[0, T]$ by [128] . Theorem 4.1.1 below extends Theorem 1 of [128] to consider the case when the function $d(t)$ is piecewise linear with jump discontinuities at finitely-many deterministic points. To this end, partition the interval $[0, T]$ so that $[0, T] = \bigcup_{j=1}^{n}[v_{j-1}, v_j)$, where v_j denotes the time of the nth jump in the signal process. It is

52

important to note that both upward and downward jumps can occur. Therefore, to simplify notation in Theorem 4.1.1, let $m_j \equiv \min\{d_j, d_j^-\}$ where $d_j = d(v_j)$ and $d_j^- = d(v_j^-)$, $j = 0, 1, \ldots, n$, and let $\boldsymbol{d} = (d_1, d_2, \ldots, d_n)'$.

Theorem 4.1.1. *Let $0 = v_0 < v_1 < \cdots < v_n = T$ denote n fixed jump times and suppose $d(v)$ is linear on $[v_{j-1}, v_j)$, $j = 1, 2, \ldots, n$ with $d(0) > 0$. Then for each $v \in [0, T]$, the complement of the crossing probability of a Brownian motion process, $\sigma W(v)$, with diffusion parameter σ is given by*

$$\mathbb{P}(\sigma W(v) < d(v)) = \mathbb{E}\left[h(W(v_1), W(v_2), \ldots, W(v_n); \boldsymbol{d})\right], \tag{4.1.3}$$

where

$$h(x_1, x_2, \ldots, x_n; \boldsymbol{d}) = \prod_{j=1}^{n} \mathbf{1}(x_j < m_j/\sigma)\Delta(v_j, v_{j-1}),$$

with

$$\Delta(v_j, v_j - 1) = 1 - \exp\left[-\frac{2[d_{j-1}/\sigma - x_{j-1}]\,[d_j^-/\sigma - x_j]}{v_j - v_{j-1}}\right],$$

and $\mathbf{1}(A)$ is the indicator function for condition A.

Proof. The proof is similar to that of Theorem 1 of [128] except that we include jump discontinuities at the interval boundaries. For a single linear boundary on the interval $[0, T]$ of the form $d(v) = av + b$, [117] proved that the (conditional) probability that a standard BM process does not cross the boundary in this interval is given by

$$\mathbb{P}(W(v) < av + b, v < T | W(T) = x) = 1 - \exp\left[-\frac{2b(aT + b - x)}{T}\right].$$

For our model, we have

$$\begin{aligned}
\mathbb{P}(\sigma W(v) < d(v), v \le T) &= \mathbb{P}\left(W(v) < \frac{d(v)}{\sigma}, v \le T\right) \\
&= \int_{-\infty}^{m_1/\sigma} \mathbb{P}\left(W(v) < \frac{d(v)}{\sigma}, v < v_1 | W(v_1) = x_1\right) \\
&\quad \times \mathbb{P}\left(W(v) < \frac{d(v)}{\sigma}, v > v_1 | W(v_1) = x_1\right) d\mathbb{P}_{v_1}(x_1), \tag{4.1.4}
\end{aligned}$$

where

$$d\mathbb{P}_v(x) = \frac{1}{\sqrt{2\pi v}} \exp\left(-x^2/2v\right) dx,$$

i.e., $d\mathbb{P}_v(x)/dx$ is the probability density function of $W(v)$. The product of (4.1.4) holds since $\{W(t) : t \geq 0\}$ possesses the strong Markov property. Using the results of [117], the first term in the integrand of (4.1.4) is given by

$$\mathbb{P}\left(W(v) < \frac{d(v)}{\sigma}, v < v_1 | W(v_1) = x_1\right) = 1 - \exp\left[-\frac{2\frac{d_0}{\sigma}(\frac{d_1^-}{\sigma} - x_1)}{v_1}\right]$$

Owing to the fact that a standard BM process has stationary and independent increments, provided that $W(v_1) = x_1$, it is clear that $W(v + v_1) - x_1$ is also a BM process starting from the origin. Arguing along the same lines as [128], for any $v \in (v_1, T]$, the second term in the integrand of (4.1.4) is

$$\mathbb{P}\left(W(v) < \frac{d(v)}{\sigma} | W(v_1) = x_1\right) = \mathbb{P}\left(W(v) < \frac{d(v + v_1)}{\sigma} - x_1, v \leq T - v_1\right)$$

$$= \int_{-\infty}^{(m_2 - x_1)/\sigma} \left(1 - \exp\left[-\frac{2(\frac{d_1}{\sigma} - x_1)(\frac{d_2^-}{\sigma} - x_1 - x_2)}{(v_2 - v_1)}\right]\right)$$

$$\times \mathbb{P}\left(W(v) < \frac{d(v + v_1)}{\sigma} - x_1, v \in (v_2 - v_1, T - v_1) | W(v_2 - v_1) = x_2\right) d\mathbb{P}_{v_2 - v_1}(x_2)$$

$$= \int_{-\infty}^{m_2/\sigma} \left(1 - \exp\left[-\frac{2(\frac{d_1}{\sigma} - x_1)(\frac{d_2^-}{\sigma} - x_2)}{(v_2 - v_1)}\right]\right)$$

$$\times \mathbb{P}\left(W(v) < \frac{d(v + v_1)}{\sigma} - x_1, v \in (v_2 - v_1, T - v_1) | W(v_2 - v_1) = x_2 - x_1\right) d\mathbb{P}_{v_2 - v_1}(x_2 - x_1)$$

$$= \int_{-\infty}^{m_2/\sigma} \left(1 - \exp\left[-\frac{2(d_1/\sigma - x_1)(d_2^-/\sigma - x_2)}{(v_2 - v_1)}\right]\right)$$

$$\times \mathbb{P}\left(W(v) < \frac{d(v + v_2)}{\sigma} - x_2, v \leq T - v_2\right) d\mathbb{P}_{v_2 - v_1}(x_2 - x_1).$$

Now, similar steps can be followed to obtain the probability

$$\mathbb{P}(W(v) < d(v + v_2)/\sigma - x_2, v \leq T - v_2) d\mathbb{P}_{v_2 - v_1}(x_2 - x_1).$$

Repeating these steps in an inductive manner, one obtains

$$\mathbb{P}\left(W(v) < \frac{d(v)}{\sigma}, v_{n-1} < v \leq T\right)$$

$$= \int_{-\infty}^{m_n/\sigma} \left(1 - \exp\left[-\frac{2(\frac{d_{n-1}}{\sigma} - x_{n-1})(\frac{d_n^-}{\sigma} - x_n)}{v_n - v_{n-1}}\right]\right) d\mathbb{P}_{v_n - v_{n-1}}(x_n - x_{n-1}).$$

where for $j = 1, 2, \ldots, n$ and $x_0 = 0$,

$$d\mathbb{P}_{v_j - v_{j-1}}(x_j - x_{j-1}) = \frac{1}{\sqrt{2\pi(v_j - v_{j-1})}} \exp\left[-\frac{(x_j - x_{j-1})^2}{2(x_j - x_{j-1})}\right] dx_j$$

54

since $\{W(t) : t \geq 0\}$ is a BM process. Finally, due to the independent increments property, we obtain

$$\mathbb{P}(W(v) < d(v)/\sigma, \, v \leq T) = \int_{-\infty}^{\frac{m_1}{\sigma}} \cdots \int_{-\infty}^{\frac{m_n}{\sigma}} \prod_{j=1}^{n} \left(1 - \exp\left[\frac{(d_{j-1}/\sigma - x_{j-1})(d_j^-/\sigma - x_j)}{v_j - v_{j-1}}\right]\right) g(\boldsymbol{x}) \mathrm{d}\boldsymbol{x}$$

(4.1.5)

where $\boldsymbol{x} = (x_1, x_2, \ldots, x_n)'$, and

$$g(\boldsymbol{x}) = \prod_{j=1}^{n} \frac{1}{\sqrt{2\pi(v_j - v_{j-1})}} \exp\left[-\frac{(x_j - x_{j-1})^2}{2(v_j - v_{j-1})}\right].$$

The result follows directly by noting that $g(\boldsymbol{x})$ is the probability density function of the random vector $(W(v_1), W(v_2), \ldots, W(v_n))$. □

Suppose the degradation signal has been sampled at k distinct times, $t_1, t_2, \ldots, t_k$, and the current time is $t_k < T$. The (deterministic) process, $\{\psi(t) : t_k < t \leq T\}$, is the future environmental profile from time t_k up to some future time T. On the interval $(t_k, T]$, the deterministic component of the degradation signal is

$$\zeta^k(v) \equiv s(t_k) + \int_{t_k}^{T} r(\psi(v)) \mathrm{d}v + J(\psi(T)) - J(\psi(t_k)).$$

(4.1.6)

Define by R_k the residual life of the component at time t_k, given that the degradation signal has not crossed the threshold on the interval $[0, t_k]$. Applying equation (4.1.3) of Theorem 4.1.1, the distribution of R_k is given by

$$\mathbb{P}(R_k \leq T | \boldsymbol{s}_k) = 1 - \mathbb{E}[h(W(v_1), W(v_2), \ldots, W(v_n); \boldsymbol{d}_k)]$$

(4.1.7)

where $v_1, v_2, \ldots, v_n$ are the transition epochs of the environment process $\{\psi(t) : t_k < t \leq T\}$ and $\boldsymbol{d}_k$ indicates the dependence of $\boldsymbol{d}$ on the observation time t_k.

Equation (4.1.7), though simple in form, is not easy to compute due to the multidimensional integration requirement of (4.1.3). To circumvent this integration, we propose a Monte-Carlo simulation approach to estimate $\mathbb{E}[h(W(v_1), W(v_2), \ldots, W(v_n); \boldsymbol{d})]$. The steps of the procedure are as follows:

Step 1: Select a sufficiently large number of realizations M' for the n-dimensional Brownian motion process $(W(v_1), \ldots, W(v_n))$, say $M' = 5000$;

Step 2: For each $j \in \{1, 2, \ldots, M'\}$, generate n independent normal random variables, say $X_1, X_2, \ldots, X_n$ such that for $i = 1, \ldots, n$, $X_i \sim \mathcal{N}(0, \sigma^2(v_i - v_{i-1}))$ with $v_0 \equiv 0$, and $w_i^j = \sum_{k=1}^{i} X_k$, for i=1,2,...,n. The vector $(w_1^j, \ldots, w_n^j)$ is the jth realization of $(W(v_1), \ldots, W(v_n))$.

Step 3: By applying the strong law of large numbers (SLLN), for sufficiently large M', we can estimate the residual lifetime distribution at time t_k by

$$\mathbb{P}(R_k \leq T | s_k) \approx 1 - \frac{1}{M'} \sum_{j=1}^{M'} h(w_1^j, \ldots, w_n^j; \boldsymbol{d}_k).$$

4.1.3 Estimating the Residual Life Distribution With Continuous Environmental States

When the future environmental condition evolves continuously, the RLD can be obtained using boundary crossing probabilities for a standard Brownian motion (BM) process with a continuous boundary. For a linear boundary, the first-passage-time of a Brownian motion process follows an inverse Gaussian distribution. However, the crossing boundary is generally not linear unless the environmental condition remains constant. In what follows, we approximate the RLD for a general continuous boundary using the techniques of tangent approximation developed by [33].

We decompose the degradation signal into its deterministic and stochastic components, respectively so that

$$S(t) = \zeta(t) + \gamma B(t),$$

where $\zeta(t) = S(0) + \int_0^t r(w(v)) dv$ is the deterministic portion of the signal, and $\gamma B(t)$ is the stochastic component. The probability that the signal is below the threshold D at time t is given by

$$\mathbb{P}\left(\max_{0 \leq v \leq t} S(v) < D\right) = \mathbb{P}\left(B(v) < \frac{D - \zeta(v)}{\gamma}, \text{ for } 0 \leq v \leq t\right),$$

where, by virtue of our modeling framework, the function $\frac{D - \zeta(t)}{\gamma}$ is a continuous function of t. For convenience, we denote this function by $d(t) = \frac{D - \zeta(t)}{\gamma}$. As demonstrated in Figure 4.1.2, the probability that the degradation signal does not exceed D is equivalent to the complementary probability that a standard BM process crosses a boundary determined by $d(t)$. The plot on the left represents the original degradation signal and its failure threshold. The plot on the right represents the transformation that incorporates $\zeta(t)$ into the failure threshold.

56
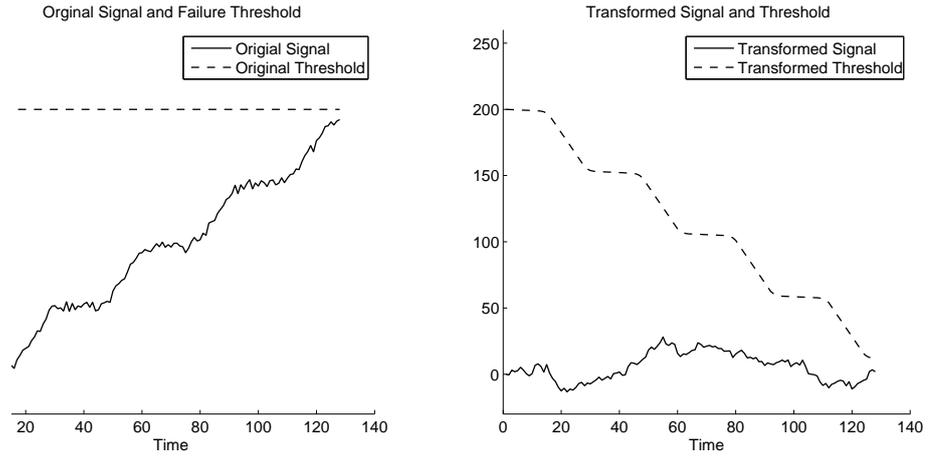
Figure 4.1.2: Relation between the RLD and the crossing probability of BM.

Estimating boundary crossing probabilities of BM processes for a curved boundary is generally very challenging. Very few exact solutions are available for specific boundaries. Even when a formula is known for a particular boundary the computation cost is very high. [33] studied the approximation of the first-passage-time (FPT) distribution of a standard Wiener process to a general boundary. Since the exact representation of this crossing probability is generally unavailable, [33] approximated the density of the FPT by using the tangent of the boundary, which is a linear function. In this case, the probability density function of the FPT is evaluated using an inverse Gaussian distribution. [33] demonstrated with numerical studies that the tangent approximation has promising performance for many continuous boundaries. Theorem 4.1.2 utilizes the tangent approximation to assesses the residual life distribution in our degradation model by estimating the equivalent distribution of the FPT.

Theorem 4.1.2. *Let R_k represent the residual lifetime of a unit at time t_k. We denote by $s(t_k)$ the observation of the signal amplitude at time t_k. Then the probability density function of R_k, denote by $g_k(t)$ is expressed as follows*

$$g_k(t) \approx \frac{a_{k,t}}{\sqrt{2\pi t^3}} \exp\left[-2a_{k,t}b_{k,t} - \frac{(d_k(t) - 2a_{k,t})^2}{2t}\right], \ where \qquad (4.1.8)$$

$$d_k(t) = \frac{1}{\gamma}\left[D - s(t_k) - \int_{t_k}^{t+t_k} r(w(v))\mathrm{d}v\right],$$

$$b_{k,t} = -\frac{r(w(t))}{\gamma}, \ and$$

$$a_{k,t} = d_k(t) + \frac{r(w(t))}{\gamma}t.$$

Proof. For any given $t > 0$, the distribution of residual life R_k is expressed as follows

$$\mathbb{P}(R_k < t) = \mathbb{P}\left(\max_{0 \le v \le t}\left[s(t_k) + \int_{t_k}^{t_k+v} r(w(u))\mathrm{d}u + \gamma B(v)\right] > D\right).$$

$s(t_k) + \int_{t_k}^{t_k+v} r(w(u))\mathrm{d}u$ represents the deterministic part of the degradation signal. We incorporate this term in the failure threshold, as shown in Figure 4.1.2, and rewrite the distribution of R_k as follows

$$\mathbb{P}(R_k > t) = \mathbb{P}\left(B(v) < d_k(v), \ for \ 0 \le v \le t\right),$$

where

$$d_k(t) = \frac{1}{\gamma}\left[D - s(t_k) - \int_{t_k}^{t+t_k} r(w(u))\mathrm{d}u\right]$$

represents the transformed boundary corresponding to standard Wiener process $B(t)$ when the current time is t_k. Subsequently, we estimate the probability density function of R_k by approximating $d_k(v)$ using its tangent. We denote by $\tilde{d}_{k,t}(\cdot)$ the tangent of $d_k(v)$ at $v = t$. The existence of $\tilde{d}_{k,t}(\cdot)$ for any $t > 0$ is guaranteed by the continuity in the environmental profile. Since environmental state $w(v)$ is a continuous function, $d_k(t)$ is differentiable for any $t > 0$.

We assume that for any given t

$$\tilde{d}_{k,t}(v) = a_{k,t} + b_{k,t}v,$$

where $a_{k,t}$ and $b_{k,t}$ represent the intercept and the slope of $\tilde{d}_{k,t}(\cdot)$, respectively. $b_{k,t}$ and $a_{k,t}$ are computed as follows

$$b_{k,t} = \left.\frac{\mathrm{d}}{\mathrm{d}v}d_k(v)\right|_{v=t} = -\frac{r(w(t))}{\gamma},$$

$$a_{k,t} = \tilde{d}_{k,t}(t) - b_{k,t}t = d_k(t) + \frac{r(w(t))}{\gamma}t.$$

58

According to [33], we approximate $g_k(t)$ using the pdf of the first-passage-time when the crossing boundary is represented by $\tilde{d}_{k,t}(\cdot)$ for each given $t > 0$. In this case, $g_k(t)$ is approximated by the pdf of an inverse Gaussian distribution, which is expressed as follows

$$g_k(t) \approx \frac{a_{k,t}}{\sqrt{2\pi t^3}} \exp\left[-2a_{k,t}b_{k,t} - \frac{(d_k(t) - 2a_{k,t})^2}{2t}\right]$$

for $t > 0$. $\qquad\qquad\qquad\qquad\qquad\qquad\qquad\qquad\qquad\qquad\qquad\qquad\qquad\qquad$ $\square$

Remarks The cumulative density function of R_k given signal observations s_k is expressed as

$$\mathbb{P}(R_k < T|s_k) = \int_0^T g_k(t)\mathrm{d}t.$$

4.1.4 An Illustrative Example

We now illustrate how to compute the residual life distribution by describing a model with a specific form of the degradation rate function and the environment-dependent jump process. The rate of degradation, as a function of the environment state, is given by

$$r(\psi(v)) = \alpha\psi(v) + \beta,$$

and the impact of jumps is captured by the function

$$J(\psi(v)) = \eta\,\psi(v),$$

where α, β and η are parameters of the degradation signal model as is σ, the diffusion coefficient. The prior marginal distributions of these parameters are as follows: $\alpha \sim \mathcal{N}(\mu_1, \sigma_1^2)$, $\beta \sim \mathcal{N}(\mu_2, \sigma_2^2)$, $\eta \sim \mathcal{N}(\mu_3, \sigma_3^2)$, and $\sigma \sim \mathcal{N}(\mu_4, \sigma_4^2)$. The parameters are assumed to be mutually independent random variables. To estimate the posterior distribution of $(\alpha, \beta, \eta, \sigma)$, or equivalently of (r, J, σ), we next derive the likelihood function of degradation model. The likelihood function of s_k, conditioned on the parameter vector $(\alpha, \beta, \eta, \sigma)$, is denoted by

$$L(s_k|\alpha, \beta, \eta, \sigma) = \prod_{i=1}^{k} \phi_i(s(t_i) - s(t_{i-1}))$$

where ϕ_i is the probability density function of a normal distribution with mean

$$\int_{t_{i-1}}^{t_i} [\alpha + \beta\psi(v)]\mathrm{d}v + \eta\,(\psi(t_i) - \psi(t_{i-1}))$$

59

and variance $\sigma^2(t_i - t_{i-1})$. To simplify notation, let $\mathcal{G}_{t_k} = \{\psi(v) : 0 \leq v \leq t_k\}$. The posterior distribution of $(\alpha, \beta, \eta, \sigma)$ is

$$v_s(\alpha, \beta, \eta, \sigma | s_k, \mathcal{G}_{t_k}) = \pi_s(\alpha, \beta, \eta, \sigma) \times \prod_{i=1}^{k} \phi_i(s(t_i) - s(t_{i-1}))$$

where $\pi_s(\alpha, \beta, \eta, \sigma) = \varphi_1(\alpha)\varphi_2(\beta)\varphi_3(\eta)\varphi_4(\sigma)$, and $\varphi_i(x) = \frac{1}{\sqrt{2\pi\sigma_i^2}} \exp\left[-\frac{(x-\mu_i)^2}{2\sigma_i^2}\right]$, for $i = 1, 2, 3, 4$.

The updated residual life distribution at time t_k is given by

$$
\begin{aligned}
\mathbb{P}(R_k \leq T | s_k, \mathcal{G}_{t_k}) &= \int_{\alpha,\beta,\eta,\sigma} \mathbb{P}(R_k \leq T | s_k) \times v_s(\alpha, \beta, \eta, \sigma | s_k, \mathcal{G}_{t_k}) \\
&= \int_{\alpha,\beta,\eta,\sigma} \mathbb{P}(R_k \leq T | s_k) \prod_{i=1}^{k} \phi_i(s(t_i) - s(t_{i-1}))\pi_s(\alpha, \beta, \eta, \sigma) \\
&= \mathbb{E}_{\pi_s}\left[\mathbb{P}(R_k \leq T | s_k) \prod_{i=1}^{k} \phi_i(s(t_i) - s(t_{i-1}))\right], \qquad (4.1.9)
\end{aligned}
$$

where $\mathbb{E}_{\pi_s}$ is the expectation operator with respect to the measure π_s. In a manner similar to that described for estimating $\mathbb{P}(R_k \leq T | s_k)$, equation (4.1.9) can be estimated using Markov chain Monte-Carlo (MCMC) techniques. Specifically, a sufficiently large number (say M') of realizations of $(\alpha, \beta, \eta, \sigma)$ can be simulated from the joint density $\pi_s(\alpha, \beta, \eta, \sigma)$ in order to estimate the corresponding values of

$$\mathbb{P}(R_k \leq T | s_k) \prod_{i=1}^{k} \phi_i(s(t_i) - s(t_{i-1})).$$

Applying the SLLN, for sufficiently large M', the updated RLD is estimated by

$$\mathbb{P}(R_k \leq T | s_k, \mathcal{G}_{t_k}) \approx \frac{1}{M'} \sum_{(\alpha,\beta,\eta,\sigma)} \left[\mathbb{P}(R_k \leq T | s_k) \prod_{i=1}^{k} \phi_i(s(t_i) - s(t_{i-1}))\right].$$

Numerical examples illustrating the quality of these estimates will be provided in Section 5. However, in Section 4.2 we first describe a more general model that allows the environment to evolve randomly over time.

4.2 Randomly-Varying Environment

While the model of Section 4.1 is potentially useful for environments that change deterministically, it cannot be applied to scenarios in which the fielded component operates in a randomly-varying conditions. Therefore, we now present a generalization of the model of Section 4.1 to account for an uncertain future environmental profile.

In the spirit of the model studied by [62], we denote by $U(t)$ the state of the environment at time t and assume that $\{U(t) : t \geq 0\}$ is an ergodic, finite continuous-time Markov chain (CTMC) on the state space $\mathcal{S} = \{1, 2, \ldots, m\}$. As before, the states in $\mathcal{S}$ are ordered by the level of severity so that $r(i) < r(j)$ if $i < j$. The CTMC has infinitesimal generator matrix Q and limiting distribution $\boldsymbol{p}$ satisfying

$$\boldsymbol{p}Q = \boldsymbol{0}, \quad \boldsymbol{p}\boldsymbol{e} = 1$$

where $\boldsymbol{0}$ is the zero vector of order m and $\boldsymbol{e}$ is a column vector ones. The degradation signal at time t is given by

$$S(t) = S(0) + \int_0^t r(U(v))\mathrm{d}v + J(U(v)) + \sigma W(t)$$

where the functions r and J are defined as in Section 4.1 as is $\sigma W(t)$. Moreover, we assume that

$$\int_0^t |r(U(v))|\mathrm{d}v < \infty, \quad t \geq 0$$

with probability 1 to ensure that the degradation path is well defined for each $t \geq 0$.

Whenever the environment occupies state i, it stays there for an exponentially-distributed time with parameter $q_i > 0$, where $q_i = -q_{ii} = \sum_{j \neq i} q_{ij}$, is the total rate of leaving state i. Let V_j denote the jth jump epoch of $\{U(t) : t \geq 0\}$ and define $U_j = U(V_j^+)$, the state of the environment just after the jth environment transition. The process $\{(U_j, V_j) : j \geq 0\}$ is a Markov renewal process; therefore, $\{U_j : j \geq 0\}$ is a discrete-time Markov chain (DTMC) with transition probability matrix $P = [p_{ij}]$ where p_{ij} is given by

$$p_{ij} = \begin{cases} \frac{q_{ij}}{q_i}, & \text{if } j \neq i, \\ 0, & \text{if } j = i. \end{cases}$$

4.2.1 Bayesian Updating Methodology

Similar to the deterministic environment model of Section 4.1, we propose a Bayesian methodology to update the parameters of $\{U(t) : t \geq 0\}$, as well as the degradation signal $\{S(t) : t \geq 0\}$, using prior information estimated from historical data and real-time degradation signals. Individual components may experience different types of environmental conditions, so we assume the parameters of the CTMC model (namely the non-negative off-diagonal elements of Q) are random. The (negative) diagonal elements follow directly from the fact that the row sums of Q are all zero. We will estimate

the prior distribution of the environment's generator matrix, Q, as well as (r, J, σ), the parameters of the degradation model.

To simplify notation in what follows, let $\boldsymbol{q} = \{q_{i,j} : i, j \in S, \ j \neq i\}$ be the set of off-diagonal elements of Q. The prior distribution of Q will be denoted by $\pi_Q(\boldsymbol{q})$, while the prior distribution of (r, J, σ) is again denoted by $\pi_s(r, J, \sigma)$. Consider an interval of time $[0, T]$ and assume the degradation signal has not crossed the threshold D by this time. The degradation signal is sampled at the discrete times $t_0, t_1, \ldots, t_k < T$ such that $0 = t_0 < t_1 < t_2 < \ldots < t_k$, and these observations are stored in the vector $\boldsymbol{s}_k = (s(0), s(t_1), s(t_2), \ldots, s(t_k))$ while the environment, $\{U(t) : t \geq 0\}$, is monitored continuously on the interval $[0, t_k]$ for some t_k. For $i, j \in S$, $j \neq i$, let $N_{i,j}(t_k)$ denote the number of environment transitions from state i to state j in the interval $[0, t_k]$, and let $R_i(t_k)$ be the total time spent by the environment in state i on this interval. It is well-known (cf. [21]) that for a continuously-monitored CTMC, the likelihood function of its infinitesimal generator matrix Q is given by

$$L(\boldsymbol{q}) = \prod_{i=1}^{m} \prod_{j \neq i} q_{i,j}^{N_{i,j}(t_k)} \exp\left[-q_{i,j} R_i(t_k)\right].$$

Our aim is to update the elements of Q using a Bayesian approach. To this end, we assume that the (i, j)th element of Q has a gamma prior distribution, i.e.,

$$q_{i,j} \sim \Gamma(k_{i,j}, \theta_{i,j}), j \neq i$$

where $k_{i,j}$ is the shape parameter and $\theta_{i,j}$ is the scale parameter of the gamma distribution. The probability density function of $q_{i,j}$ is

$$\frac{q_{i,j}^{k_{i,j}-1} \exp(-q_{i,j}/\theta_{i,j})}{\Gamma(k_{i,j})\theta_{i,j}^{k_{i,j}}}$$

We choose the gamma distribution as a prior distribution for a few pragmatic reasons. First, each of the off-diagonal elements of Q is a non-negative, real number. Second, the gamma distribution encompasses a number of important distributions including the exponential, Erlang, and chi-square distributions. Moreover, the shape and scale parameters can be chosen to model distributions with varying degrees of skewness. Finally, the gamma prior distribution results in a closed-form posterior distribution that facilitates easy implementation. By applying Bayes' formula, the posterior

distribution of Q, ν_Q, can be obtained by noting that

$$\nu_Q(\boldsymbol{q}|\mathcal{F}_{t_k}) \propto \pi_Q(\boldsymbol{q}) \times L(\boldsymbol{q})$$

where $\mathcal{F}_{t_k} = \{U(v) : 0 \le v \le t_k\}$ is the history of the environment process up to time t_k, and $n_{i,j}(t_k)$ and $r_i(t_k)$ are the realizations of $N_{i,j}(t_k)$ and $R_i(t_k)$, respectively. Theorem 4.2.1 establishes that the posterior distribution of $q_{i,j}$ also follows a gamma distribution and gives the explicit form of its parameters.

Theorem 4.2.1. *Suppose the environment process is observed continuously up to time t_k, that $N_{i,j}(t_k) = n_{ij}(t_k)$, and $R_i(t_k) = r_i(t_k)$ for $i, j \in S$ such that $j \ne i$. Then the posterior distribution of $q_{i,j}$ is the gamma distribution with parameters $(\tilde{k}_{i,j}, \tilde{\theta}_{i,j})$ where*

$$\tilde{k}_{i,j} = k_{i,j} + n_{i,j}(t_k), \text{ and } \tilde{\theta}_{i,j} = \left[\theta_{i,j}^{-1} + r_i(t_k)\right]^{-1}.$$

Proof. Let $\mathcal{F}_{t_k} = \{U(v) : 0 \le v \le t_k\}$ be the history of the environment process up to observation time t_k and suppose $N_{i,j}(t_k) = n_{i,j}(t_k)$ and $R_i(t_k) = r_i(t_k)$ during $[0, t_k]$. By applying Bayes' formula and the likelihood function $L(\boldsymbol{q})$, we can write

$$
\begin{aligned}
\nu_Q(\boldsymbol{q}|\mathcal{F}_{t_k}) \quad &\propto \quad \pi_Q(\boldsymbol{q})L(\boldsymbol{q}) \\
&= \quad \left(\prod_{i=1}^{m}\prod_{j\ne i} \frac{q_{i,j}^{k_{i,j}-1}\exp(-q_{i,j}/\theta_{i,j})}{\Gamma(k_{i,j})\theta_{i,j}^{k_{i,j}}}\right)\left(\prod_{j=1}^{m}\prod_{j\ne i} q_{i,j}^{n_{i,j}(t_k)} \exp\left[-q_{i,j}r_i(t_k)\right]\right) \\
&\propto \quad \left(\prod_{i=1}^{m}\prod_{j\ne i} q_{i,j}^{k_{i,j}+n_{i,j}(t_k)-1}\exp(-q_{i,j}(1/\theta_{i,j} + r_i(t_k)))\right)
\end{aligned}
$$

Therefore,

$$\nu_Q(\boldsymbol{q}|\mathcal{F}_{t_k}) = \prod_{i=1}^{m}\prod_{j\ne i} \frac{q_{i,j}^{\tilde{k}_{i,j}-1}\exp(-q_{i,j}/\tilde{\theta}_{i,j})}{\Gamma(\tilde{k}_{i,j})\tilde{\theta}_{i,j}^{\tilde{k}_{i,j}}}$$

where

$$\tilde{k}_{i,j} = k_{i,j} + n_{i,j}(t_k),$$

and

$$\tilde{\theta}_{i,j} = \left[\theta_{i,j}^{-1} + r_i(t_k)\right]^{-1}.$$

That is, the posterior distribution of $q_{i,j}$ is the gamma distribution with parameters $\tilde{k}_{i,j}$ and $\tilde{\theta}_{i,j}$. $\quad\square$

To update the signal model, we use a procedure analogous to the one described in Section 4.1. Using the same definitions in that section the posterior distribution of (r, J, σ) is

$$\nu_s(r, J, \sigma | \boldsymbol{s}_k) = \pi_s(r, J, \sigma) \times f_s(\boldsymbol{s}_k | r, J, \sigma).$$

The updated degradation model will be used together with the environment process to dynamically update the residual life distribution of the component.

4.2.2 Estimating the Residual Life Distribution

Here, we describe two separate schemes for estimating the residual life distribution for a system that degrades in a randomly-evolving environment. The first scheme is a sample path approach that simulates a large number of future environment profiles and applies the deterministic model of Section 4.1 to each of these profiles. The second approach uses the limiting distribution of $\{U(t) : t \geq 0\}$ to estimate the future environmental profile. The latter technique, while less computationally intensive, but may not adequately represent the environment's evolution in finite time.

4.2.2.1 Approach I: Sample Path Averaging

Suppose the environment is observed continuously on $[0, t_k]$. In this approach, we simulate the environment process $\{U(t) : t_k < t \leq T\}$ for some T. That is, we simulate the evolution of the environment starting from the observed environment state at time t_k until the end of some time horizon. Because each simulated sample path represents a single environmental profile (that behaves deterministically), we can estimate the residual life distribution for each profile independently using Theorem 4.1.1. Subsequently, the set of c.d.f.s are averaged to obtain the estimate of the RLD. The procedure is formalized as follows:

Step 1: Select the number of future environment profiles to simulate, I;

Step 2: Simulate I sample paths of the environment process on the interval $[t_k, T]$, i.e., simulate $\{U_i(t) : t_k < t \leq T\}$ for $i = 1, 2, \ldots, I$;

Step 3: For sample path i, obtain $\zeta_i(t_k)$, $i = 1, 2, \ldots, I$, using equation (4.1.6);

Step 4: For sample path i, compute the residual life distribution at time t_k by

$$\mathbb{P}_i(R_k \leq T | \boldsymbol{s}_k) = 1 - \mathbb{E}\left[h(W(v_1), \ldots, W(v_n); \boldsymbol{d}_k^i)\right], \quad i = 1, 2, \ldots, I,$$

using equation (4.1.7) and the simulation method described thereafter;

Step 5: For I sufficiently large, estimate the remaining life distribution at time t_k by

$$\mathbb{P}(R_k \leq T | \boldsymbol{s}_k) \approx I^{-1} \sum_{i=1}^{I} \mathbb{P}_i(R_k \leq T | \boldsymbol{s}_k).$$

Approach I allows us to consider a large number of potential future environment profiles that the component might encounter. However, this approach is computationally expensive as we must simulate a large number of these profiles, and the evolution of the stochastic component of the degradation signal.

4.2.2.2 *Approach II: Stationary Environment*

Approach II circumvents the need to simulate future profiles by assuming that the environment is operating in its limiting regime at observation time t_k. We estimate the residual lifetime at time t_k in two different ways, depending on the length of the time horizon.

Case 1: Let i_k be the observed state of the environment at time t_k (i.e., $U(t_k) = i_k$). Due to the memoryless property, the remaining time in state i_k, call it Y_{i_k}, is exponentially distribution with parameter q_{i_k}. Therefore, if $\mathbb{P}(Y_{i_k} \leq T - t_k) < \epsilon'$ for some tolerance value $\epsilon' > 0$, then we assume there are no environment transitions during $[t_k, T]$, and the current environment state serves to approximate the future environmental profile. In such case, the RLD has the inverse Gaussian distribution, i.e.,

$$\mathbb{P}(R_k \leq T | \boldsymbol{s}_k) \approx \Phi\left(\sqrt{\frac{\lambda_k}{T}}\left(\frac{T}{\vartheta_k} - 1\right)\right) + \exp\left(\frac{2\lambda_k}{\vartheta_k}\right)\Phi\left(-\sqrt{\frac{\lambda_k}{T}}\left(\frac{T}{\vartheta_k} + 1\right)\right)$$

where Φ is the standard normal c.d.f.,

$$\lambda_k = \frac{[D - s(t_k)]^2}{\sigma^2}, \quad \vartheta_k = \frac{D - s(t_k)}{r(i_k)},$$

and $s(t_k)$ and i_k are the signal and environment observations at time t_k, respectively. A reasonable tolerance value is $\epsilon' = 10^{-4}$.

Case 2: In case $\mathbb{P}(Y_{i_k} \leq T - t_k) > \epsilon'$, then assume the environment is operating in its limiting regime and partition $[t_k, T]$ into m disjoint intervals such that the fraction of $[t_k, T]$ spent in state i is p_i, the ith element of the stationary distribution $\boldsymbol{p}$, for each $i \in \mathcal{S}$. Note that the expected proportion of time is therefore $p_i(T - t_k)$. Therefore, we must consider the $m!$ different permutations of these intervals that correspond to $m!$ potential future environmental profiles.

65

For the ith permutation, compute the residual life distribution at time t_k by

$$\mathbb{P}_i(R_k \leq T | s_k) = 1 - \mathbb{E}\left[h(W(v_1), \ldots, W(v_n); \boldsymbol{d}_k^i)\right], \quad i = 1, 2, \ldots, m!,$$

using equation (4.1.7) and the simulation method described thereafter. Finally, we estimate the RLD using

$$\mathbb{P}(R_k \leq T | s_k) \approx \frac{1}{m!} \sum_{i=1}^{m!} \mathbb{P}_i(R_k \leq T | s_k).$$

The advantage of Approach II over Approach I is that it does not require simulation of the future environmental profiles, only enumeration of the $m!$ permutations and their resulting residual life distributions.

4.2.3 An Illustrative Example

Here, we illustrate the degradation model and Bayesian updating framework when the environment evolves as a CTMC. We first use observations of the degradation signal and environment state to update the degradation model as well as the environmental process; subsequently, we compute the RLD with the updated information.

First, let us assume that the prior distribution of $q_{i,j}$ is the gamma distribution with probability density function

$$\frac{q_{i,j}^{k_{i,j}-1} \exp(-q_{i,j}/\theta_{i,j})}{\Gamma(k_{i,j})\theta_{i,j}^{k_{i,j}}}$$

where $k_{i,j}$ is the shape parameter and $\theta_{i,j}$ is the scale parameter. By Theorem 4.2.1, the posterior distribution of Q, given the history of the process up to time t_k, is

$$\nu_Q(\boldsymbol{q}|\mathcal{F}_{t_k}) = \prod_{i=1}^{m} \prod_{j \neq i} \frac{q_{i,j}^{\tilde{k}_{i,j}-1} \exp(-q_{i,j}/\tilde{\theta}_{i,j})}{\Gamma(\tilde{k}_{i,j})\tilde{\theta}_{i,j}^{\tilde{k}_{i,j}}}.$$

Next, to characterize the signal model, the functions r and J are assumed to be

$$r(U(v)) = \alpha U(v) + \beta \quad \text{and} \quad J(U(v)) = \eta U(v)$$

where $\alpha, \beta,$ and η are random parameters. As before, the prior distributions of these parameters are assumed to be normal, i.e., $\alpha \sim \mathcal{N}(\mu_1, \sigma_1^2)$, $\beta \sim \mathcal{N}(\mu_2, \sigma_2^2)$, $\eta \sim \mathcal{N}(\mu_3, \sigma_3^2)$, and $\sigma \sim \mathcal{N}(\mu_4, \sigma_4^2)$, and they are all mutually independent. As for the deterministic model, let $\pi_s(\alpha, \beta, \eta, \sigma)$ denote their joint prior distribution. To estimate the posterior distributions of $(\alpha, \beta, \eta, \sigma)$ we need to derive the

likelihood function of degradation model. Recall that the degradation signal observations up to time t_k comprise the vector s_k. The likelihood function of s_k is

$$f_s(s_k|(\alpha, \beta, \eta, \sigma)) = \prod_{i=1}^{k} \phi_i(s(t_i) - s(t_{i-1}))$$

where for $i = 1, 2, \ldots, k$, $\phi_i(\cdot)$ is the p.d.f. of a normal random variable with mean

$$\int_{t_{i-1}}^{t_i} (\alpha + \beta u(v)) \mathrm{d}v + \eta(u(t_i) - u(t_{i-1}))$$

and variance $\sigma^2(t_i - t_{i-1})$. The term $u(v)$ in the integrand is the realization of the environment at time v. The posterior distribution of $(\alpha, \beta, \eta, \sigma)$ is thereby obtained as

$$\nu_s(\alpha, \beta, \eta, \sigma|s_k, \mathcal{F}_{t_k}) = \pi_s(\alpha, \beta, \eta, \sigma) \times \prod_{i=1}^{k} \phi_i(s(t_i) - s(t_{i-1}))$$

where $\pi_s(\alpha, \beta, \eta, \sigma) = \varphi_1(\alpha)\varphi_2(\beta)\varphi_3(\eta)\varphi_4(\sigma)$, and

$$\varphi_i(x_i) = \frac{1}{\sqrt{2\pi\sigma_i^2}} \exp\left(\frac{(x_i - \mu_i)^2}{2\sigma_i^2}\right), \quad i = 1, 2, 3, 4.$$

Therefore, using the degradation observations up to time t_k, the updated RLD is

$$\mathbb{P}(R_k \leq T|s_k, \mathcal{F}(t_k)) = \int_{q} \int_{(\alpha, \beta, \eta, \sigma)} \mathbb{P}(R_k \leq T|s_k, q, \alpha, \beta, \eta, \sigma)\, \nu_s(\alpha, \beta, \eta, \sigma|s_k, \mathcal{F}_{t_k})\, \nu_Q(q|\mathcal{F}_{t_k}). \quad (4.2.1)$$

The first term in the integrand of (4.2.1) can be estimated using the MCMC technique described in Section 4.1. The last term in the integrand is obtained via Theorem 4.2.1. In the next section, we provide a few numerical illustrations of these procedures via simulation experiments.

4.3 Numerical Results

In this section, we illustrate the degradation models and the performance of our Bayesian updating approach via a few numerical examples and a real case study. To this end, we simulate degradation signals under two scenarios: (1) when the environment evolves deterministically, and (2) when the environment evolves as a CTMC. For each numerical study, we simulated 1000 sample degradation signals (sample paths) until each first hits a fixed degradation threshold. The 1000 sample paths are partitioned into two sets: the first 500 paths are used to estimate parameters of the prior distributions, while the remaining 500 are used to illustrate real-time residual life prediction.

For the first two experiments, simulated sample paths serve as our benchmark, whereas real observed failures are used for the third experiment. Therefore, we assess our real-time RLD estimates by computing the mean and variance of the prediction error percentage. For the simulation experiments, let L_i denote the lifetime of the ith simulated path, and let $\hat{L}_i$ be the estimated lifetime (using our updating procedure). Then the prediction error (%) for the ith sample path is given by

$$\delta_i = \frac{|L_i - \hat{L}_i|}{L_i} \times 100. \tag{4.3.1}$$

Denoting δ as the true error, we estimate the mean and variance of the prediction error, respectively, by

$$\mathbb{E}(\delta) \approx \bar{\delta} = \frac{1}{500} \sum_{i=501}^{1000} \delta_i, \tag{4.3.2}$$

and

$$\mathrm{Var}(\delta) \approx \frac{1}{499} \sum_{i=501}^{1000} (\delta_i - \bar{\delta})^2. \tag{4.3.3}$$

Additionally, when the environment is deterministic, we compare our techniques to two existing approaches which are special cases of our model, namely those of [48] and [37]. [48] modulate the degradation signal by assuming a time-varying degradation rate and jumps that occur at environment transition epochs; however, they assume that the future environmental profile is unchanged when predicting the RLD. [37] presented a degradation model in which the time-varying (deterministic) environment modulates the degradation rate, but they do not consider jumps in the degradation signal. Using a time transformation, they developed an expression for the lifetime distribution. Clearly, these two models can be obtained as special cases of the degradation model presented herein.

When the environment evolves randomly, we compare our predicted residual lifetime only with the simulated results. The main objective of these experiments is to examine and illustrate the sensitivity of the Bayesian approach to a few of the model's parameters. Finally, the case study of Section 4.3.3 uses a deterministic environment as the benchmark.

4.3.1 Simulated Degradation Signals: Deterministic Environment

The first experiment mirrors the illustration provided in Section 4.1. The functions r and J are given by $r(\psi(t)) = \alpha \psi(t) + \beta$ and $J(\psi(t)) = \eta \psi(t)$, $t \geq 0$. The prior distributions of the degradation

model parameters are $\alpha \sim \mathcal{N}(\mu_1, \sigma_1^2)$, $\beta \sim \mathcal{N}(\mu_2, \sigma_2^2)$, $\eta \sim \mathcal{N}(\mu_3, \sigma_3^2)$, $\sigma \sim \mathcal{N}(\mu_4, \sigma_4^2)$, a collection of mutually independent random variables. Recall that [37] does not consider jumps in the degradation signals, and [48] assumes that the future environmental profile is unchanged. To investigate the effects of jumps, we conduct numerical studies with various values of the prior mean and variance of η: $\mu_3 = 0.0$, 10.0, 20.0 and $\sigma_3^2 = 0.1\mu_3$. The other parameter values are chosen according to Table 4.3.1. For each numerical study, we simulated 1000 degradation signals and denote the ith simulated signal at time t by $s_i(t)$, $i = 1, 2, \ldots, 1000$ using the parameters in Table 4.3.1.

Table 4.3.1: Prior distribution parameter values: deterministic environment.

Model parameter	Mean of prior p.d.f.	Variance of prior p.d.f.
α	$\mu_1 = 0.3$	$\sigma_1^2 = 0.03$
β	$\mu_2 = 0.5$	$\sigma_2^2 = 0.05$
σ	$\mu_4 = 3.0$	$\sigma_4^2 = 0.30$

For these experiments, the failure threshold is $D = 350$ units, and we assume $S(0) = 0$ with probability 1. The environment alternates between only two states so that ($\mathcal{S} = \{1, 2\}$), and its evolution is given by the step function

$$\psi(v) = \begin{cases} 1, & 0 \le v < 100, \\ 2, & 100 \le v < 200 \\ 1, & 200 \le v < 300 \\ 2, & v \ge 300. \end{cases}$$

The following procedure was used to simulate $s_i(t)$, $i = 1, 2, \ldots, 1000$:

Step 1: For $i = 1, 2, \ldots, 1000$, sample from the prior distributions of α, β, η and σ according to the parameters provided in Table 4.3.1. The resulting realizations are denoted by $\alpha_i, \beta_i, \eta_i$, and γ_i.

Step 2: Using $\alpha_i, \beta_i, \eta_i, \gamma_i$, and $\psi(t)$, simulate the degradation signal $s_i(t)$ according to

$$s_i(t) = \int_0^t (\alpha_i \psi(v) + \beta_i) \mathrm{d}v + \eta_i \psi(v) + \gamma_i W(t)$$

until it first hits the failure threshold D, i.e., simulate until time L_i where

$$L_i = \inf\{u \geq 0 : s_i(u) \geq D\}.$$

For each simulated signal $s_i(t)$, we re-sample degradation signals at discrete epochs $t_1, t_2, t_3, \ldots, t_{k_i}$, where t_{k_i} is the actual lifetime of signal $s_i(t)$. For simplicity, we let $t_j = j$, $j = 1, 2, \ldots, k_i$. The first 500 degradation signals can be viewed as a historical data set, and the remaining 500 degradation signals are used to test online prediction of the RLD. A two-stage procedure was employed to estimate the prior distributions of $(\alpha, \beta, \eta, \sigma)$, i.e., μ_k and σ_k^2, $k = 1, 2, 3, 4$. The details are attached in the Appendix.

Next, we use equation (4.1.9) with the estimated prior distributions of $\alpha, \beta, \eta, \sigma$ to assess online prediction of the RLD using the remaining degradation signals (signals $501, \ldots, 1000$). We estimate the component lifetime by observing the degradation signal up to the 50th and 90th percentiles of the lifetime and then compute the average and sample variance of the prediction error via equations (4.3.2) and (4.3.3), respectively. The results are compared with those obtained using the models of [48] and [37] in Figure 4.3.1 where technique (a) represents the prediction error obtained via [48], technique (b) represents results from [37], and technique (c) represents results from our method.
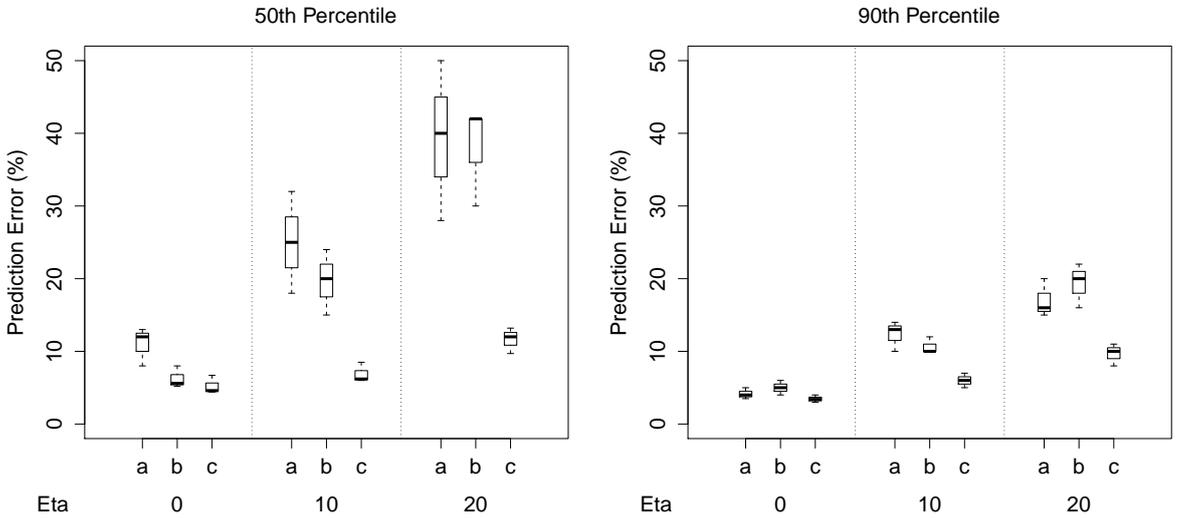

Figure 4.3.1: Comparison of prediction error as a function of η: deterministic environment.

Figure 4.3.1 indicates that our online updating technique yields the smallest mean prediction

error, and substantially smaller variation in the results. This is due, in part, to the fact that we completely characterize the features of simulated signals and utilize online data from the degradation signals.

4.3.2 Simulated Degradation Signals: Random Environment

In this subsection, we test online prediction of the RLD under a variety of scenarios in which the degradation model and environment process are updated online. We start with a baseline framework with parameter values chosen according to Table 4.3.2. As before, we set the degradation threshold to $D = 350$ and assume $S(0) = 0$ with probability 1. Initially, the environment has only two states so that $S = \{1, 2\}$, i.e., $m = 2$.

Table 4.3.2: Baseline parameter values: random environment.

Model parameter	Mean of prior p.d.f.	Variance of prior p.d.f.
α	$\mu_1 = 0.3$	$\sigma_1^2 = 0.03$
β	$\mu_2 = 0.5$	$\sigma_2^2 = 0.05$
η	$\mu_3 = 1.0$	$\sigma_3^2 = 0.10$
σ	$\mu_4 = 3.0$	$\sigma_4^2 = 0.30$
$q_{1,2}$	$k_{1,2} = 0.2$	$\theta_{1,2} = 0.1$
$q_{2,1}$	$k_{2,1} = 0.2$	$\theta_{2,1} = 0.1$

For this analysis, we change the value of one parameter while holding all others fixed. Additionally, we assess the effect of the number of environment states on RLD prediction. To make fair comparisons among simulation experiments, we fix the average state holding time for each state and assume the environment process chooses the next state according to a uniform distribution. The details of the simulation experiments are provided in what follows:

Group 1: (Assessing the effect of η). Let μ_3 assume the values $1, 2, \ldots, 50$ and set $\sigma_3^2 = 0.1\mu_3$;

Group 2: (Assessing the effect of σ). Let μ_4 assume the values $1, 2, \ldots, 50$ and set $\sigma_4^2 = 0.1\mu_4$;

Group 3: (Assessing the effect of Q). Let m assume the values $2, 3, \ldots, 15$. Given m, set $k_{i,j} = 0.2/(m-1)$ and $\theta_{i,j} = 0.1$, for $j \neq i$. Then, $q_{i,j}$ has mean $\theta_{i,j}k_{i,j} = 0.02/(m-1)$ for $j \neq$

i, the mean holding time in each state is $1/0.02$, and the environment transitions to next state according to a uniform distribution (i.e., it visits any one of the other states with equal probability) at the next transition.

We assess the quality of RLD prediction for different values of η and σ but fix $\alpha, \beta, S(0)$ and D. These values are fixed because increasing α or β and/or decreasing $D - S(0)$ have the same effect on prediction accuracy as decreasing the parameter σ; hence, we focus on parameters involving σ. For each instance, we simulate degradation signals via the following procedure:

Step 1: Simulate the environment's evolution.

1. Generate an m-state generator matrix Q using the prior distributions. That is, for each $i, j \in S$ such that $j \neq i$, generate a realization of $q_{i,j}$, denoted by $q_{i,j}^*$, from a $\Gamma(k_{i,j}, \theta_{i,j})$ p.d.f. and define $q_i^* = \sum_{j \neq i} q_{i,j}^*$;

2. Choose an initial environment state from S randomly (i.e., any state is chosen with probability $1/m$);

3. If the current state is i, generate an exponential holding time with parameter q_i^*;

4. The environment next transitions to state j with probability $q_{i,j}^*/q_i^*$;

5. Return to Step 1(c) until the total elapsed time reaches $T_{max} = 10000$. The resulting sample path can be viewed as a deterministic function of t denoted by $u^*(t)$.

Step 2: Simulate degradation signals subject to the environment process $u^*(t)$. The procedure is identical to the deterministic case described in Section 4.3.1.

Figures 4.3.2 depicts the simulation results for a number of instances using Approach I (sample path averaging) and Approach II (assuming a stationary environment) to compute the RLD as described in Section 4.2.

The graphs in the left-hand column plot the average prediction error whereas those in the right-hand column plot the variance of the prediction error as functions of m, σ, and η. From these figures, we deduce the following general conclusions: (1) For large η, jumps caused by environment transitions dominate, i.e., system failure can primarily be attributed to shocks. (2) For large σ, the
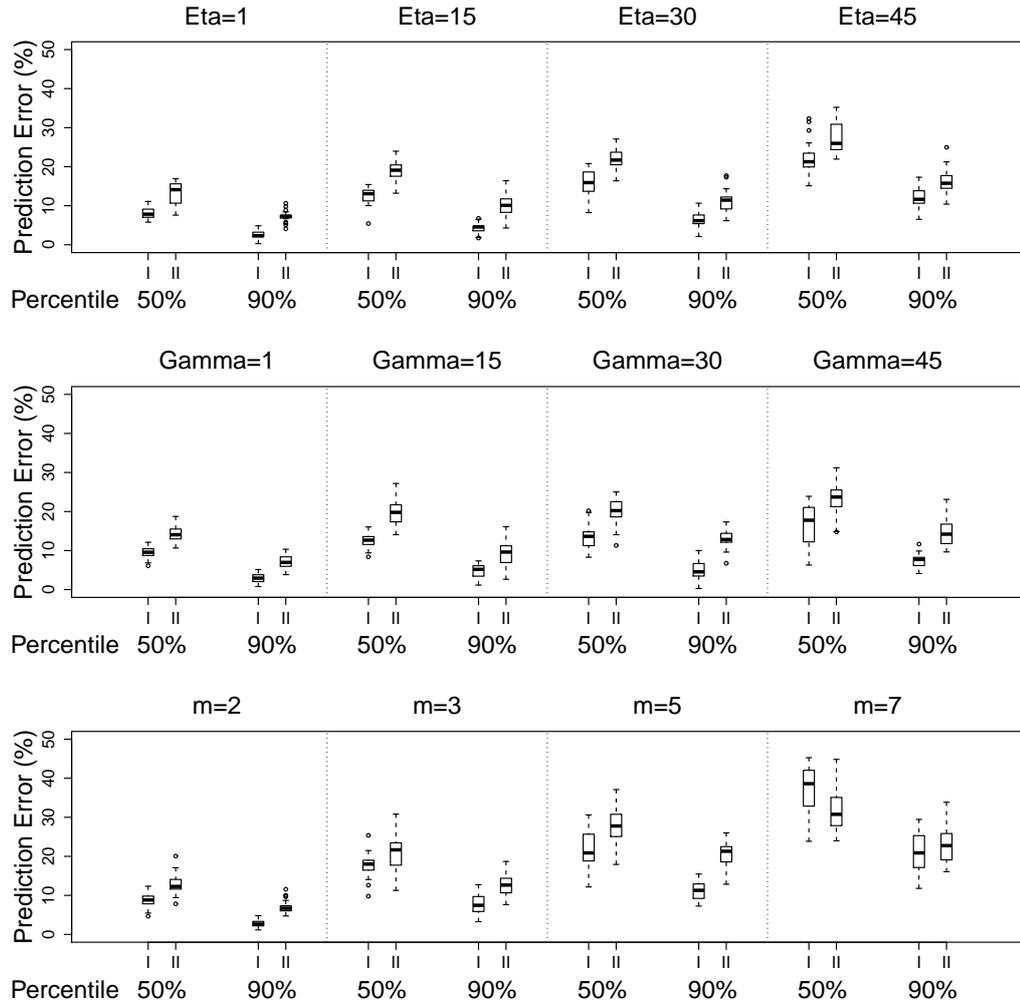
Figure 4.3.2: RLD prediction error using Approach I and Approach II.

diffusion term of the degradation signal dominates, and the effect of the environment can almost be ignored. (3) An increase in the number of environment states (m) results in a sharp increase in the mean and variance of the prediction error.

Figure 4.3.2 suggests that moderate parameter values should be chosen for the prior distributions. For example, $\eta < 20$, $\sigma < 20$, $m < 10$ are reasonable for the experiments we conducted. As compared to using Approach I, computing the RLD via Approach II sacrifices about 7% of average prediction accuracy at the 50th percentile and 2% of average prediction accuracy at the 90th percentile. However, Approach II reduces the computational burden drastically by circumventing the simulation of future profiles.

4.3.3 A Case Study

In this subsection, we present a case study that involves ball bearings operating under deterministic environmental profiles. We use vibration-based degradation signals generated from an experimental test rig that is designed to perform accelerated degradation tests on ball bearings using different loads and rotational speeds. Bearing failure has been widely studied in the literature, and vibration monitoring is considered as one of the most widely used techniques for monitoring bearing degradation ([51]). In fact, vibration signals contain distinctive frequencies that are related to various types of bearing defects ([48]). Figure 4.3.3 shows how the vibration spectra from a degrading bearing evolve as the rotational speed changes. It also shows that the system experiences a significant shock as the bearing transitions from one operating condition to another. This observation lends credence to our degradation signal model, i.e., signal jumps are more prominent as the component transitions from one operating condition to another.

We construct the vibration-based degradation signals based on the fact that the vibration amplitude of bearing-specific defective frequencies is generally correlated with the severity of the bearing's degradation. In particular, we compute the average amplitude of the defective frequency and its first five harmonics. We limit ourselves to the first five harmonics since higher-order harmonics have been observed to behave erratically. Furthermore, we define bearing failure based on the root mean square (RMS) value of the overall vibration of the test rig. According to industrial standards for machinery vibration, ISO 2372, 2.0–2.2 G (G denotes gravitational acceleration) represents a

Figure 4.3.3: Evolution of the vibration spectra of a degrading bearing.

vibration-based danger level for applications involving general purpose mid-size machinery. We use this standard to identify a corresponding failure threshold of 0.025 Vrms (Root Mean Square Volts).

In this study, we examine the effects of two environmental factors: the load applied to the bearing and the rotational speed of the bearing. In particular, two different loads (400 lbs and 500 lbs) and two different rotational speeds (2,200 rpm and 2,600 rpm) are considered; therefore, initially there are four distinct environmental conditions: (2,200 rpm, 400 lbs), (2,200 rpm, 500 lbs), (2,600 rpm, 400 lbs), and (2,600 rpm, 500 lbs). To construct the mapping from the environmental conditions to the environmental state space, we examine the degradation rate in each environmental condition and determine the environmental states so that state 1 represents the environmental condition with the lowest degradation rate and state 4 the highest degradation rate. Let $r(s, l)$ denote the degradation rate when the rotational speed is s (rpm), and the load is l (lbs). Since higher load or speed accelerates the degradation of bearings ([94]), we obtain the following inequalities of degradation rates in various environment states:

1. $r(2,200 \text{ rpm}, 400 \text{ lbs}) < r(2,200 \text{ rpm}, 500 \text{ lbs}) < r(2,600 \text{ rpm}, 500 \text{ lbs})$,

2. $r(2,200 \text{ rpm}, 400 \text{ lbs}) < r(2,600 \text{ rpm}, 400 \text{ lbs}) < r(2,600 \text{ rpm}, 500 \text{ lbs})$.

To establish a complete ordering of the degradation rates in all four environmental conditions, we evaluate r(2,200 rpm, 500 lbs) and r(2,600 rpm, 400 lbs) using the vibration data. Our analysis, which is based on the hypothesis testing procedure, indicates that r(2,200 rpm, 500 lbs) $< r$(2,600 rpm, 400 lbs). Therefore, the final ordering of degradation rates (from least severe to most severe) is $r(2200, 400) < r(2200, 500) < r(2600, 400) < r(2600, 500)$. The resulting environmental states included in $\mathcal{S}$ are summarized in Table 4.3.3.

Table 4.3.3: Definition of ordered environmental states.

Environmental condition	Environmental state
(2,200 rpm, 400 lbs)	1
(2,200 rpm, 500 lbs)	2
(2,600 rpm, 400 lbs)	3
(2,600 rpm, 500 lbs)	4

We conducted two groups of bearing tests. The first set of 12 experiments was used to estimate prior distribution parameters for the degradation model, and these are designated as ID 1 to 12. The second set of 3 experiments are used for validation, and these are labeled as ID 13 to 15. The experimental setups for these two groups are summarized in Table 4.3.4. Moreover, the real observed degradation signals used for validation are depicted in Figure 4.3.4). Applying the approach described in Section 5.1, we estimate the prior distributions of model parameters using the degradation signals from experiments 1-12. Subsequently, we assess online prediction of the RLD using the degradation signals from experiments 13-15.

We predict the component's lifetime by observing the degradation signal and updating the degradation model at the 30th, 60th and 90th percentiles of the lifetime. The means of the estimated lifetimes and the corresponding prediction errors are presented in Table 4.3.5. We observe that the prediction errors at the 90th percentile of the lifetime are relatively small. This is, in part, because the environmental condition remains constant for all of the three online experiments after the 90th percentile of the lifetime.
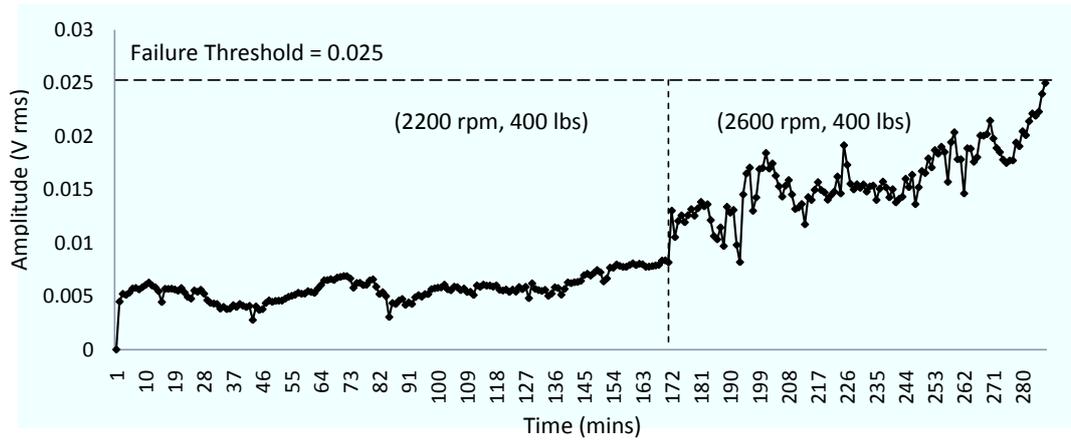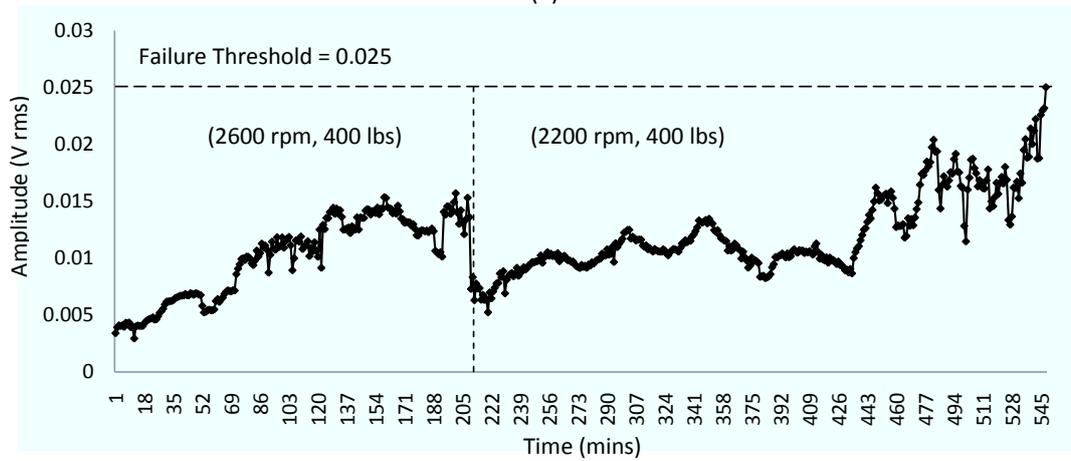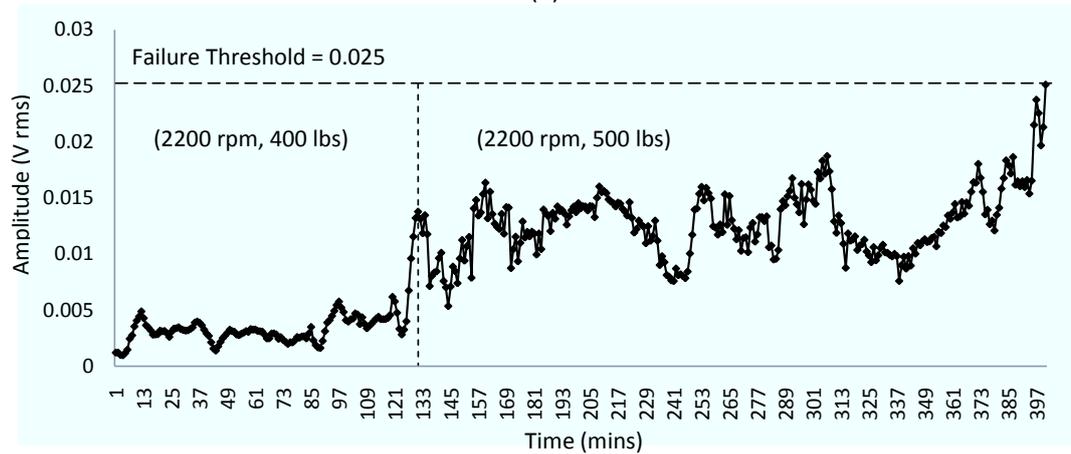
Figure 4.3.4: Degradation signals for online validation.

Table 4.3.4: Experiments for prior information and online validation.

Experiment ID	Operating conditions	Number of bearings
1	(2,200 rpm, 400 lbs)	4
2	(2,200 rpm, 500 lbs)	4
3	(2,600 rpm, 400 lbs)	4
4	(2,600 rpm, 500 lbs)	4
5	(2,200 rpm, 400 lbs) → (2,200 rpm, 500 lbs)	2
6	(2,200 rpm, 500 lbs) → (2,200 rpm, 400 lbs)	2
7	(2,600 rpm, 400 lbs) → (2,600 rpm, 400 lbs)	2
8	(2,600 rpm, 400 lbs) → (2,600 rpm, 400 lbs)	2
9	(2,200 rpm, 400 lbs) → (2,600 rpm, 400 lbs)	2
10	(2,600 rpm, 400 lbs) → (2,200 rpm, 400 lbs)	2
11	(2,600 rpm, 400 lbs) → (2,200 rpm, 400 lbs)	2
12	(2,200 rpm, 400 lbs) → (2,600 rpm, 400 lbs)	2
13	(2,200 rpm, 400 lbs) → (2,600 rpm, 400 lbs)	1
14	(2,600 rpm, 400 lbs) → (2,200 rpm, 400 lbs)	1
15	(2,200 rpm, 400 lbs) → (2,200 rpm, 500 lbs)	1

Table 4.3.5: Prediction of lifetime for validation data.

ID	Actual Lifetime	30th Percentile	60th Percentile	90th Percentile
13	283	318.28 (12.5% error)	301.31 (6.5% error)	289.81 (2.4% error)
14	546	489.56 (10.3% error)	575.14 (5.3% error)	563.32 (3.1% error)
15	402	440.24 (9.5% error)	432.21 (7.5% error)	387.86 (3.8% error)

CHAPTER V

STOCHASTIC FRAMEWORK FOR SYSTEMS WITH DISCRETE

INTERACTIVE DEGRADATION SIGNALS

This chapter focuses on modeling degradation-rate-interactions (DRIs) that occur in a discrete manner. Specifically, changes in the degradation rate of a component occur when other stochastically dependent components reach pre-specified degradation levels, i.e., when their degradation signals reach specific amplitudes or amplitude ranges. From a practical perspective, discrete-type DRIs can take place in applications where, for example, different levels of wear or plastic deformation result in categorically different effects on the degradation processes of other components. Our approach rests on the idea that degradation signals from interdependent components can be divided into amplitude ranges that correspond to discrete degradation states. When a component transitions from one state to a more severe state, it triggers a DRI, which results in increasing the degradation rates of other dependent components. Consequently, the times at which DRIs take place correspond to change-points in the degradation rates of the components of the system. Using this approach, we develop a stochastic degradation modeling framework where the evolution of degradation signals is modeled as a continuous-time stochastic process, and in which degradation interactions are modeled as change-points in the growth rate of the signals. A change-point detection algorithm is utilized to identify the times that correspond to degradation interactions. Historical degradation signals are used to estimate the model parameters and their prior distributions. However, the main benefit of this approach lies in the ability to utilize *in-situ* degradation signals from the components of fielded systems to update the model parameters in a Bayesian manner, and predict their residual life distributions.

The remainder of this chapter is organized as follows : Section 5.1 describes a multi-state degradation model that captures the discrete-type DRIs among the components of a system. In Section 5.2, we present a series of simulation studies that evaluate the performance of the proposed model and report our analysis.

5.1 Degradation Model for Discrete-Type Degradation-Rate-Interactions

Consider a system with n interdependent components, $C_1, C_2, \ldots, C_n$, with corresponding degradation signals denoted by $S_1(t), S_2(t), \ldots, S_n(t)$. For notational convenience, we let

$$S(t) = (S_1(t), S_2(t), \ldots, S_n(t))'.$$

Based on the amplitude of $S_i(t)$, a component C_i can be classified into different degradation states, e.g., "good", "degraded", "failed", etc. Let $h_i(\cdot)$ define the degradation state of component C_i, $i = 1, \ldots, n$, such that $h_i : \mathbb{R} \to \mathbb{Z}^+$ is a piecewise constant function expressed as follows:

$$h_i(S_i(t)) = \begin{cases} 0 & S_i(t) < g_{i,1} \\ 1 & g_{i,1} \leq S_i(t) < g_{i,2} \\ \ldots & \ldots \\ M_i - 1 & S_i(t) \geq g_{i,M_i-1} \end{cases} \tag{5.1.1}$$

where M_i represents the number of degradation states for component C_i, and $g_{i,1}, \ldots, g_{i,M_i-1}$ represent the signal thresholds for different degradation states such that $g_{i,1} < \ldots < g_{i,M_i-1}$. For example, when $M_i = 3$, the degradation state of component C_i can occupy three states, state 0 (for $S_i(t) < g_{i,1}$), state 1 (for $g_{i,1} \leq S_i(t) < g_{i,2}$), and state 2 (for $S_i(t) \geq g_{i,2}$). Generally, a component can occupy at least two states "good" and "failed", i.e., $M_i \geq 2$. We define $d_i \equiv g_{i,M_i-1}$ as the failure threshold of component C_i. As a result, the failure state is a special case of the degradation states characterized by $h_i(S_i(t))$.

Next, we denote the degradation rate of component C_i at time t by $r_i(t)$ and assume that $r_i(t)$ consists of two parts: (1) κ_i, which represents the inherent degradation rate of component C_i, i.e., the degradation rate of component C_i without the effect of any DRIs, and (2) $\boldsymbol{h}(\boldsymbol{S}(t))$, where $\boldsymbol{h}(\boldsymbol{S}(t)) = (h_1(S_1(t)), \ldots, h_n(S_n(t)))'$ represents the degradation states of all the other interdependent components of the system. Thus, the overall degradation rate of component C_i can be expressed as $r_i(t) = r_i[t; \kappa_i, \boldsymbol{h}(\boldsymbol{S}(t))]$. As mentioned earlier, we use degradation signals to model the underlying physical degradation process. The degradation signal of a component C_i can therefore be expressed as follows:

$$S_i(t) = S_i(0) + \int_0^t r_i[v; \kappa_i, \boldsymbol{h}(\boldsymbol{S}(v))]\mathrm{d}v + \epsilon_i(t), \tag{5.1.2}$$

where $S_i(0)$ represents an initial signal amplitude that directly precedes degradation, and $\epsilon_i(t)$ is used to model the noise level of the signal.

5.1.1 Base-Case DRI Model

Equation (5.1.2) presents a general DRI modeling framework. Here, we focus on a base-case stochastic model with the following assumptions :

Assumption (1): A DRI event (degradation-rate-interaction event) occurs when one component transitions to a more severe degradation state, which increases the degradation rates of all other interdependent components. We refer to the former as the "influencing component" and the latter as the "affected components". By virtue of our model, the probability that two DRI events occur at the same time is 0. This because a DRI event occurs when the degradation signal of a certain component, say $S_i(t)$, crosses the interaction thresholds. Since $S_i(t)$ is a continuous stochastic process for $i = 1, \ldots, n$, the probability that two crossing events occurs at the same time is 0. Therefore, at each DRI event there is exactly one influencing component, and at least one affected component.

Assumption (2): When an influencing component, say C_j, transitions to a more severe state, it increases the degradation rate of every other affected component, say C_i, by an amount $\delta_{j,i}$. In this paper, we limit our development to the case where $\delta_{j,i}$ is constant and does not depend on the age nor degradation states of components C_i or C_j. In addition, we assume that the degradation rate of the influencing component C_j remains unchanged, i.e., $\delta_{j,j} = 0$.

Assumption (3): The degradation rate of a component, say C_i, is a linear function of its inherent degradation rate and the degradation states of other influencing components. Specifically, $r_i(t) = \kappa_i + \sum_{j \neq i} \delta_{j,i} h_j(S_j(t))$.

Assumption (4): $\epsilon_i(t) = B_i(t)$, where $B_i(t)$ is assumed to follow a stationary Brownian motion process with diffusion parameter σ_i^2, i.e., $B_i(t) \sim N(0, \sigma_i^2 t)$.

The resulting base-case degradation model for component, say C_i, can be expressed as follows:

$$S_i(t) = S_i(0) + \int_0^t \left[\kappa_i + \sum_{j \neq i} \delta_{j,i} h_j(S_j(v)) \right] dv + B_i(t). \tag{5.1.3}$$

Model parameters are divided into deterministic and stochastic parameters. Deterministic parameters are generally fixed and determined by the characteristics of a given system, i.e., its configuration, operating conditions, and constituent components. We assume that $\delta_{i,j}$'s are deterministic. For notational convenience, we let $\Delta = [\delta_{i,j}]$. On the other hand, stochastic parameters capture variations among similar components that are due to manufacturing processes, materials inhomogeneities, and other random factors. In our model, κ_i's and σ_i^2's are assumed to be stochastic. The

vector forms of these parameters are denoted by $\kappa = (\kappa_1, \ldots, \kappa_n)$ and $\sigma^2 = (\sigma_1^2, \ldots, \sigma_n^2)$. Note that κ and σ^2 are fixed for components of a specific system, but take different values across different systems. The randomness of κ and σ^2 is modeled using prior distributions. As will be shown later in Section 5.1.2, the values of Δ as well as the prior distributions of κ and σ^2 can be estimated using a historical sample of degradation signals.
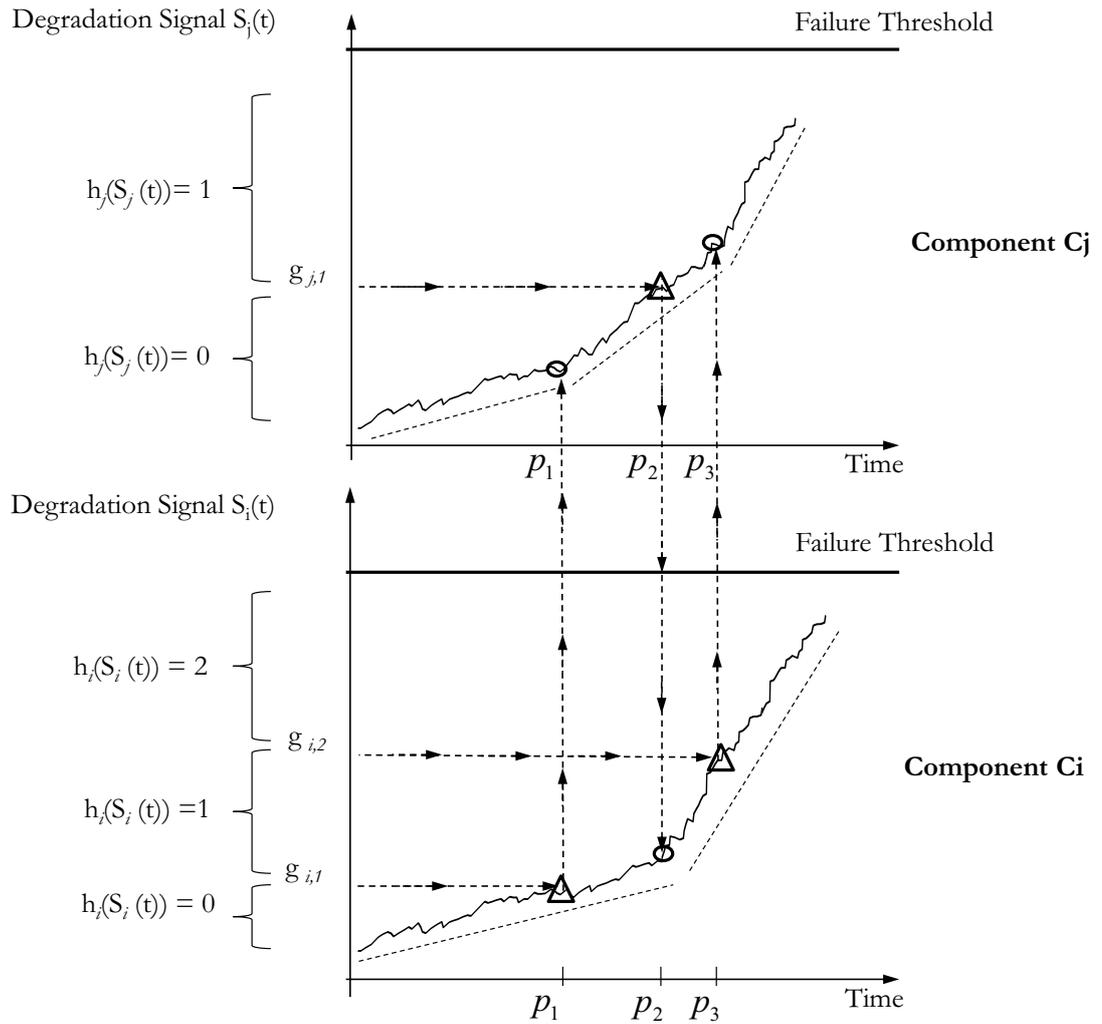
Figure 5.1.1: Degradation-rate-interactions between the degradation processes of components. $\triangle$ represents the influencing component, and $\circ$ the affected component.

Figure 5.1.1 illustrates a possible scenario for two dependent components and their corresponding DRIs using the based-case model expressed in equation (5.1.3). The figure displays the degradation signals of two interdependent components C_i and C_j. The dashed line segments adjacent to the signals represent the underlying degradation rate of the respective components at different stages of their degradation. The arrows define the direction of influence at each DRI event. In total, there are three DRI events, and they occur at times p_1, p_2, and p_3. These events correspond to change-points in the degradation rates of the two interacting components. At time p_1, we say that the degradation state of component C_i transitions from state 0 to state 1, and at p_3 it transitions to state 2. The transition thresholds corresponding to these degradation states are given by $g_{i,1}$ and $g_{i,2}$, respectively. Once the degradation signal of component C_i crosses $g_{i,1}$, it impacts the degradation rate of component C_j by increasing its degradation rate by an amount $\delta_{i,j}$. This is represented by the increased slopes of the dashed line segments at times p_1 in the degradation signal of C_j (upper graph of Figure 5.1.1). A similar scenario occurs at p_3. At p_1 and p_3, we refer to component C_i as the "influencing component", and component C_j as the "affected component". This is illustrated by the direction of the arrows. A reverse scenario occurs at time p_2, where C_j takes one the role of the influencing component, and C_i becomes the affected component.

In Section 5.1.2, we discuss how to estimate the values of Δ as well as the prior distributions of κ and σ^2 using a sample of historical degradation signals. In Section 5.1.3, we discuss how to update the distributions of κ and σ using real-time observations of degradation signals from a system operating in the field, which allows for more accurate predictions of the residual life distributions.

5.1.2 Parameter Estimation Using Historical Degradation Signals

To estimate the parameters of the model, we exploit assumption (2) of section 5.1.1 which states that when a component transitions to a more severe state, it increases the degradation rates of other dependent components by a constant amount $\delta_{i,j}$. As mentioned earlier, the points at which these interactions occur represent change-points in the degradation rates as shown in Figure 5.1.1. We use this assumption as the basis for estimating the parameters of the degradation state function $h_i(\cdot)$, namely, M_i and $g_{i,\ell}$, for $i = 1, \ldots, n$ and $\ell = 1, \ldots, M_i - 1$.

To estimate the change-points of degradation rates, we consider the increments of the degradation signals. For a given system, we denote the observed component degradation signals at time t by $s(t)$, where $s(t) = (s_1(t), \ldots, s_n(t))'$. Note that $s(t) \in \mathbb{R}^n$ represents the realization of random variable $S(t)$. Thus, the observed degradation signals at $t_0, t_1, \ldots, t_q$ can be expressed as $s(t_0), s(t_1), \ldots, s(t_q)$. Without loss of generality, assume $t_1 - t_0 = t_2 - t_1 = \ldots = t_q - t_{q-1} = \epsilon_t$ and let $y_m = \frac{s(t_m) - s(t_{m-1})}{t_m - t_{m-1}}$, for $m = 1, \ldots, q$. y_m can be expressed as a vector $y_m = (y_{m,1}, \ldots, y_{m,i}, \ldots, y_{m,n})'$ where $y_{m,i} = \frac{1}{t_m - t_{m-1}} \int_{t_{m-1}}^{t_m} \left(\kappa_i + \sum_{j \neq i} \delta_{j,i} h_j(s_j(v)) \right) dv + \frac{B_i(t_m) - B_i(t_{m-1})}{t_m - t_{m-1}}$ (using equation (5.1.3)). For applications where the interval between two consecutive monitoring epochs is short (i.e. ϵ_t is small), we can use the following approximation for $y_{m,i}$: $\frac{1}{t_m - t_{m-1}} \int_{t_{m-1}}^{t_m} \left(\kappa_i + \sum_{j \neq i} \delta_{j,i} h_j(s_j(v)) \right) dv \approx \kappa_i + \sum_{j \neq i} \delta_{j,i} h_j(s_j(t_{m-1}))$. Recall that $r_i(t_{m-1}) = \kappa_i + \sum_{j \neq i} \delta_{j,i} h_j(s_j(t_{m-1}))$. Thus, the distribution of $y_{m,i}$ can be approximated using a normal distribution with the following parameters,

$$y_{m,i} \sim N(r_i(t_{m-1}), \sigma_i^2/(t_m - t_{m-1})).$$

Therefore, $y_m \sim \text{MVN}\left(r(t_m), \frac{1}{\epsilon_t}\Sigma \right)$, where $r(t) \in \mathbb{R}^n$, $r(t) = (r_1(t), \ldots, r_n(t))'$, $\Sigma \in \mathbb{R}^{n \times n}$, and $\Sigma = \text{diag}\{\sigma_1^2, \ldots, \sigma_n^2\}$. Furthermore, the times at which DRIs occur correspond to the change-points in the mean of y_m for $m \in \{1, 2, \ldots, q\}$. If we denote the number of change-points by L ($L < q$) and let $\mathbb{G} = \{t_0, t_1, t_2, \ldots, t_q\}$ represent the set of observation times, we can define $p = (p_1, p_2, \ldots, p_L)'$ where $p \in \mathbb{G}^L$, as the vector of change-points in $r(t)$.

As a result, $r(t) = (r_1(t), \ldots, r_n(t))'$ such that $r_i(t)$ represents the degradation rate of component C_i at time t; and $p_1, p_2, \ldots, p_L$ represent the times at which DRI events occur. Recall that we assume when a DRI event occurs, it changes the degradation rates of the affected components. Hence, for any two consecutive DRI times, say $p_{\ell-1}$ and p_ℓ, the vector of degradation rates $r(t)$ remains a constant vector, which is denoted by μ_ℓ, as shown in Figure 5.1.2. In this figure, the degradation rates of components are represented by the slopes of dashed line segments. Therefore, $r(t)$ is a
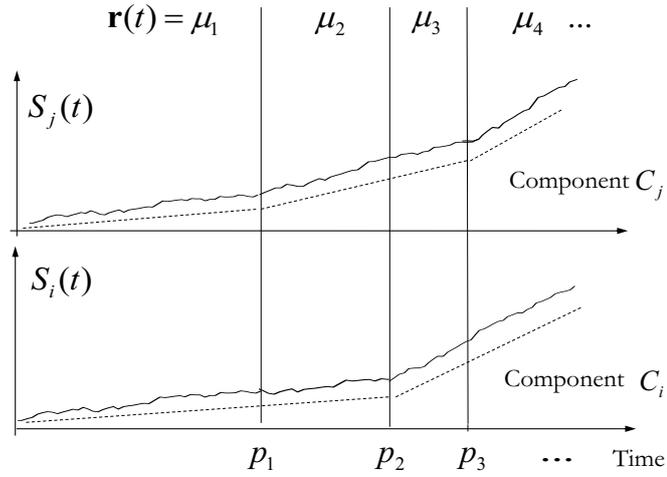
85

Figure 5.1.2: $r(t)$ as a piecewise constant function.

piecewise constant function and can be expressed as follows:

$$r(t) = \begin{cases} \mu_1 & t_0 \leq t < p_1 \\ \mu_2 & p_1 \leq t < p_2 \\ \ldots & \ldots \\ \mu_L & p_{L-1} \leq t < p_L \\ \mu_{L+1} & p_L \leq t \leq t_q. \end{cases}$$

The challenge now is to identify these change-points. Many researchers have addressed the problem of change-point detection using various approaches, such as Schwarz criterion ([111]), the Bayesian approach ([69]), the non-parametric approach ([72]), the penalized likelihood approach ([8]) and other techniques. In [111], the authors developed Schwarz' criterion (BIC) for model selection with independent and identically distributed observations from the exponential family. In [144], the authors examined Schwarz' criterion for change-point detection and established the consistency of the estimator for the number of change-points. In our framework, we present a three-step algorithm based on Schwarz' criterion to estimate the change-points in $r(t)$, and hence the function, $h(\cdot)$.

First, we estimate the vector p for a given number of change-points, L, where $L = 1, \ldots, L_{\max}$.

Here, $L_{\max}$ can be a pre-specified maximum value of L. Next, the optimal value of L and the corresponding p is then chosen using Schwarz' criterion. In the third step, we identify the "influencing component" at each interaction and estimate the corresponding interaction thresholds. Once the interaction state function has been estimated, it can be used to estimate κ and σ^2.

Step 1: Fix the number of change-points L and compute the MLEs of $p, \mu_1, \ldots, \mu_\ell, \ldots, \mu_{L+1}$, and σ^2 by maximizing the following likelihood function:

$$f_p(p, \mu_1, \ldots, \mu_{L+1}, \sigma^2 | y_1, \ldots, y_q)$$

$$= \left(\frac{\epsilon_t}{\sqrt{(2\pi)^n |\Sigma|}} \right)^q \prod_{\ell=0}^{L} \left[\exp \left(-\frac{\epsilon_t}{2} \sum_{t_m \in \mathbb{G}}^{p_\ell \le t_m < p_{\ell+1}} (y_m - \mu_{\ell+1})' \Sigma^{-1} (y_m - \mu_{\ell+1}) \right) \right], \qquad (5.1.4)$$

where $p_0 \equiv t_0$, $p_{L+1} \equiv t_q$, and $|\Sigma|$ represents the determinant of Σ.

For moderate values of L, we can maximize likelihood function f_p for each given p, and obtain a global maximum for f_p for all possible values p. Given p, the likelihood function is maximized at $\sigma^2 = \hat{\sigma}_p^2$ and $\mu_\ell = \hat{\mu}_{p,\ell}$ where,

$$\hat{\mu}_{p,\ell} = \frac{\epsilon_t}{p_\ell - p_{\ell-1}} \sum_{t_m \in \mathbb{G}}^{p_{\ell-1} \le t_m < p_\ell} y_m \quad \text{and} \quad \hat{\sigma}_p^2 = \frac{\epsilon_t}{q} \sum_{\ell=0}^{L} \sum_{t_m \in \mathbb{G}}^{p_\ell \le t_m < p_{\ell+1}} (y_m - \hat{\mu}_{p,\ell+1})^2.$$

Here, the square of any vector x is defined as $x^2 \equiv (x_1^2, x_2^2, \ldots, x_n^2)'$ for $x = (x_1, x_2, \ldots, x_n)'$.

For each $p \in \mathbb{G}^L$ with constraint $p_1 < p_2 < \ldots < p_L$, we substitute $\hat{\sigma}_p^2$ and $\hat{\mu}_{p,\ell}$ in $f_p(p, \mu_1, \ldots, \mu_{L+1}, \sigma^2 | y_1, \ldots, y_q)$ for $\ell = 1, \ldots, L$. Note that $p_0 \equiv t_0$ and $p_{L+1} \equiv t_q$. The likelihood function is maximized at $p = \hat{p}_L$ where,

$$\hat{p}_L = \underset{p \in \mathbb{G}, p_1 < \ldots < p_L}{\arg \max} f_p(p, \hat{\mu}_{p,1}, \ldots, \hat{\mu}_{p,L+1}, \hat{\sigma}_p^2 | y_1, \ldots, y_q).$$

This procedure works well for moderate values of L. For large L (e.g. $L > 6$), we can utilize the dynamic programming technique developed by [5].

Step 2: This step focuses on selecting the optimal number of change-points, L, using Schwarz' criterion. The Schwarz' criterion (BIC) is expressed as follows:

$$SC(L) = \frac{q}{2} \log \|\hat{\sigma}_L\|^2 + L \log q,$$

where $\|\hat{\sigma}_L\|$ is the Euclidean norm of $\hat{\sigma}_L$, and $\hat{\sigma}_L^2$ is the calculated MLE of σ^2 that corresponds to $\hat{p}_L$.

If we let $\hat{L}$ denote an estimate of the optimal value of L, then $\hat{L}$ minimizes based on Schwarz' criterion given below,

$$\hat{L} = \operatorname*{arg\,min}_{L=1,2,\ldots,L_{\max}} \left[\frac{q}{2} \log \|\hat{\sigma}_L\|^2 + L \log q \right]. \tag{5.1.5}$$

Once $\hat{L}$ is calculate, we denote the corresponding estimates of $\boldsymbol{p}_L$, σ_L^2, and $\boldsymbol{\mu}_\ell$ as $\hat{\boldsymbol{p}}$, $\hat{\sigma}^2$, and $\hat{\boldsymbol{\mu}}_\ell$, respectively. These values will be used to estimate the parameters of $\boldsymbol{h}(\cdot)$, namely M_i's and $g_{i,m}$'s, in the following step.

Step 3: This step focuses on estimating the parameters of $\boldsymbol{h}(\cdot)$, namely M_i's and $g_{i,m}$'s. As mentioned earlier, during each DRI event the degradation rates of the affected component increase, while that of the influencing component remains unchanged. Hence, it is reasonable to assume that at each DRI event, the influencing component is the component with the smallest change in degradation rate (considering the signal noise). In other words, the influencing component at change-point $\hat{p}_\ell$ is the component that corresponds to the minimal element of $|\hat{\boldsymbol{\mu}}_{\ell+1} - \hat{\boldsymbol{\mu}}_\ell|$. Formally, let $I : \mathbb{G} \to \{1, \ldots, n\}$ such that $I(\hat{p}_\ell)$ is a function that returns the index of the influencing component at $\hat{p}_\ell$, where $\hat{\boldsymbol{p}} = (\hat{p}_1, \ldots, \hat{p}_\ell, \ldots, \hat{p}_{\hat{L}})'$. That is,

$$I(\hat{p}_\ell) = \operatorname*{arg\,min}_{i=1,\ldots,n} |\hat{\mu}_{\ell+1,i} - \hat{\mu}_{\ell,i}|,$$

where $\hat{\mu}_{\ell,i}$ is the ith element of vector $\hat{\boldsymbol{\mu}}_\ell$ for $i = 1, \ldots, n$ and $\ell = 1, \ldots, \hat{L}$, and $C_{I(\hat{p}_\ell)}$ represents the influencing component at time $\hat{p}_\ell$.

Recall that at each DRI event there is exactly one influencing component, and at least one affected component. Furthermore, each DRI event signals the transition of the influencing component to a more severe degradation state. Thus, the number of transitions for a component, say C_i, is equal to its number of degradation states minus one, $M_i - 1$. If we let $\widehat{M}_i$ denote the estimate of M_i, then we have,

$$\widehat{M}_i = 1 + \sum_{\ell=1}^{\hat{L}} \mathbf{1}(I(\hat{p}_\ell) = i), \tag{5.1.6}$$

where $\mathbf{1}(A)$ is the indicator function of condition A.

To estimate the signal thresholds for each degradation state, we begin by identifying the influencing component at change-point $\hat{p}_1$, $C_{I(\hat{p}_1)}$, using the function $I(\hat{p}_\ell)$. Next, we estimate $g_{\{I(\hat{p}_1),1\}}$ using the amplitude of the degradation signal of $C_{I(\hat{p}_1)}$ at time $\hat{p}_1$, i.e., $\hat{g}_{\{I(\hat{p}_1),1\}} = s_{I(\hat{p}_1)}(\hat{p}_1)$. For change-point $\hat{p}_2$, if the influencing component is still $C_{I(\hat{p}_1)}$, i.e., $I(\hat{p}_1) = I(\hat{p}_2)$, we set $\hat{g}_{\{I(\hat{p}_1),2\}} = $

$s_{I(\hat{p}_1)}(\hat{p}_2)$; otherwise, we set $\hat{g}_{\{I(\hat{p}_2),1\}} = s_{I(\hat{p}_2)}(\hat{p}_2)$. We continue this procedure for $\hat{p}_3, \ldots, \hat{p}_{\hat{L}}$ and obtain the estimate of all $g_{i,l}$ for $m = 1, \ldots, \widehat{M}_i - 1$. Given $\widehat{M}_i$'s and $\hat{g}_{i,m}$, $h_i(\cdot)$ is estimated as follows:

$$
\hat{h}_i(s_i(t)) = \begin{cases} 0 & s_i(t) < \hat{g}_{i,1} \\ 1 & \hat{g}_{i,1} \le s_i(t) < \hat{g}_{i,2} \\ \ldots & \ldots \\ \widehat{M}_i & s_i(t) \ge \hat{g}_{i,\widehat{M}_i-1} \end{cases}.
\tag{5.1.7}
$$

Given $\hat{h}_i(s_i(t))$'s and $\hat{\sigma}_i^2$'s, the MLE of κ and Δ can be expressed using equation (5.1.3),

$$
f_d(\kappa, \Delta | y_1, \ldots, y_q, \hat{h}, \hat{\sigma}^2)
$$
$$
= \prod_{m=1}^{q} \left(\sqrt{\frac{\epsilon_t}{(2\pi)^n |\hat{\Sigma}|}} \exp \left\{ -\frac{\epsilon_t}{2} [y_m - (\kappa + \Delta' \times \hat{h}(s(t)))]' \hat{\Sigma}^{-1} [y_m - (\kappa + \Delta' \times \hat{h}(s(t)))] \right\} \right),
$$

where $\hat{\Sigma} = \text{diag}\{\hat{\sigma}_1^2, \ldots, \hat{\sigma}_n^2\}$ and $\hat{h}(s(t)) = (\hat{h}_1(s_1(t)), \ldots, \hat{h}_n(s_n(t)))'$. $f_d(\kappa, \Delta | y_1, \ldots, y_q)$ is maximized at $\Delta = \widehat{\Delta}$ and $\kappa = \hat{\kappa}$, where $A = [a_{i,j}]$, $B = [b_{i,j}]$, $e = (e_1, \ldots, e_n)'$, and

$$
\widehat{\Delta} = A^{-1} B,
\tag{5.1.8}
$$

$$
\hat{\kappa} = \frac{s(t_q)}{t_q} - \frac{1}{q} \widehat{\Delta} \sum_{m=1}^{q} s(t_{m-1}),
\tag{5.1.9}
$$

$$
a_{i,j} = \frac{\epsilon_t}{q} \sum_{m=1}^{q} \hat{h}_i(s_i(t_m)) \sum_{m=1}^{q} \hat{h}_j(s_j(t_m)) - \epsilon_t \left(\sum_{m=1}^{q} \hat{h}_i(s_i(t_m)) \hat{h}_j(s_j(t_m)) \right),
\tag{5.1.10}
$$

$$
b_{i,j} = \frac{s_j(t_q)}{q} \sum_{m=1}^{q} \hat{h}_j(s_j(t_m)) - \sum_{m=1}^{q} [s_j(t_m) - s_j(t_{m-1})] \hat{h}_i(s_i(t_m)).
\tag{5.1.11}
$$

The proposed algorithm and equations (5.1.8)–(5.1.11) provide the MLEs of $(\kappa, \sigma^2, \Delta)$ for components of a single system. We can also use a historical data set that consists of degradation signals from N independent systems. In this case, we can apply a two-stage procedure similar to the one proposed in [84] to obtain estimates for the N systems. To do this, we first obtain the MLEs of $(\kappa, \sigma^2, \Delta)$ for each individual system. Since Δ is deterministic, it can be estimated using a sample average of its MLEs. For $\hat{\kappa}$ and $\hat{\sigma}^2$, we fit their MLEs obtained from the individual systems to the desired prior distributions. Once these parameters are estimated, the degradation model can now be applied to estimate the residual lifetimes of interdependent components of systems that are functioning in the field. Real-time signal observations from the components of these fielded systems are

used to update the stochastic parameters of the degradation model based on the latest degradation states of these components and their interactions. Consequently, more accurate predictions of their residual life distributions can be obtained.

5.1.3 Updating the Degradation Model Using Real-Time Degradation Signals

In this section, we discuss a Bayesian updating framework that utilizes *in-situ* degradation signals from components of fielded systems in order to update their residual lifetime predictions. Specifically, the observed degradation signals are used to update the prior distributions of κ and σ^2. First, we assume that the prior distribution of σ_i^2 follows an inverse Gamma distribution, i.e. $\sigma_i^2 \sim \Gamma^{-1}(\xi_i, \theta_i)$. $\Gamma^{-1}(\xi, \theta)$ represents an inverse Gamma distribution with shape parameter ξ and scale parameter θ. Conditional on σ_i^2, assume that κ_i has a normal prior distribution $\kappa_i | \sigma_i^2 \sim N(\mu_i, \tau_i \sigma_i^2)$ for $i = 1, \ldots, n$, where $N(\mu, \sigma^2)$ represents a normal distribution with mean μ and variance σ^2. These two prior distributions are chosen for a few pragmatic reasons. First, the gamma distribution encompasses a number of important distributions (e.g., exponential, Erlang, and chi-square); second, the normal distribution is widely used to model a mixture of populations; third, such prior distributions yield a closed-form density function of the posterior distributions (see Proposition 5.1.1 by Berger (1985)) that is easy to use.

Now, consider a system operating in the field that consists of n critical components. Assume that we can monitor (in real-time) the degradation signals of these critical components at times $t_0^*, t_1^*, \ldots, t_k^*$, where t_k^* represents the time of the most recent observation epoch. Denote the corresponding signal observations by $s(t_0^*), s(t_1^*), \ldots, s(t_k^*)$, respectively, where $s(t_m^*) = (s_1(t_m^*), s_2(t_m^*), \ldots, s_n(t_m^*))'$, for $m = 0, 1, \ldots, k$. Furthermore, assume $\epsilon_t^* = t_1^* - t_0^* = t_2^* - t_1^* = \ldots = t_k^* - t_{k-1}^*$. Let $\mathcal{S}_k^*$ represent the set of real-time signal observations up to time t_k^*, i.e., $\mathcal{S}_k^* = (s(t_0^*), s(t_1^*), \ldots, s(t_k^*))$. Using Proposition 5.1.1, we can express the posterior distributions of (κ_i, σ_i^2) given $\mathcal{S}_k^*$, where κ_i is the inherent degradation rate of component C_i and σ_i^2 is its diffusion parameter.

Proposition 5.1.1. *(Berger, 1985) Given $\mathcal{S}_k^*$, the posterior probability density function (p.d.f.) of (σ_i^2, κ_i), denoted by $\pi_i(\kappa_i, \sigma_i^2 | \mathcal{S}_k^*)$, is given by*

$$\pi_i(\kappa_i, \sigma_i^2 | \mathcal{S}_k^*) = \pi_{i,1}(\kappa_i | \sigma_i^2, \mathcal{S}_k^*) \pi_{i,2}(\sigma_i^2 | \mathcal{S}_k^*),$$

where $\pi_{i,1}(\kappa_i|\sigma_i^2, \mathcal{S}_k^*)$ represents the p.d.f. of a normal distribution with mean $\tilde{\mu}_i$ and variance $\tilde{\tau}_i \sigma_i^2$, and $\pi_{i,2}(\sigma_i^2|\mathcal{S}_k^*)$ represents the p.d.f. of an inverse Gamma distribution with shape parameter $\tilde{\xi}_i$ and scale parameter $\tilde{\theta}_i$. Here, $\tilde{\mu}_i, \tilde{\tau}_i, \tilde{\xi}_i$, and $\tilde{\theta}_i$ for $i = 1, \ldots, n$ are computed as follows:

$$\tilde{\mu}_i = \frac{\mu_i + \epsilon_t^* \tau_i \sum_{m=1}^{k} x_{i,m}}{1 + k\tau_i \epsilon_t^*},$$

$$\tilde{\tau}_i = \frac{1}{k\epsilon_t^* \tau_i + 1} \tau_i,$$

$$\tilde{\xi}_i = \xi_i + k/2,$$

$$\tilde{\theta}_i = \theta_i + \frac{\epsilon_t^*}{2} \sum_{m=1}^{k} (x_{i,m} - \bar{x}_i)^2 + \frac{k\epsilon_t^*(\bar{x}_i - \mu_i)^2}{2(1 + k\epsilon_t^* \tau_i)}$$

where $x_{i,m} = \frac{s_i(t_m^*) - s_i(t_{m-1}^*)}{\epsilon_t^*} - \sum_{j \neq i} s_j(t_m^*)\delta_{j,i}$ and $\bar{x}_i = \frac{1}{k} \sum_{m=1}^{k} x_{i,m}$ for $m = 1, \ldots, k$.

Given the observed degradation signals, $\mathcal{S}_k^*$, the posterior distribution of σ_i^2 follows an inverse Gamma distribution, i.e., $\sigma_i^2|\mathcal{S}_k^* \sim \mathbf{\Gamma}^{-1}(\tilde{\xi}_i, \tilde{\theta}_i)$, and the posterior distribution of $\kappa_i|\sigma_i^2$ follows a normal distribution, i.e., $\kappa_i|\sigma_i^2, \mathcal{S}_k^* \sim N\left(\tilde{\mu}_i, \tilde{\tau}\sigma_i^2\right)$. In Proposition 5.1.2, we show that the posterior marginal distribution of κ_i for $i = 1, \ldots, n$ follows a $\mathcal{T}$ distributions.

Proposition 5.1.2. *If $\sigma_i^2 \sim \mathbf{\Gamma}^{-1}(\xi_i, \theta_i)$ and $\kappa_i|\sigma_i^2 \sim N(\mu_i, \tau_i\sigma_i^2)$, the marginal distribution of κ_i follows $\mathcal{T}$ distribution $\mathcal{T}(2\xi_i, \mu_i, \tau_i/(\xi_i\theta_i))$.*

Proof. The p.d.f. of a random variable X, which follows $\mathcal{T}$ distribution $\mathcal{T}(\alpha, \mu, \gamma^2)$, is expressed as follows

$$f_{\mathcal{T}}(x) = \frac{\Gamma[(\alpha + 1)/2]}{\gamma(\alpha\pi)^{1/2}\Gamma(\alpha/2)} \left(1 + \frac{(x - \mu)^2}{\alpha\gamma^2}\right)^{-(\alpha+1)/2}.$$

Proposition 5.1.2 can be proven by integrating over σ_i^2 the joint probability density of κ_i and σ_i^2. The details are omitted in this paper. □

Thus, by Proposition 5.1.2, the posterior marginal distribution of κ_i denoted by $\kappa_i|\mathcal{S}_k^*$ follows a $\mathcal{T}$ distribution expressed as $\kappa_i|\mathcal{S}_k^* \sim \mathcal{T}\left(2\tilde{\xi}_i, \tilde{\mu}_i, \frac{\tilde{\tau}}{\tilde{\xi}_i\tilde{\theta}_i}\right)$ for $i = 1, \ldots, n$. If we let κ_i^* and σ_i^{*2} denote the posterior means of κ_i and σ_i^2, then κ_i^* and σ_i^{*2} can be estimated using the following expressions.

$$\kappa_i^* = \mathbb{E}(\kappa_i|\mathcal{S}_k^*) = \tilde{\mu}_i, \quad \text{and } \sigma_i^{*2} = \mathbb{E}(\sigma_i^2|\mathcal{S}_k^*) = \frac{\tilde{\theta}_i}{(\tilde{\xi}_i - 1)}. \tag{5.1.12}$$

The updated values of κ_i^* and σ_i^{*2} can be used to revise the predicted residual life distribution of component C_i, for $i = 1, \ldots, n$. The updating process can be performed each time when new degradation signals are observed.

5.1.4 Estimating the Residual Life Distributions of Components Using Real-Time Degradation Signals

The residual life distribution of a partially degraded component is the distribution of the time it takes for a partial degradation signal to reach a predefined failure threshold. If we let $R_{i,k}$ denote the first-passage time of the degradation signal $S_i(t)$ to a threshold level d_i, given that it has not crossed d_i up to time t_k^*, then the random variable $R_{i,k}$ represents the residual lifetime of component C_i at time t_k. Thus, the residual lifetime can be written as $R_{i,k} = \inf\{u > 0 : S_i(t_k^* + u) \geq d_i\}$ and express its cumulative distribution function (c.d.f.) given $(\kappa_i^*, \sigma_i^{*2}, S_k^*)$ as follows:

$$\mathbb{P}(R_{i,k} \leq t - t_k^* | \kappa_i^*, \sigma_i^{*2}, S_k^*) = \mathbb{P}\left(\sup_{t_k^* < u \leq t} S_i(u) \geq d_i \middle| \kappa_i^*, \sigma_i^{*2}, S_k^* \right). \tag{5.1.13}$$

We note that given $(\kappa_i^*, \sigma_i^{*2}, S_k^*)$, the degradation signal can be characterized by two terms

$$S_i(t) = \vartheta_{i,k}(t) + \sigma_i^* W_i(t - t_k^*)$$

where $W_i(t)$ represents a standard Wiener process, and $\vartheta_{i,k}(v) = s_i(t_k^*) + \int_{t_k^*}^t \left(\kappa_i^* + \sum_{j \neq i} \delta_{j,i} h_j(S_j(v)) \right) \mathrm{d}v$ represents the underlying path of the degradation process for component C_i after time t_k^*. In Figure 5.1.2, $\vartheta_{i,k}(t)$ is represented by the dashed line segments and the $S_i(t)$ is represented by the curves. Hence, $\vartheta_{i,k}(t)$ captures the major degradation characteristics of component C_i and and its DRIs with other components. Since the actual degradation process $\vartheta_{i,k}(t)$ is not observable due to the signal noise in many applications, we estimate the properties of $\vartheta_{i,k}(t)$ by examining the degradation signal $S_i(t)$.

The decomposition above can be used to evaluate the distribution of $R_{i,k}$ through the expression below.

$$\mathbb{P}(R_{i,k} > t - t_k^* | \kappa_i^*, \sigma_i^{*2}, S_k^*) = \mathbb{P}\left(W_i(v - t_k^*) < \frac{d_i - \vartheta_{i,k}(v)}{\sigma_i^*}, \forall t_k^* < v < t \right). \tag{5.1.14}$$

Recall that due to interactions between the degradation processes, the degradation of component C_i is affected by the influencing component C_j, for $j \neq i$. This can be seen by noting that $\vartheta_{i,k}(v)$ depends on $S_j(v)$, for any $j \neq i$. Since $S_j(v)$ is a stochastic process with its own Brownian motion term $W_j(v)$ representing signal noise, this makes $\vartheta_{i,k}(v)$ directly dependent on $W_j(v)$'s. Due to this dependency, estimating the exact future evolution of $\vartheta_{i,k}(v)$, and hence the distribution of $R_{i,k}$ becomes very challenging.

To overcome this issue, we propose an approximation for the future evolution of $\vartheta_{i,k}(v)$ by dropping the Brownian motion term $W_j(v)$ in $S_j(v)$. Since $W_j(v)$ only represents the signal noise for component C_j, this assumption can be considered a reasonable one. As a result, $\vartheta_{i,k}(t)$ can be approximated as

$$\widehat{\vartheta}_{i,k}(t) = s_i(t_k^*) + \int_{t_k^*}^{t} \left(\kappa_i^* + \sum_{j \neq i} \delta_{j,i} h_j(\widehat{\vartheta}_{j,k}(v)) \right) \mathrm{d}v.$$

The approximated degradation path $\widehat{\vartheta}_{i,k}(t)$ is a deterministic piecewise linear function in t for $t > t_k^*$. To see this, assume that at time t_k, there are n_k future DRI events that occur at the following times $v_1, v_2, \ldots, v_{n_k}$, such that $t_k^* \equiv v_0 < v_1 < v_2 < \ldots < v_{n_k}$. This implies that during the interval $[v_{\ell-1}, v_\ell)$, the degradation state function $h_j(\widehat{\vartheta}_{j,k}(t))$ remains constant for $t \in [v_{\ell-1}, v_\ell)$, $\ell = 1, \ldots, n_k$. Thus, if $h_j(\widehat{\vartheta}_{j,k}(t)) = \zeta_{j,\ell}$ for $t \in [v_{\ell-1}, v_\ell)$, the slope of $\widehat{\vartheta}_{i,k}(t)$ can be expressed as $\kappa_i^* + \sum_{j \neq i} \delta_{j,i} \zeta_{j,\ell}$. A similar scenario occurs at subsequent time intervals, i.e., after the DRI event at time v_ℓ, the slope changes due to the effect of degradation interaction from other components and become $\kappa_i^* + \sum_{j \neq i} \delta_{j,i} \zeta_{j,\ell+1}$, and so forth.

We can therefore use this approximation to estimate the probability distribution expressed by equation (5.1.14) as follows:

$$\mathbb{P}(R_{i,k} > t - t_k^* | \kappa_i^*, \sigma_i^{*2}, \mathcal{S}_k^*) = \mathbb{P}\left(W_i(v - t_k^*) < \frac{d_i - \widehat{\vartheta}_{i,k}(v)}{\sigma_i^*}, \forall t_k^* < v < t \right). \tag{5.1.15}$$

If we let $b_{i,k}(t) \equiv \frac{d_i - \widehat{\vartheta}_{i,k}(t)}{\sigma_i^*}$, the problem of estimating the distribution of the residual life becomes equivalent to finding the first passage time probability of a Brownian motion given a piecewise linear boundary. It should be noted that boundary crossing probabilities for BM processes have been well-studied in the literature (cf. [117], [128]). For instance, Siegmund [117] derived the (conditional) probability that a BM process crosses the linear boundary in this interval, i.e., when the function $b_{i,k}(t)$ is linear in $[t_k^*, t]$. This result was later extended to the case where the boundary was a piecewise linear function by Wang and Potzelberger in [128]. In this work, we rely on Theorem 1 of [128] to approximately estimate the residual life distribution of a partially degraded component that experiences degradation interactions with other components of a given system.

Theorem 5.1.1. *(Wang and Potzelberger, 1997) Let $t_k^* \equiv v_0 < v_1 < v_2 < \ldots < v_{n_k} < t$. Suppose $b_{i,k}(t)$ is linear on $[v_{\ell-1}, v_\ell]$, $\ell = 1, \ldots, n_k$. Then for each $v \in [t_k^*, t]$, the complement of the first*

passage probability of a Brownian motion process, $W_i(t)$, is given by

$$\mathbb{P}\left(W_i(v - t_k^*) < b_{i,k}(v), \forall t_k^* < v < t\right) \approx \mathbb{E}[H_{i,k}(W_i(v_1), \ldots, W_i(v_{n_k}))], \qquad (5.1.16)$$

where

$$H_{i,k}(x_1, x_2, \ldots, x_{n_k}) = \prod_{\ell=1}^{n_k} \left\{ \mathbf{1}(x_\ell < b_{i,k}(v_\ell)) \left(1 - \exp\left[-\frac{2(b_{i,k}(v_{\ell-1}) - x_{\ell-1})(b_{i,k}(v_\ell) - x_\ell)}{v_\ell - v_{\ell-1}} \right] \right) \right\}.$$

Equation (5.1.16) is not easy to compute because it requires multidimensional integration. To circumvent this complication, we use a Monte-Carlo simulation procedure to estimate the right-hand side of (5.1.16). The details can be found in [128].

5.2 Numerical Studies

In this section, we investigate the performance of our proposed DRI degradation model. We focus on evaluating the accuracy of predicting the residual lifetimes of partially degraded components from a hypothetical system in which components are assumed to exhibit degradation interactions. We study several scenarios for various key model parameters. Specifically, we investigate the impact of different levels of degradation signal noise, which is captured by σ_i^2 of our model. This is important because it allows us to evaluate the maximum signal noise level beyond which changes in the degradation rates, which result from interaction, are masked by the noise. Second, we investigate the impact of different magnitudes of degradation interaction. In other words, we study the effects of different levels by which the rate of the degradation signal changes at a DRI event, i.e., $\delta_{i,j}$ for any two components C_i and C_j. This enables us to identify the lowest level of rate changes resulting from DRIs at which our model becomes almost equivalent to models that do not consider any interactions between the degradation processes or simply assume independence. Finally, we study the effect of the number of degradation states M_i on the accuracy of predicting the residual lifetime.

As a case in point, we consider a system with three constituent components. These components are assumed to be interdependent, and thus their degradation processes exhibit interactions that are manifested in their degradation signals. For the purpose of this study, we simulate degradation signals for all three components using equation (5.1.3) with $n = 3$. To simulate degradation signals for the different scenarios, we consider two experimental settings. The first experiment, Experiment

94

I, focuses on different combinations of noise and interaction magnitude. We begin by considering σ_i^2 which represents the level of signal noise for some component C_i. Recall that σ_i^2 is the diffusion parameter of the signal model and has a prior distribution that is assumed to be an inverse-Gamma distribution, i.e., $\sigma_i^2 \sim \mathbf{\Gamma}^{-1}(\xi_i, \theta_i)$. Next, we note that $\delta_{i,j}$ represents the magnitude of the DRI event, i.e., the incremental change in the degradation rate of component C_j when component C_i transitions to a more severe state. To facilitate our simulation, we start with a baseline setup with parameter values chosen according to Table 5.2.1. We then define two scale factors, m_1 and m_2. m_1 is used to define different noise levels whereas m_2 is used to scale $\delta_{i,j}$. Thus, for the first experiment, we use the following simulation settings.

Experiment I: (Assessing the effects of σ_i^2 and $\delta_{i,j}$). Suppose

$$(\theta_i, \delta_{i,j}) \in \{(m_1 \times \theta_i^{\text{base}}, m_2 \times \delta_{i,j}^{\text{base}}) : m_1, m_2 = 1, 2, \dots, 20\}.$$

Thus, the prior mean of σ_i^2 equals $0.1, 0.2, \dots, 1.9, 2.0$.

In the second experiment, we study the relationship between the accuracy of the predicted RLDs and the number of degradation states M_i. We also define a scaling factor m_3 for the number of degradation states. The simulation settings for Experiment II are summarized below.

Experiment II: (Assessing the effect of M_i). Suppose $M_i \in \{M_i^{\text{base}} + m_3 : m_3 = 0, 1, \dots, 9\}$.

For each scenario, we simulate component degradation signals for 100 systems. For each system, the degradation signals of its components are simulated using the following procedure:

Step C.1: For $i = 1, \dots, 3$, sample from the prior distributions of σ_i^2 and κ_i according to Experiments I and II. The realizations are denoted by $\tilde{\sigma}_i^2$ and $\tilde{\kappa}_i$.

Step C.2: Set $s_i(0) = 0$, use $\tilde{\sigma}_i^2$ and $\tilde{\kappa}_i$ to simulate the degradation signal $s_i(t)$, $i = 1, \dots, 3$ according to the model below until it first hits the failure threshold d_i, i.e., simulate until time L_i, where $L_i = \inf\{u \geq 0 : s_i(u) \geq d_i\}$ represents the lifetime of component C_i:

$$s_i(t) = s_i(0) + \int_0^t \left[\tilde{\kappa}_i + \sum_{j \neq i} \delta_{j,i} h_j(s_j(v)) \right] dv + \tilde{\sigma}_i W_i(t).$$

Table 5.2.1: Baseline parameter values for the discrete model.

Component Index	Component C_1	Component C_2	Component C_3
d_i	300	300	300
M_i^{base}	3	3	3
μ_i	1.8	1.4	2.3
τ_i	0.2	0.3	0.1
ξ_i	92	92	92
θ_i^{base}	9.1	9.1	9.1
$\delta_{1,i}^{\text{base}}$	0	0.12	0.23
$\delta_{2,i}^{\text{base}}$	0.04	0	0.02
$\delta_{3,i}^{\text{base}}$	0.05	0.07	0

Table 5.2.2: Results for estimated baseline parameters.

Component Index	Component C_1	Component C_2	Component C_3
$\widehat{M}_i^{\text{base}}$	3	3	3
$\hat{\mu}_i$	1.82	1.43	2.23
$\hat{\tau}_i$	0.32	0.26	0.18
$\hat{\xi}_i$	87	95	98
$\hat{\theta}_i^{\text{base}}$	9.2	8.9	9.0
$\hat{\delta}_{1,i}^{\text{base}}$	0	0.119	0.231
$\hat{\delta}_{2,i}^{\text{base}}$	0.043	0	0.022
$\hat{\delta}_{3,i}^{\text{base}}$	0.046	0.077	0
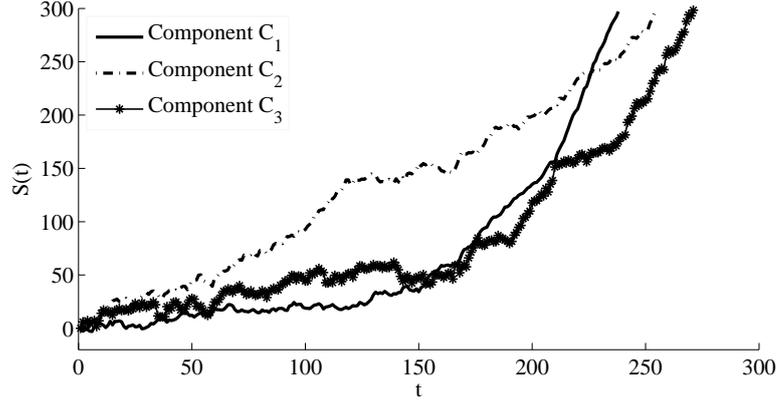
Figure 5.2.1: Example of simulated degradation signals from a system of three components.

Figure 5.2.1 provides a plot of a sample of simulated degradation signals using the baseline values defined in Table 5.2.1 and the following values for scaling factors: $m_1 = 3$, $m_2 = 10$, and $m_3 = 0$. The degradation signals are divided equally into two groups. The first group consists of 50 randomly chosen degradation signals. This group represents the historical degradation database and is used to estimate the deterministic and stochastic parameters of our degradation model. Specifically, these degradation signals are used to estimate matrix Δ, and the prior distributions of κ and σ^2. The results of the estimated baseline parameters are summarized in Table 2. The second group consists of the remaining 50 signals, hereafter referred to as validations signals. These signals are used to emulate *in-situ* component degradation signals that are observed from systems still operating in the field. The individual signal observations associated with each component are used to update the prior distributions of the stochastic model parameters, and in turn revise its predicted residual life distribution. Equation (5.1.15) is used to compute the updated RLDs using the validation signals.

To evaluate the performance of our proposed model, we compare the predicted lifetime of each component at different life percentiles with its actual failure time T_i for $i = 1, \ldots, 3$. Specifically, the predicted lifetimes are evaluated at the 50th, 70th, and 90th life percentiles. To do this, let $\hat{T}_i$ be the predicted lifetime of component C_i. $\hat{T}_i$ is calculated using the following expression, $\hat{L}_i = t_k^* + \hat{R}_{i,k}$, where $\hat{R}_{i,k}$ is the median of the posterior RLD updated using the degradation signals of component C_i (for $i = 1, \ldots, 3$) that have been observed up to time t_k^*. Note that $\hat{T}_i$ is evaluated at each life percentile. In other words, for the three life percentiles defined above, $t_k^* = 0.5T_i$, $t_k^* = 0.7T_i$, and

97

$t_k^* = 0.9T_i$. Corresponding prediction errors are then computed for each life percentile using the following expression

$$e_i = \frac{|T_i - \hat{T}_i|}{T_i} \times 100.$$

The overall prediction error for all three components of a given system is given by $\bar{e} = \sum_{i=1}^{3} e_i/3$.

To demonstrate the importance of modeling degradation interactions, we apply a benchmark model that was developed in [47] to the same set of simulated signals. We also compute the corresponding prediction errors at the same life percentiles. We could have chosen other benchmark approaches, but we focus on this specific model for the following reasons: (1) this benchmark model is similar in spirit to our proposed model in that it models that degradation signal as a stochastic process with a Brownian error term, however unlike our modeling approach it does not account for any component interdependencies and degradation interactions; and (2) similar to our approach, this benchmark model also utilizes real-time degradation signals to update the degradation model and the component RLDs. Therefore, using this benchmark is a reasonable choice because it helps demonstrate that any potential improvements in the accuracy of predicting residual lifetimes originate solely from the consideration of component DRIs.

Results of Experiment I. In Experiment I, we study how different levels of signal noise and interaction magnitudes affect the accuracy of predicting a component's residual lifetime. Figure 2(a) shows six plots of the mean prediction error (in %) evaluated at three designated life percentiles. The upper row summarizes the prediction errors from our proposed DRI model and the lower row plots those resulting from applying the benchmark model. In both cases, the prediction errors are computed using the validation degradation signals. Furthermore, prediction errors are evaluated for 20 different levels of signal noise, i.e., $\theta_i = m_1 \times \theta_i^{\text{base}}$ where $m_1 = 1, \ldots, 20$, and 20 different levels of DRI magnitudes by which the degradation rate of an affected component can change at a DRI event, i.e., $\delta_{i,j} = m_2 \times \delta_{i,j}^{\text{base}}$ for $m_2 = 1, \ldots, 20$. The corresponding sample variance of the prediction errors are shown in (Figure 2(b)).

The plots in Figure 2(a) illustrate that the average prediction errors (%) increase as the magnitude of interaction parameter $\delta_{i,j}$ increases. A similar trend can also bee seen as the signal noise
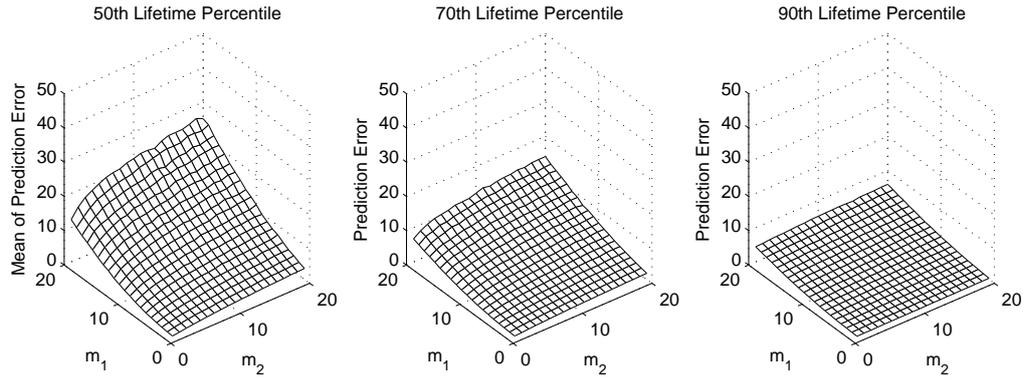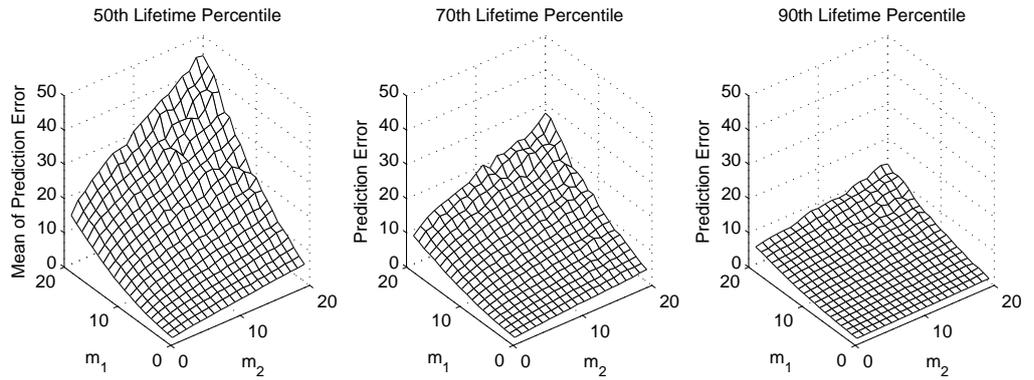
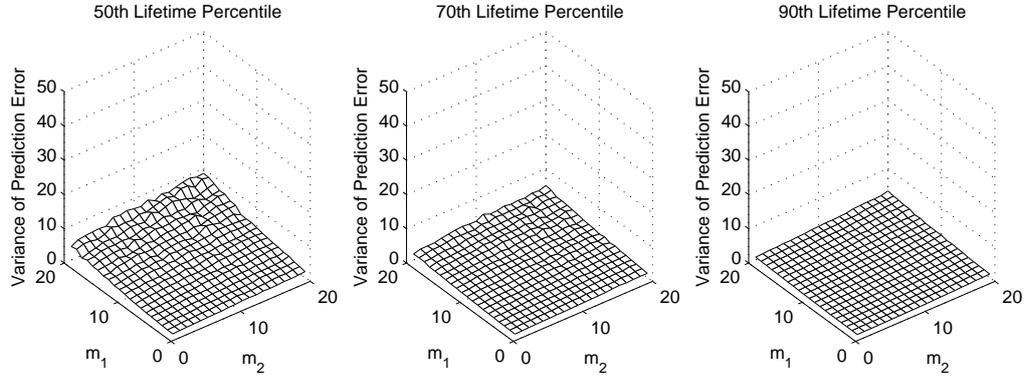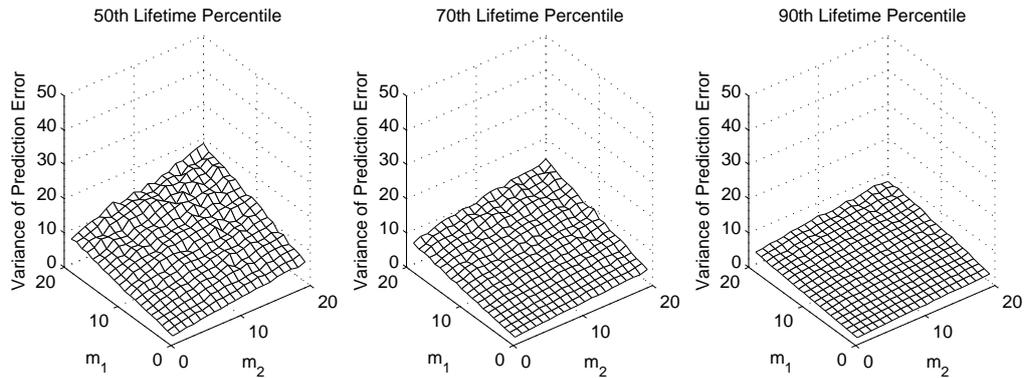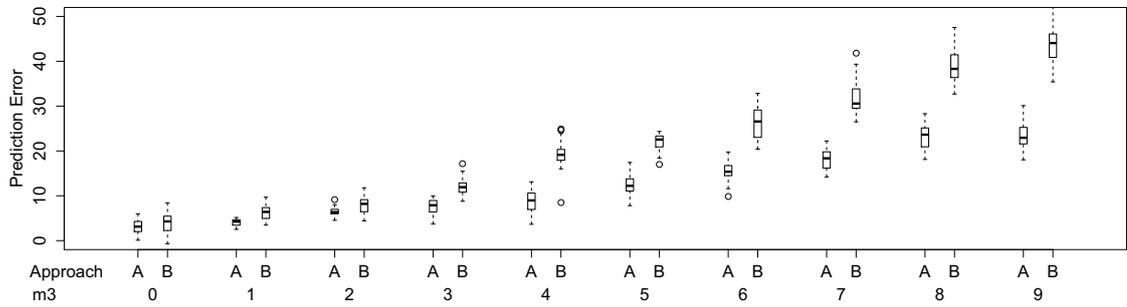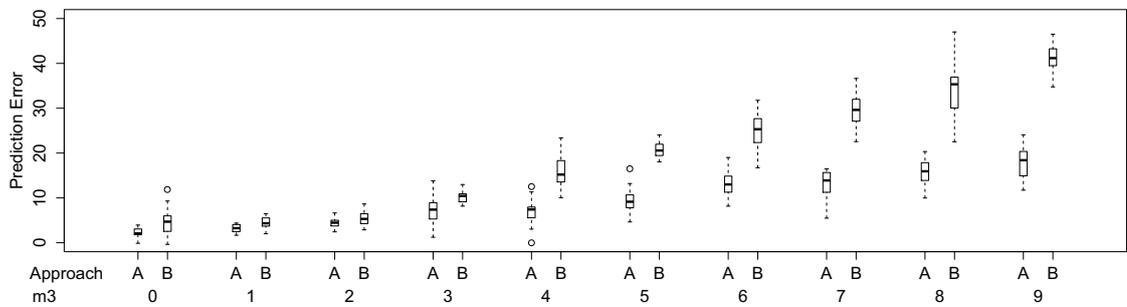(a) Sample Mean of Prediction Error

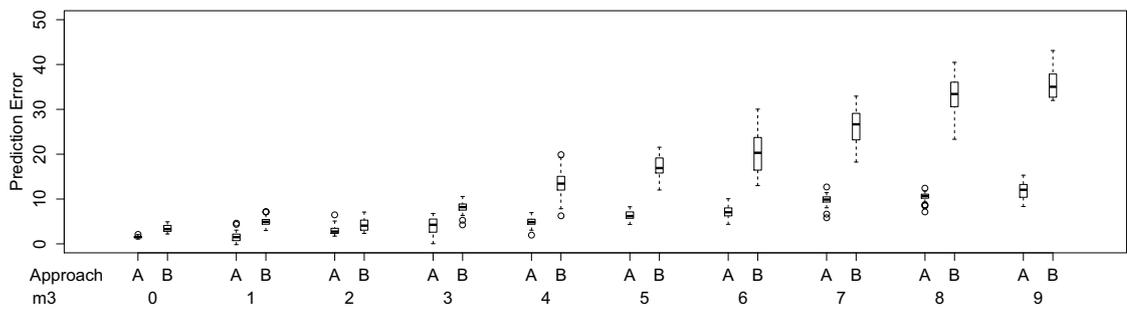(b) Sample Variance of Prediction Error

Figure 5.2.2: Prediction error from Group 1 simulation study. m_1: signal noise. m_2: component

(a) 50th Life Percentile

(b) 70th Life Percentile

(c) 90th Life Percentile

Figure 5.2.3: Prediction error from Group 2 simulation study. m_3: the number of degradation states. Approach A: our proposed model. Approach B: the benchmark model.

increases. If we focus on the small values of m_2, for example $m_2 = 0$, it is obvious that the prediction error increases as m_1—scale parameter associated with the signal noise—increases for both the DRI model and the benchmark model.

On the other hand, by comparing the plots of the upper and lower rows of Figure 2(a) along the m_2 axis, we can see that although the prediction error increases our approach performs significantly better than the benchmark model. Intuitively speaking, increasing m_2 implies that the effects of degradation interactions become more pronounced, i.e., the changes in the degradation rates are greater. It is therefore reasonable to conclude that our approach outperforms the benchmark model because it captures the effects of DRIs.

By studying the plots from left to right, we can see that the average prediction error decreases when the prediction is made at later life percentiles. We believe that one of the primary reasons for this is the Bayesian updating procedure which incorporates the real-time behavior of each component. Furthermore, the difference in prediction errors of our approach and those of the benchmark decrease for predictions made at later life percentile. In fact, there is little difference between the two models for relatively smaller values of m_1 and m_2 (< 10), at the 90th life percentile. One may attribute this phenomenon to the fact that we expect to see significantly fewer degradation interactions beyond the 90th percentile compared, for example, to the 50th percentile.

The plots of the variance of the prediction error shown in Figure 2(b) show that the values of the error variance resulting from our approach are significantly lower than the benchmark. The differences become more pronounced for larger values of m_1 and m_2. This observation may indicate the relative robustness of our approach.

Results of Experiment II. This numerical experiment examines how the number of degradation states affects the accuracy of predicting component RLDs. Recall that the degradation signals are simulated with the number of degradation states $M_i = M_i^{\text{base}} + m_3, m_3 = 0, \ldots, 9$. Thus, M_i increases as m_3 increases. Figure 5.2.3 presents boxplots for prediction errors resulting from our approach versus the benchmark model for different values of m_3. Approach A represents the results of our proposed model, and Approach B corresponds to the benchmark model [47].

It is clear that as the number of degradation states (characterized by m_3) increases, the mean and the variance of the prediction errors associated with the benchmark model (Approach B) increase

significantly, whereas those corresponding to our model (Approach A) are relatively less affected. We believe that when m_3 increases, DRI events that take place between the components become more evident. Since the benchmark model does not capture the effects of DRIs, which results in higher prediction errors.

We can also see that the prediction errors at the 90th life percentile are lower than those at the that at the 50th. Once again, we believe that this is because at the 90th percentile more real-time degradation signals are used to update the degradation model. This observation echoes with our observation from Experiment I, which indicates that updating the RLD using real-time signal improves the prediction accuracy.

CHAPTER VI

STOCHASTIC FRAMEWORK FOR SYSTEMS WITH CONTINUOUS

INTERACTIVE DEGRADATION SIGNALS

This chapter focuses on modeling degradation-rate-interactions (DRIs) that occur in a continuous manner. Specifically, changes in the degradation rate of a component is continuously affected by the amplitudes of degradation signals of other components. To model such dynamics among the degradation signals of components in a given system, we utilize the approach of SDE systems, the coefficient matrix of which characterizes the inter-dependency among system components. One major advantage of using an SDE approach is that we can exploit the mathematical tools of Ito's formulae and express the component RLDs in closed-form expressions. Once the degradation model is established, we utilize the real-time degradation signals from the components of a system functioning in the field to update the model parameters and the component/system residual life distributions in a Bayesian manner. To validate our methodology, we conduct a series of simulation studies for testing the prediction accuracy with various of model parameters. The results are compared with a benchmark model, which does not consider component interactions. We demonstrate that incorporating the effects of component interactions significantly improves the prediction accuracy of RLDs.

The remainder of this chapter is organized as follows : Section 6.1 describes a SDE degradation model that captures the continuous DRIs among the constituent components of a given multi-component system with two special cases. In Section 6.3, we discuss how to estimate the model parameters using a historical data set and update the established model as well as the component/system RLDs using the real-time observations of degradation signals. In Section 6.4, we present a series of simulation studies that evaluate the performance of the proposed model.

6.1   General Stochastic Degradation Framework

In this section, we present a method for stochastically modeling the degradation signals of dependent components and how their degradation processes affect each other. We consider a system of n interconnected components, $C_1, C_2, \ldots, C_n$ with degradation signals denoted by $S_1(t), S_2(t), \ldots, S_n(t)$, respectively. For notational convenience, we let $\boldsymbol{S}(t) = (S_1(t), S_2(t), \ldots, S_n(t))'$.

We define $r_i(t)$ as the rate at which the degradation signal of component C_i increases (or decreases) over time. Hereafter, we refer to this as the degradation rate since the amplitude of the

signal is correlated with physical degradation. Let $\boldsymbol{r}(t) = (r_1(t), \ldots, r_n(t))'$. Assume that $\boldsymbol{r}(t)$ consists of two parts: (1) $\boldsymbol{\kappa}$, where $\boldsymbol{\kappa} = (\kappa_1, \ldots, \kappa_n)'$ represents the natural degradation rates of system components, i.e., κ_i represents the degradation rate of component C_i without the effect of any interactions from other components; and (2) $\boldsymbol{h}(\boldsymbol{S}(t))$, which captures the effects of DRIs (degradation-rate-interactions) on the degradation rate. We assume that the degradation rates of system components can be expressed as $\boldsymbol{r}(t) = \boldsymbol{\kappa} + \boldsymbol{h}(\boldsymbol{S}(t))$. Using this setup, the degradation signals of different components in a system can be described by the following equation

$$\mathrm{d}\boldsymbol{S}(t) = [\boldsymbol{\kappa} + \boldsymbol{h}(\boldsymbol{S}(t))]\mathrm{d}t + \mathrm{d}\boldsymbol{\epsilon}(t), \tag{6.1.1}$$

where $\boldsymbol{\epsilon}(t) \in \mathbb{R}^n$ represents the noise content in the degradation signals.

Equation (6.1.1) presents our stochastic DRI modeling framework. In other words, the amplitude of the degradation signal and the path that it follows, both capture the degradation level of the respective component in addition to the degradation effects resulting from other components in the system. In this framework we make the following key assumptions:

(1) If two components exhibit a DRI, the degradation rate of one component is linearly increasing in the degradation level of the other. That is, the function $\boldsymbol{h}(\boldsymbol{S}(t))$ assumes a linear form $\boldsymbol{h}(\boldsymbol{S}(t)) = \boldsymbol{\Delta} \times \boldsymbol{S}(t)$, where $\boldsymbol{\Delta} \in \mathbb{R}^{n \times n}$ characterizes the magnitudes of DRIs. Recall that $\boldsymbol{S}(t)$ is the amplitudes of the degradation signals and represents the degradation levels of components.

(2) Signal noise follows a Brownian motion process. That is, $\boldsymbol{\epsilon}(t) = \boldsymbol{B}(t)$, where

$$\boldsymbol{B}(t) = (B_1(t), \ldots, B_n(t))'.$$

Here, $B_1(t), \ldots, B_n(t)$ are independent Brownian motion processes with diffusion parameters $\sigma_1^2, \ldots, \sigma_n^2$, respectively, i.e., $B_i(t) \sim N(0, \sigma_i^2 t)$ for $i = 1, \ldots, n$. In other words, $\boldsymbol{B}(t) \sim MVN(\boldsymbol{0}, \boldsymbol{\Pi_0} t)$, where $\boldsymbol{\Pi_0} = \mathrm{diag}\{\sigma_1^2, \ldots, \sigma_n^2\}$.

(3) $\boldsymbol{\Delta}$ is a deterministic parameter that is fixed and determined by the characteristics of the systems, including the structure, the function, the operating condition of the systems as well as the types of individual components, which can also be estimated using data.

(4) κ and σ^2, where $\sigma^2 = (\sigma_1^2, \sigma_2^2, \ldots, \sigma_n^2)'$, are stochastic parameters that may vary even among identical components due to the variations in the manufacturing processes, material inhomogeneities, and other factors, and other factors (cf. [47, 133]). Hence, these parameters are assumed to follow some distributional form across the population of units, with those of the individual device being an unknown "draw" from the population.

Given these assumptions, equation (6.1.1) can be rewritten in the following form:

$$\mathrm{d}S(t) = [\kappa + \Delta \times S(t)]\mathrm{d}t + \mathrm{d}B(t). \tag{6.1.2}$$

Figure 6.1.1 provides an example of degradation signals from a system of 3 components with continuous DRIs.
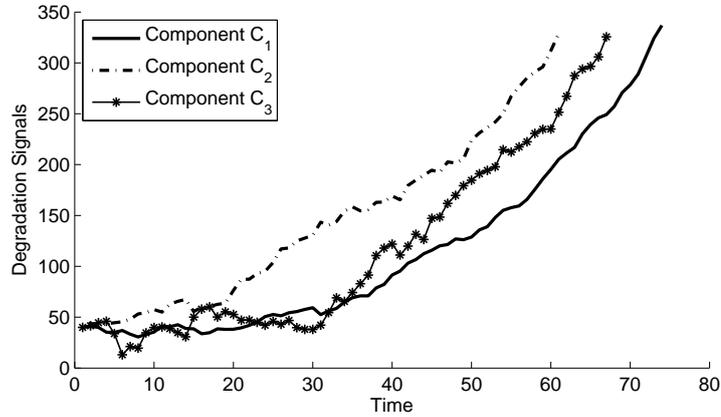

Figure 6.1.1: Example of degradation signals with continuous interactions in a 3-component system.

6.1.1 Estimating Component Lifetime Distributions

For each component, say C_i, we assume that failure occurs when its degradation signal $S_i(t)$ crosses a pre-specified threshold d_i. We let T_i be the failure time of component C_i. In this case, T_i is the first-passage-time of $S_i(t)$ to d_i. However, estimating the first-passage probability of $S_i(t)$ is generally very challenging, and a closed-form expression is usually unavailable. Here, we circumvent this challenge by introducing an approximation:

$$\mathbb{P}(T_i > t) \approx \mathbb{P}(S_i(t) < d_i). \tag{6.1.3}$$

106

Similar approximations of failure probability have been utilized in many reliability publications such as [132], [47], [134], and other papers. This technique is a very reasonable when the signal noise (σ_i^2) is not too large. Hereafter, we use the "=" sign, instead of "≈", in the expression of (remaining) lifetime distributions.

To evaluate the probability in equation (6.1.3), we need to understand how degradation signals $S(t)$ evolve in future. To this end, we solve the system of stochastic differential equations (SDEs) as described in equation (6.1.2) with initial condition $S(0) = s_0$, where s_0 represents the vector of initial degradation levels for components in the system. [61] presented a general procedure for the solving the system linear SDEs. Proposition 6.1.1 below applies this procedure and provides a closed-form expression for the transition of $S(t)$ given the values of (κ, σ^2).

Proposition 6.1.1. *For any t > 0, the solution to SDE system given* (κ, σ^2)

$$\mathrm{d}S(t) = [\kappa + \Delta \times S(t)]\mathrm{d}t + \mathrm{d}B(t)$$

$$S(0) = s_0$$

is expressed as follows

$$S(t)|(\kappa, \sigma^2) = \exp(t\Delta) \times s_0 + \int_0^t \exp[(t-s)\Delta] \times \kappa\,\mathrm{d}s + \int_0^t \exp[(t-s)\Delta]\mathrm{d}B(s). \qquad (6.1.4)$$

1

Proof. To solve for the SDE system, we introduce an integrating factor $\exp(-t\Delta)$, which is a matrix exponential. Recall that for any matrix A, where $A \in \mathbb{R}^{n \times n}$, matrix exponential $\exp(A)$ is defined as $\exp(A) = \sum_{\ell=0}^{\infty} \frac{1}{\ell}A^\ell$. Here, $\exp(-t\Delta)$ satisfies the following equation

$$\mathrm{d}\exp(-t\Delta) = -\Delta \times \exp(-t\Delta)\mathrm{d}t \qquad (6.1.5)$$

Next, we consider the differentiation of $\exp(-t\Delta) \times S(t)$. By Ito's formula in n-dimensions, we have

$$\mathrm{d}(\exp(-t\Delta) \times S(t)) = \mathrm{d}\exp(-t\Delta) \times S(t) + \exp(-t\Delta) \times \mathrm{d}S(t) + \mathbf{0}.$$

Plug in equations (6.1.2) and (6.1.5) for the expressions of $d \exp(-t\Delta)$ and $dS(t)$, respectively. We have

$$d(\exp(-t\Delta) \times S(t)) = -\Delta \exp(-t\Delta)S(t)dt + \exp(-t\Delta)\{[\kappa + \Delta \times S(t)]dt + dB(t)\} \quad (6.1.6)$$

$$= \exp(-t\Delta) \times \kappa \, dt + \exp(-t\Delta)dB(t) \quad (6.1.7)$$

Integrating both sides from 0 to t, we have

$$\exp(-t\Delta \times S(t)) - s_0 = \int_0^t \exp(-s\Delta) \times \kappa \, ds + \int_0^t \exp(-s\Delta)dB(s),$$

where the integration is calculated matrix-coefficient-wise. For instance, we denote the $(i, j)^{th}$ element of matrix $\exp(-s\Delta)$ by $e_{i,j}(s)$, which a function of variable s. Thus, the first integral $\int_0^t \exp(-s\Delta) \times \kappa \, ds$ can be expressed as follows

$$\int_0^t \exp(-s\Delta) \times \kappa \, ds = \left(\int_0^t \sum_{j=1}^n e_{1,j}(s)\kappa_j \, ds, \ldots, \int_0^t \sum_{j=1}^n e_{n,j}(s)\kappa_j \, ds \right)'$$

$$= \left(\sum_{j=1}^n \kappa_j \int_0^t e_{1,j}(s)ds, \ldots, \sum_{j=1}^n \kappa_j \int_0^t e_{n,j}(s)ds \right)'.$$

Similarly, the second integral $\int_0^t \exp(-s\Delta)dB(s)$ can be expressed as

$$\int_0^t \exp(-s\Delta)dB(s) = \left(\sum_{j=1}^n \int_0^t e_{1,j}(s)dB_1(s), \ldots, \sum_{j=1}^n \int_0^t e_{n,j}(s)dB_n(s) \right)'.$$

Note that the inverse matrix of $\exp(t\Delta)$ is $\exp(-t\Delta)$. We multiply both sides by $\exp(t\Delta)$ and solve for $S(t)$:

$$S(t) = \exp(t\Delta) \times s_0 + \int_0^t \exp[(t-s)\Delta] \times \kappa \, ds + \int_0^t \exp[(t-s)\Delta]dB(s).$$

$\square$

Based on the results of Proposition 6.1.1, $S(t)|(\kappa, \sigma^2)$ is a multivariate Gaussian process. Thus, for any $t > 0$, $S(t)|(\kappa, \sigma^2)$ follows a multivariate normal distribution. Proposition 6.1.2 below provides the mean vector and the covariance matrix of $S(t)$, given the values of κ and σ^2.

Proposition 6.1.2. *For any given $t > 0$, $S(t)|(\kappa, \sigma^2)$ follows a multivariate normal distribution with mean vector $\mu(t)|(\kappa, \sigma^2)$ and covariance matrix $\Sigma(t)|(\kappa, \sigma^2)$, where*

$$\mu_0(t)|(\kappa, \sigma^2) = \exp(t\Delta) \times s_0 + \int_0^t \exp[(t-s)\Delta] \times \kappa ds \quad (6.1.8)$$

$$\Sigma_0(t)|(\kappa, \sigma^2) = \int_0^t \exp[(t-s)\Delta] \times \Pi_0 \times \exp[(t-s)\Delta]^T ds \quad (6.1.9)$$

Proof. Based on Equation (6.1.4),

$$\boldsymbol{\mu}_0(t) = \mathbb{E}(\exp(t\boldsymbol{\Delta}) \times s_0) + \mathbb{E}\left(\int_0^t \exp[(t-s)\boldsymbol{\Delta}] \times \boldsymbol{\kappa} \mathrm{d}s\right) + \mathbb{E}\left(\int_0^t \exp[(t-s)\boldsymbol{\Delta}] \mathrm{d}\boldsymbol{B}(s)\right).$$

Note that $\exp(t\boldsymbol{\Delta}) \times s_0$ and $\int_0^t \exp[(t-s)\boldsymbol{\Delta}] \times \boldsymbol{\kappa} \mathrm{d}s$ are deterministic values for any give t, whereas $\mathbb{E}[\int_0^t \exp[(t-s)\boldsymbol{\Delta}] \mathrm{d}\boldsymbol{B}(s)] = 0$. Thus,

$$\boldsymbol{\mu}_0(t) = \exp(t\boldsymbol{\Delta}) \times s_0 + \int_0^t \exp[(t-s)\boldsymbol{\Delta}] \times \boldsymbol{\kappa} \mathrm{d}s.$$

Using the same facts, we have

$$\begin{aligned}\boldsymbol{\Sigma}_0(t) &= \mathrm{cov}\left(\int_0^t \exp[(t-s)\boldsymbol{\Delta}] \mathrm{d}\boldsymbol{B}(s)\right) \\ &= \mathbb{E}\left[\left(\int_0^t \exp[(t-s)\boldsymbol{\Delta}] \mathrm{d}\boldsymbol{B}(s)\right) \times \left(\int_0^t \exp[(t-s)\boldsymbol{\Delta}] \mathrm{d}\boldsymbol{B}(s)\right)'\right]\end{aligned}$$

As discussed in the proof of Proposition 6.1.1, $\exp[(t-s)\boldsymbol{\Delta}]$ is an $n \times n$ matrix, each element of which is function depending on $(t-s)$. We denote the $(i,j)^{th}$ element of $\exp[(t-s)\boldsymbol{\Delta}]$ by $e_{i,j}(t-s)$. The multi-dimensional Ito's integral is expressed as

$$\int_0^t \exp[(t-s)\boldsymbol{\Delta}] \mathrm{d}\boldsymbol{B}(s) = \left(\sum_{\ell=1}^n \int_0^t e_{1,\ell}(t-s) \mathrm{d}B_\ell(s), \ldots, \sum_{\ell=1}^n \int_0^t e_{n,\ell}(t-s) \mathrm{d}B_\ell(s)\right)'.$$

Thus, the $(i,j)^{th}$ element of $\boldsymbol{\Sigma}_0(t)$, denoted by $\Sigma_{i,j}(t)$, is calculated as follows

$$\begin{aligned}\Sigma_{i,j}(t) &= \mathbb{E}\left[\left(\sum_{\ell_1=1}^n \int_0^t e_{i,\ell_1}(t-s) \mathrm{d}B_{\ell_1}(s)\right) \times \left(\sum_{\ell_2=1}^n \int_0^t e_{j,\ell_2}(t-s) \mathrm{d}B_{\ell_2}(s)\right)\right] \\ &= \sum_{\ell_1=1}^n \sum_{\ell_2=1}^n \mathbb{E}\left(\int_0^t e_{i,\ell_1}(t-s) \mathrm{d}B_{\ell_1}(s) \times \int_0^t e_{j,\ell_2}(t-s) \mathrm{d}B_{\ell_2}(s)\right)\end{aligned} \tag{6.1.10}$$

Since $B_{\ell_1}(t)$ and $B_{\ell_2}(t)$ are two independent Brownian motion processes for $\ell_1 \neq \ell_2$,

$$\mathbb{E}\left(\int_0^t e_{i,\ell_1}(t-s) \mathrm{d}B_{\ell_1}(s) \times \int_0^t e_{j,\ell_2}(t-s) \mathrm{d}B_{\ell_2}(s)\right) = 0.$$

Hence, we can simplify the expression of $\Sigma_{i,j}(t)$ as follows

$$\begin{aligned}\Sigma_{i,j}(t) &= \sum_{\ell=1}^n \mathbb{E}\left(\int_0^t e_{i,\ell}(t-s) \mathrm{d}B_\ell(s) \times \int_0^t e_{j,\ell}(t-s) \mathrm{d}B_\ell(s)\right) \\ &= \sum_{\ell=1}^n \int_0^t e_{i,\ell}(t-s) e_{j,\ell}(t-s) \sigma_\ell^2 \mathrm{d}s \\ &= \int_0^t \exp[(t-s)\boldsymbol{\Delta}]_{i\cdot} \times \boldsymbol{\Pi_0} \times \exp[(t-s)\boldsymbol{\Delta}']_{\cdot j} \mathrm{d}s,\end{aligned}$$

where $\exp[(t-s)\Delta]_{i\cdot}$ represents the ith row of matrix $\exp[(t-s)\Delta]$, and $\exp[(t-s)\Delta']_{\cdot j}$ the jth column of matrix $\exp[(t-s)\Delta']$. Therefore, the covariance matrix $\Sigma(t)$ can be expressed as follows

$$\Sigma_0(t) = \int_0^t \exp[(t-s)\Delta] \times \Pi_0 \times \exp[(t-s)\Delta^T] \mathrm{d}s.$$

$\square$

This result provides a closed-form expression for the distribution of $S(t)$ given (κ, σ^2). The resulting expressions of mean vector $\mu_0(t)|(\kappa, \sigma^2)$ and covariance matrix $\Sigma_0(t)|(\kappa, \sigma^2)$ are in the form of multi-dimensional integrals that depend explicitly on matrix exponential $\exp[(t-s)]$. Both of expressions (6.1.8) and (6.1.9) can be computed directly using mathematical software, such as Matlab and Mathematica.

Proposition 6.1.2 can be used to compute the point estimate and the confidence interval of component lifetimes, T_i's. We denote the $(100\alpha)^{th}$ percentile of T_i by $t_{(i,\alpha)}$. For any $0 < \alpha < 1$, $t_{(i,\alpha)}$ can be computed by solving the following equation: $\mathbb{P}(S_i(t_{(i,\alpha)}) > d_i) = \alpha$. Hence, we can compute the median estimate of T_i (i.e. $t_{(i,0.5)}$), and the 95% confidence interval of T_i (i.e. $(t_{(i,0.025)}, t_{(i,0.975)})$).

This result herein generalizes the method in [140], which presented a similar SDE model with the assumption that Δ is a full rank matrix. This assumption may not necessarily be satisfied in many real world applications.

Example:

Here, we provide an illustrative example for using Proposition 6.1.2. We assume that model parameters $(\Delta, s_0, \kappa, \sigma^2)$ take the following values:

$$\Delta = \begin{pmatrix} 0 & 0 \\ 1 & 0 \end{pmatrix}, \quad s_0 = \begin{pmatrix} 1 \\ 0 \end{pmatrix}, \quad \kappa = \begin{pmatrix} 1 \\ 0.5 \end{pmatrix}, \quad \text{and } \sigma^2 = \begin{pmatrix} 1 \\ 4 \end{pmatrix}.$$

Thus, the DRI model $\mathrm{d}S(t) = [\kappa + \Delta \times S(t)]\mathrm{d}t + \mathrm{d}B(t)$ can be written as follows:

$$\mathrm{d}S_1(t) = \mathrm{d}t + \mathrm{d}B_1(t) \tag{6.1.11}$$

$$\mathrm{d}S_2(t) = [S_1(t) + 0.5]\mathrm{d}t + \mathrm{d}B_2(t) \tag{6.1.12}$$

with initial conditions $S_1(0) = 1$ and $S_2(0) = 0$. Here, $B_1(t)$ and $B_2(t)$ are independent Brownian motion processes with diffusion parameters 1 and 4, respectively, i.e., $B_1(t) \sim N(0,t)$ and $B_2(t) \sim N(0,4t)$.

110

In this example, there exists a one-way DRI between Components C_1 and C_2. Specifically, the degradation level of C_1 affects the degradation rate of C_2 but not the vice versa. In terms of their degradation signals, $S_1(t)$ is a Brownian motion process independent from $S_2(t)$, and $S_2(t)$ is affected by the amplitude of $S_1(t)$. It can be shown directly using Equation (6.1.11) that $S_1(t) = S_1(0) + t + B_1(t)$ follows a normal distribution $N(1 + t, t)$ for any $t > 0$.

Next, we apply the results of Proposition 6.1.2 to compute the mean vector and covariance matrix of $S(t)$. We can compute the expressions of $\boldsymbol{\mu}_0(t)|(\kappa, \sigma^2)$ and $\boldsymbol{\Sigma}_0(t)|(\kappa, \sigma^2)$ using the symbolic function of Matlab for any $\boldsymbol{\Delta} \in \mathbb{R}^{n \times n}$. The results are expressed as follows:

$$\boldsymbol{\mu}_0(t)|(\kappa, \sigma^2) = \begin{pmatrix} t + 1 \\ t + \frac{(t+0.5)^2}{2} - \frac{1}{8} \end{pmatrix} \tag{6.1.13}$$

$$\boldsymbol{\Sigma}_0(t)|(\kappa, \sigma^2) = \begin{pmatrix} t & \frac{t^2}{2} \\ \frac{t^2}{2} & \frac{[t(t^2+12)]}{3} \end{pmatrix}. \tag{6.1.14}$$

In the expression above, the mean of $S_1(t)$ is $t + 1$, and its variance is t. This is consistent with the model of $S_1(t)$ in Equation (6.1.11).

6.1.2 Two Special Cases of the Continuous DRI Model

In this subsection, we discuss two special cases of our proposed degradation model that considers two different assumptions of $\boldsymbol{\Delta}$.

6.1.2.1 Special case (1): $\boldsymbol{\Delta}$ is a Diagonal Matrix.

We consider the case where a system components are independent and there is not form of degradation interaction. Thus for a system with n independent components we have $\boldsymbol{\Delta} = \text{diag}\{\lambda_1, \ldots, \lambda_n\}$, where $\lambda_1, \ldots, \lambda_n \in \mathbb{R}$. The magnitude of DRIs between any pair of components 0. Hence, equation (6.1.2) collapses to n independent equations: $dS_i(t) = [\kappa_i + \lambda_i S_i(t)]dt + dB_i(t)$, for $i = 1, \ldots, n$, where each equation characterizes the degradation signal of an individual component. Corollary 6.1.1 and Corollary 6.1.2 below provide the expression and the distribution of $S_i(t)$, respectively, when $\boldsymbol{\Delta}$ is a diagonal matrix.

Corollary 6.1.1. *If $\boldsymbol{\Delta}$ is a diagonal matrix expressed as $\boldsymbol{\Delta} = diag\{\lambda_1, \ldots, \lambda_n\}$, for any $i = 1, \ldots, n$,*

the future evolution of any component's degradation signal is expressed as follows

$$S_i(t)|(\kappa_i, \sigma_i^2) = e^{\lambda_i t} s_{0,i} + \frac{\kappa_i}{\lambda_i}\left(e^{\lambda_i t} - 1\right) + \int_0^t e^{\lambda_i(t-s)}\mathrm{d}B_i(s), \tag{6.1.15}$$

where $s_0 = (s_{0,1}, \ldots, s_{0,n})'$.

Proof. According to Proposition 6.1.1, the future evolution of $S(t)$ can be expressed as

$$S(t) = \exp(t\Delta) \times s_0 + \int_0^t \exp[(t-s)\Delta] \times \kappa\, \mathrm{d}s + \int_0^t \exp[(t-s)\Delta]\mathrm{d}B(s) \tag{6.1.16}$$

Note that the matrix exponential $\exp[t\Delta]$ is a diagonal matrix expressed as $\mathrm{diag}\{\exp(\lambda_1 t), \ldots, \exp(\lambda_n t)\}$. Hence, the multi-dimensional integral $\int_0^t \exp[(t-s)\Delta] \times \kappa$ can be expressed as follows

$$\int_0^t \exp[(t-s)\Delta] \times \kappa \mathrm{d}s$$
$$= \left(\int_0^t \exp[(t-s)\lambda_1]\kappa_1 \mathrm{d}s, \ldots, \int_0^t \exp[(t-s)\lambda_n]\kappa_n \mathrm{d}s\right)^T$$
$$= \left(\frac{\kappa_1}{\lambda_1}(e^{\lambda_1 t} - 1), \ldots, \frac{\kappa_n}{\lambda_n}(e^{\lambda_n t} - 1)\right)^T \tag{6.1.17}$$

Similarly,
$$\exp(t\Delta) \times s_0 = \left(e^{\lambda_1 t}s_{0,1}, \ldots, e^{\lambda_n t}s_{0,n}\right)^T$$
$$\int_0^t \exp[(t-s)\Delta]\mathrm{d}B(t) = \left(\int_0^t \exp[(t-s)\lambda_1]\mathrm{d}B_1(t), \ldots, \int_0^t \exp[(t-s)\lambda_n]\mathrm{d}B_n(t)\right)^T.$$

Therefore, for any $i = 1, \ldots, n$, the future evolution of $S_i(t)$ can be expressed as follows:

$$S_i(t) = e^{\lambda_i t}s_{0,i} + \frac{\kappa_i}{\lambda_i}\left(e^{\lambda_i t} - 1\right) + \int_0^t e^{\lambda_i(t-s)}\mathrm{d}B_i(s).$$

$\square$

Corollary 6.1.2. *For any given $t > 0$, $S_i(t)$'s are independent with mean and variance expressed as follows:*

$$\mathbb{E}(S_i(t))|(\kappa_i, \sigma_i^2) = e^{\lambda_i t}s_{0,i} + \frac{\kappa_i}{\lambda_i}\left(e^{\lambda_i t} - 1\right) \tag{6.1.18}$$

$$var(S_i(t))|(\kappa_i, \sigma_i^2) = \frac{\sigma_i^2}{2\lambda_i}\left(e^{2\lambda_i t} - 1\right) \tag{6.1.19}$$

Proof. The expression of $\mathbb{E}(S_i(t))$ follows directly by taking the expectation of $S_i(t)$ in equation (6.1.15). Recall we prove in Proposition 6.1.2 that

$$\boldsymbol{\Sigma}(t) = \int_0^t \exp[(t-s)\boldsymbol{\Delta}] \times \boldsymbol{\Pi_0} \times \exp[(t-s)\boldsymbol{\Delta}^T].$$

When $\boldsymbol{\Delta} = \text{diag}\{\lambda_1, \ldots, \lambda_n\}$, we have

$$\exp[(t-s)\boldsymbol{\Delta}] = \exp[(t-s)\boldsymbol{\Delta}^T] = \text{diag}\{\exp[(t-s)\lambda_1], \ldots, \exp[(t-s)\lambda_n]\}.$$

Hence, $\boldsymbol{\Sigma}(t)$ is also a diagonal matrix, which is expressed as follows:

$$\begin{aligned}
\boldsymbol{\Sigma}(t) &= \text{diag}\left\{\sigma_1^2 \int_0^t \exp[2(t-s)\lambda_1]\mathrm{d}s, \ldots, \sigma_n^2 \int_0^t \exp[2(t-s)\lambda_n]\mathrm{d}s\right\} \\
&= \text{diag}\left\{\frac{\sigma_1^2}{2\lambda_1}\left(e^{2\lambda_1 t} - 1\right), \ldots, \frac{\sigma_n^2}{2\lambda_n}\left(e^{2\lambda_n t} - 1\right)\right\}
\end{aligned} \tag{6.1.20}$$

Therefore, $S_i(t)$'s are independent for $i = 1, \ldots, n$ with $\text{var}(S_i(t)) = \frac{\sigma_i^2}{2\lambda_i}\left(e^{2\lambda_i t} - 1\right)$. $\qquad\square$

Based on Corollary 6.1.2, the lifetime distribution of each component, say component C_i, can be estimated independently:

$$\mathbb{P}(T_i < t|(\kappa_i, \sigma_i^2)) \approx \mathbb{P}(S_i(t) \geq d_i|(\kappa_i, \sigma_i^2)) = \Phi\left(\left.\frac{\mathbb{E}(S_i(t)) - d_i}{\sqrt{\text{var}(S_i(t))}}\right|(\kappa_i, \sigma_i^2)\right).$$

$$\mathbb{P}(T_i < t) \approx \mathbb{P}(S_i(t) \geq d_i) = \Phi\left(\frac{\mathbb{E}(S_i(t)) - d_i}{\sqrt{\text{var}(S_i(t))}}\right).$$

Also, when $\lambda_1 = \cdots = \lambda_n = 0$, this special case collapses to the conventional degradation model for individual components (cf. [84], [47]).

6.1.2.2 *Special case (2):* $\boldsymbol{\Delta}$ *is a Diagonalizable Matrix on* $\mathbb{R}$.

When $\boldsymbol{\Delta}$ is a diagonalizable matrix on $\mathbb{R}$. That is, there exists matrix $V \in \mathbb{R}^{n \times n}$ such that $V^{-1}\boldsymbol{\Delta}V$ is a diagonal matrix. Matrix V can be found using eigen-decomposition. In particular, assume that $\boldsymbol{\Delta}$ has eigen values $\lambda_1, \ldots, \lambda_n$ and the corresponding eigen vectors $\boldsymbol{v_1}, \ldots, \boldsymbol{v_n}$. Let $V = (\boldsymbol{v_1}, \ldots, \boldsymbol{v_n})$, thus $V^{-1}\boldsymbol{\Delta}V = \text{diag}\{\lambda_1, \ldots, \lambda_n\}$. This case encompasses a large variety of components whose degradation processes interact with each other. For example, a real symmetric matrix is diagonalizable on $\mathbb{R}$. When $\boldsymbol{\Sigma}$ is a real symmetric matrix, i.e., $\boldsymbol{\Delta} = [\delta_{i,j}]$ where $\delta_{i,j} = \delta_{j,i}$, for $i, j = 1, \ldots, n$, equation (6.1.2) characterizes the degradation signals from a system with n identical components with

similar interaction characteristics among their degradation processes. In such systems, the DRI effects between any pair of components are identical, since the constituent components in the system are identical. Corollary 6.1.3 and Corollary 6.1.4 below provide the expression and the distribution of $S(t)$ when Δ is a diagonalizable matrix.

Corollary 6.1.3. *Assume that Δ is a diagonalizable matrix on $\mathbb{R}$, the future evolution of $S(t)$ can be expressed by*

$$S(t)|(\kappa, \sigma^2) = VD_1(t)V^{-1} \times s_0 + VD_2(t)V^{-1} \times \kappa + V \times \int_0^t D_1(t-s)V^{-1}\mathrm{d}B(s), \qquad (6.1.21)$$

where $D_1(t) = diag\left\{e^{\lambda_1 t}, \ldots, e^{\lambda_n t}\right\}$ and $D_2(t) = diag\left\{\frac{e^{\lambda_1 t}-1}{\lambda_1}, \ldots, \frac{e^{\lambda_n t}-1}{\lambda_n}\right\}$.

Proof. Since $V^{-1}\Delta V = \mathrm{diag}\{\lambda_1, \ldots, \lambda_n\}$, matrix exponential $\exp(t\Delta)$ can be expressed as

$$\exp(t\Delta) = V \times \mathrm{diag}\{\exp(\lambda_1 t), \ldots, \exp(\lambda_n t)\} \times V^{-1} = V \times D_1(t) \times V^{-1}.$$

Similarly, $\exp((t-s)\Delta) = V \times \mathrm{diag}\{\exp(\lambda_1(t-s)), \ldots, \exp(\lambda_n(t-s))\} \times V^{-1}$. Thus, the multi-dimensional integral $\int_0^t \exp((t-s)\Delta) \times \kappa \mathrm{d}s$ can be expressed as follows:

$$\begin{aligned}
\int_0^t \exp((t-s)\Delta) \times \kappa \mathrm{d}s &= \int_0^t V \times \mathrm{diag}\{\exp(\lambda_1(t-s)), \ldots, \exp(\lambda_n(t-s))\} \times V^{-1} \times \kappa \mathrm{d}s \\
&= V \times \int_0^t \mathrm{diag}\{\exp(\lambda_1(t-s)), \ldots, \exp(\lambda_n(t-s))\}\,\mathrm{d}s \times V^{-1} \times \kappa \\
&= V \times \mathrm{diag}\left\{\frac{e^{\lambda_1 t}-1}{\lambda_1}, \ldots, \frac{e^{\lambda_n t}-1}{\lambda_n}\right\} \times V^{-1} \times \kappa \\
&= V \times D_2(t) \times V^{-1} \times \kappa \qquad (6.1.22)
\end{aligned}$$

Similarly, $\int_0^t \exp((t-s)\Delta)\mathrm{d}B(s)$ can be expanded as

$$\int_0^t \exp((t-s)\Delta)\mathrm{d}B(s) = \int_0^t V \times D_1(t-s) \times V^{-1}\mathrm{d}B(s) = V \times \int_0^t D_1(t-s) \times V^{-1}\mathrm{d}B(s).$$

Therefore, based on equation (6.1.4), the expression of $S(t)$ can be written as

$$S(t) = VD_1(t)V^{-1} \times s_0 + VD_2(t)V^{-1} \times \kappa + V \times \int_0^t D_1(t-s)V^{-1}\mathrm{d}B(s).$$

$\square$

Corollary 6.1.4. *Assume that Δ is a diagonalizable matrix on $\mathbb{R}$. For any given $t > 0$, $S(t)$ follows a multivariate normal distribution with mean vector $\mu(t)$ and covariance matrix $\Sigma(t)$, where*

$$\mu_0(t)|(\kappa, \sigma^2) = VD_1(t)V^{-1} \times s_0 + VD_2(t)V^{-1} \times \kappa \tag{6.1.23}$$

$$\Sigma_0(t)|(\kappa, \sigma^2) = V \times \int_0^t D_1(t-s)V^{-1} \times \Pi_0 \times (V^{-1})^T D_1(t-s)\mathrm{d}s \times V^T \tag{6.1.24}$$

Proof. The expression of $\mu(t)$ follows by taking the expectation of $S(t)$ in equation (6.1.21). Based on Proposition 6.1.2, $\Sigma(t)$ can be expressed as

$$
\begin{aligned}
\Sigma(t) &= \int_0^t VD_1(t-s)V^{-1} \times \Pi_0 \times (VD_1(t-s)V^{-1})^T \mathrm{d}s \\
&= \int_0^t VD_1(t-s)V^{-1} \times \Pi_0 \times (V^{-1})^T D_1(t-s)V^T \mathrm{d}s \\
&= V \times \int_0^t D_1(t-s)V^{-1} \times \Pi_0 \times (V^{-1})^T D_1(t-s)\mathrm{d}s \times V^T
\end{aligned}
$$

$\square$

Remark 6.1.1. *Corollary 6.1.3 and Corollary 6.1.4 are developed on the assumption that Δ is diagonalizable on $\mathbb{R}$. Variations of Corollary 6.1.3 and Corollary 6.1.4 can be developed to obtain the expression of $S(t)$ with other forms of Δ. For example, when Δ is diagonalizable on $\mathbb{C}$, a modified version of Corollary 6.1.3 and Corollary 6.1.4 can be developed. Note that Δ is a real-valued matrix. The complex eigenvalues of Δ show up in conjugate pairs. In this case, we would not be able to obtain n separate SDEs by diagonalizing Δ. However, the resulting SDEs corresponding to the complex eigenvalues can still be solved in pairs. In other words, we can equivalently solve multiple SDE systems, each of which has two linear equations.*

6.2 DRI Model with Instantaneous Component Replacement

In this section, we extend the proposed DRI model described by Equation (6.1.2) and consider the scenario, in which the failed component is replaced instantaneously by a new component.

6.2.1 Estimating Time to the Next Replacement

We consider a relatively structured system where components are assumed to belong to two different categories of lifetimes. One class of components has a relatively longer lifetime compared to the other. In other words, we expect that components with shorter lifetime will be replaced multiple

times before any of the components that belong to the category of longer lifetimes. For illustrative purposes, Figure 6.2.1 shows the replacement strategy for a hypothetical two-component system. Assume that C_1 has a relatively longer lifetime compared to C_2 and that C_1 and C_2 are replaced instantaneously once their degradation signals reach a predetermined failure threshold.
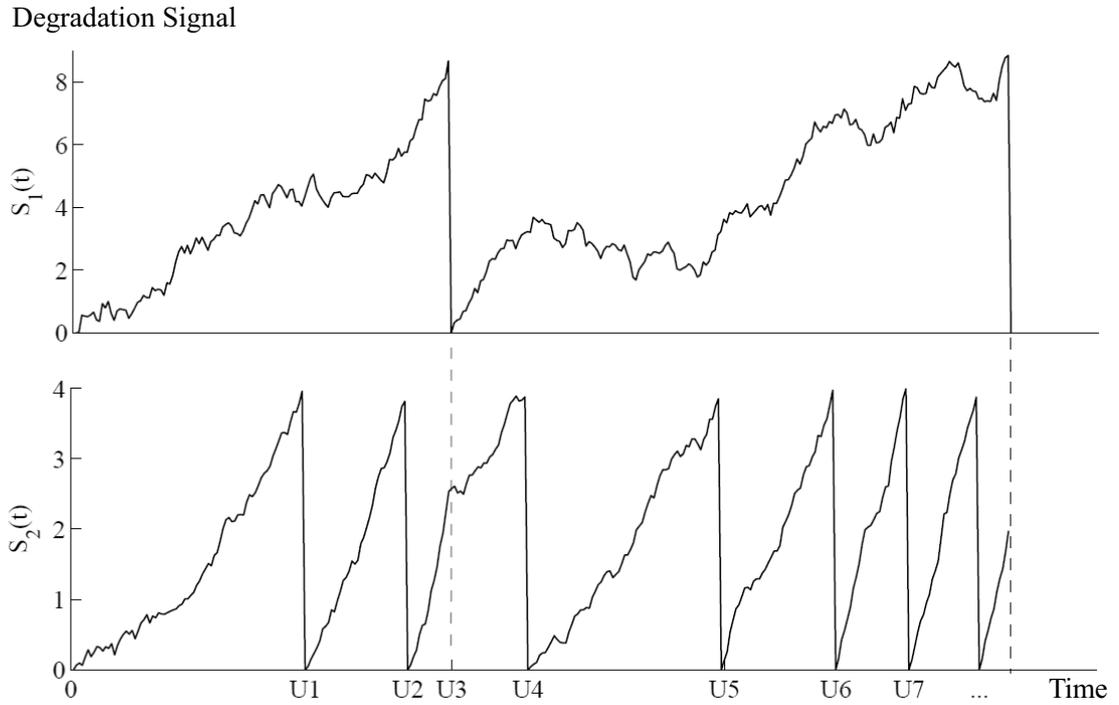

Figure 6.2.1: Degradation signals of a two-component systems with instantaneous replacement.

The upper and lower plots in Figure 6.2.1 show the degradation signals of components C_1 and C_2, respectively. We denote the time for the ℓth replacement by U_ℓ, for $\ell = 1, 2, \ldots$. Note that C_1 is replaced at time U_3 while C_2 being the component with the shorter lifetime is replaced more often at times, $U_1, U_2, U_4, \ldots, U_7$. Within the context of our DRI framework, we note that the replacement points of the C_2 become increasingly more frequent as the degradation signal of C_1 increases. This can be seen by observing the difference between U_5, U_6 and U_7. In other words, as soon as component C_2 is replaced, its degradation rate will follow a path that is dictated by the amplitude of the degradation signal of component C_1. The relationship between the two paths of the

116

two degradation signals is governed by the DRI model that was discussed earlier in equation (6.1.2). For instance, at U_1 component C_2 is replaced with a new unit. However, its lifetime becomes significantly shorter, i.e., $U_2 - U_1 < U_1$ due to its DRI with component C_1. Similar observations can be noticed for $U_5 - U_4, U_6 - U_5$, and $U_7 - U_6$.

Characterizing the dynamics of component DRIs with replacement is very challenging. In what follow, we propose an iterative procedure to estimate the replacement times of components in a series system. That is, the system fails if any of its constituent component fails. We assume that the initial degradation states of all the components in the system are observable, which are represented by a deterministic vector s_0. Based on the proposed DRI model, we can estimate the failure time of the system as the first failure time of components in the system. When the failure of a component occurs, we replace the failed component with a new component (with degradation level 0) and monitor the degradation states of all components in the system. Using the observed degradation states, we can again use the proposed DRI model and estimate the distribution of the next replacement time. Hence, we can iteratively estimate the future replacement times for a finite replacement horizon.

- **Replacement 1: Estimating U_1 given $S(0) = s_0$.**

  U_1 is equivalent to the time, at which the first failure event occurs. That is $U_1 = \min\{T_1, \ldots, T_n\}$, where $T_i, i = 1, \ldots, n$, represents the lifetime of component C_i. Hence, the distribution of U_1, given s_0, can be computed as follows

$$
\begin{aligned}
\mathbb{P}(U_1 > t | S(0) = s_0, (\kappa, \sigma^2)) &= \mathbb{P}(T_1 > t, \ldots, T_n > t | S(0) = s_0, (\kappa, \sigma^2)) \\
&\approx \mathbb{P}(S_1(t) < d_1, \ldots, S_n(t) < d_n | S(0) = s_0, (\kappa, \sigma^2)) \\
&= \mathbb{P}(S(t) < d | S(0) = s_0, (\kappa, \sigma^2)) \quad (6.2.1)
\end{aligned}
$$

By Proposition 6.1.2, $S(t)$, given $S(0) = s_0$, follows a multivariate normal distribution

$$
MNV(\mu_0(t)|(\kappa, \sigma^2), \Pi_0(t)|(\kappa, \sigma^2)).
$$

Thus, the distribution of U_1 can be computed as follows:

$$
\mathbb{P}(U_1 > t | S(0) = s_0, (\kappa, \sigma^2)) = \varphi_{0,t}(d),
$$

117

where $\varphi_{0,t}(\cdot)$ is the c.d.f. of the multivariate normal distribution with mean vector $\boldsymbol{\mu}_0(t)|(\boldsymbol{\kappa}, \sigma^2)$ and covariance matrix $\boldsymbol{\Pi}_0(t)|(\boldsymbol{\kappa}, \sigma^2)$.

- **Replacement 2: Estimating U_2 given $(U_1 = u_1, S(u_1) = s(u_1))$.**

  Let u_1 be a realization of U_1. We replace the failed component and monitor the degradation signals of the rest of the components in the system. Let the observed degradation signals at U_1 be denoted by $s(u_1)$. The future evolution of degradation signals $S(t)$ before the second replacement U_2 can be described by the following expressions:

$$\mathrm{d}S(t) = [\boldsymbol{\kappa} + \boldsymbol{\Delta} \times S(t)]\mathrm{d}t + \mathrm{d}B(t), \text{ for } t > u_1, \tag{6.2.2}$$

$$S(u_1) = s(u_1).$$

  Once again, using Proposition 6.1.2 we see that $S(t)|(U_1 = u_1, S(u_1) = s(u_1), \boldsymbol{\kappa}, \sigma^2)$ follows a multivariate normal distribution. We denote the mean vector and the covariance matrix of $S(t)|(U_1 = u_1, S(u_1) = s(u_1), \boldsymbol{\kappa}, \sigma^2)$ at time u_1 as $\boldsymbol{\mu}_1(t)|(\boldsymbol{\kappa}, \sigma^2)$ and $\boldsymbol{\Sigma}_1(t)|(\boldsymbol{\kappa}, \sigma^2)$, respectively. Hence, the conditional distribution of U_2 can be computed as

$$\mathbb{P}(U_2 > t|U_1 = u_1, S(u_1) = s(u_1), \boldsymbol{\kappa}, \sigma^2) = \varphi_{1,t}(\boldsymbol{d}),$$

  where $\varphi_{1,t}(\cdot)$ is the c.d.f. of the multivariate normal distribution with mean vector $\boldsymbol{\mu}_1(t)|(\boldsymbol{\kappa}, \sigma^2)$ and covariance matrix $\boldsymbol{\Sigma}_1(t)|(\boldsymbol{\kappa}, \sigma^2)$. This procedure can be repeated iteratively until replacement ℓ.

- **Replacement ℓ: Estimating U_ℓ given $(U_{\ell-1} = u_{\ell-1}, S(u_{\ell-1}) = s(u_{\ell-1}))$.**

  For the ℓth replacement, the conditional distribution of U_ℓ can be computed as

$$\mathbb{P}(U_\ell > t|U_{\ell-1} = u_{\ell-1}, S(u_{\ell-1}) = s(u_{\ell-1}), \boldsymbol{\kappa}, \sigma^2) = \varphi_{\ell-1,t}(\boldsymbol{d}),$$

  where $\varphi_{\ell-1,t}(\boldsymbol{d})$ can be obtained by solving equation:

$$\mathrm{d}S(t) = [\boldsymbol{\kappa} + \boldsymbol{\Delta} \times S(t)]\mathrm{d}t + \mathrm{d}B(t), \text{ for } t > u_{\ell-1}, \tag{6.2.3}$$

$$S(u_{\ell-1}) = s(u_{\ell-1}).$$

The proposed procedure provides the estimated time for the next replacement activity when a failed component is replaced. By incorporating real-time observations of degradation signals,

this approach is useful for decision making regarding maintenance/replacement activities in the short term. For decision making about component replacement in the long term, we can utilize the property of conditional probability to obtain the joint probability distributions of $(U_1, \ldots, U_\ell)$. The results can be used to schedule the next ℓ replacement activities in future. The details are not discussed here.

6.2.2 Determining Replacement Policy for System With Component DRIs

As noted in Section 6.2.1, DRIs among the components of a system may affect the lifetimes or the residual lifetimes of components in a system. Typically, when the degradation level of one component is high, it may significantly increase the degradation rates of its interconnected components and decrease their lifetimes. Hence, in a system with significant component-to-component interactions, the total replacement cost could be very high, if each component is replaced individually at their own failure thresholds without considering the interactions among them.

Here, we propose a policy for determining the replacement thresholds of components in a system with inter-dependent components while account for the DRIs among the components. Our goal is choose the replacement thresholds for each component so that we can minimize the total cost of replacement in the system. In particular, we determine the replacement thresholds for individual components so that the limiting average replacement cost of the entire system is minimized. The limiting average replacement cost, A_v, for a system with n components can be expressed as follows:

$$A_v = \lim_{k \to \infty} \sum_{i=1}^{n} \frac{e_i}{\mathbb{E}_k(T_i | f_1, f_2, \ldots, f_n)}, \tag{6.2.4}$$

where e_i represents the replacement cost of component C_i for one replacement, f_i represents the replacement threshold for component C_i, and $\mathbb{E}_k(T_i | f_1, f_2, \ldots, f_n)$ is the expected lifetime of component C_i after the kth replacement. As discussed earlier, $\mathbb{E}_k(T_i | f_1, f_2, \ldots, f_n)$ is determined by the replacement thresholds of all components in the system, namely $f_1, \ldots, f_n$, and $\mathbb{E}_k(T_i | f_1, f_2, \ldots, f_n)$ can be computed based on the our proposed DRI models.

We consider the limiting average replacement for two important reasons: (1) this criterion can be equivalently converted to other measures of system performance, such as the availability of the system (cf. [135].) (2) The computational cost is relatively low compared with other decision

making tool, such as Markov decision process (MDP), the computation cost of which increases significantly as the number of components increases ($n \geq 2$).

However, due to the uncertainty associated with the degradation process of each component, the limit in equation (6.2.4) does not generally exist. Instead, we develop a conservative policy that minimize the upper bound of A_v. The optimization formulation is expressed as follows:

$$\min_{f_1,\ldots,f_n} \quad \limsup_{k \to \infty} \sum_{i=1}^{n} \frac{e_i}{\mathbb{E}_k(T_i | f_1, f_2, \ldots, f_n)} \tag{6.2.5}$$

$$\text{s.t.} \qquad 0 < f_i \leq d_i, \quad \text{for } i = 1, \ldots, n. \tag{6.2.6}$$

Recall that the degradation level of a new component is defined to be 0, and the failure threshold of component C_i is denoted by d_i. The constraint in expression (6.2.6) guarantees that any component is replaced before the component failure occurs due to safety and security conditions. Also, when a component fails, it is usually replaced by a new component.

Determining the optimal values of $f_1, \ldots, f_n$ requires solving the non-linear optimization problem expressed in expressions (6.2.5) and (6.2.5). For a medium size system ($n \leq 5$), this optimization problem can be solved directly using mathematical software. For larger systems, the development of advanced optimization technique is required. In what follows, we provide an illustrative example of a system with two inter-dependent components to demonstrate the proposed procedure.

6.2.3 Illustrative Example

We consider a system of two-components, which exhibit continuous DRIs, for the purpose of demonstration. The proposed approach can be generalized to a system with n components and discrete DRIs.

Degradation signals of a two-component system with continuous component interactions can be characterized by the following equations.

$$dS_1(t) = [S_2(t)\delta_{2,1} + \kappa_1]dt + \sigma_1 dW_1(t) \tag{6.2.7}$$

$$dS_2(t) = [S_1(t)\delta_{1,2} + \kappa_2]dt + \sigma_2 dW_2(t) \tag{6.2.8}$$

Let $\mu_1(t) = \mathbb{E}[S_1(t)]$ be the mean of $S_1(t)$. Based on the proposed DRI model, $\mu_1(t)$ can be expressed as follows

$$\mu_1(t) = s_2(t_0^k) \frac{\sqrt{\delta_{1,2}\delta_{2,1}}}{2\delta_{2,1}} \left[\exp((t - t_0^k)\sqrt{\delta_{1,2}\delta_{2,1}}) - \frac{1}{\exp((t - t_0^k)\sqrt{\delta_{1,2}\delta_{2,1}})} \right] \tag{6.2.9}$$

$$+ \frac{s_1(t_0^k)}{2} \left[\exp((t - t_0^k)\sqrt{\delta_{1,2}\delta_{2,1}}) + \frac{1}{\exp((t - t_0^k)\sqrt{\delta_{1,2}\delta_{2,1}})} \right] - \frac{\kappa_2}{\delta_{2,1}} \tag{6.2.10}$$

$$+ \frac{\exp((t - t_0^k)\sqrt{\delta_{1,2}\delta_{2,1}})}{2\delta_{2,1}} \left[\kappa_2 + \frac{\kappa_2 - (\delta_{2,1}\kappa_1)/\sqrt{\delta_{1,2}\delta_{2,1}}}{\exp(2(t - t_0^k)\sqrt{\delta_{1,2}\delta_{2,1}})} + \frac{\delta_{2,1}\kappa_1}{\sqrt{\delta_{1,2}\delta_{2,1}}} \right] \tag{6.2.11}$$

$\mu_2(t)$ can be obtained in a similar way, with a symmetric form to $\mu_1(t)$.

Moreover, we approximate $\mathbb{E}_k[T_1|f_1, f_2]$ using the median of T_1, which can be obtained by solving $\mu_1(t) = f_1$. The resulting expression of $\mathbb{E}_k[T_1|f_1, f_2]$ is represented as follows:

$$\mathbb{E}_k[T_1|f_1, f_2] \approx \frac{1}{\sqrt{\delta_{1,2}\delta_{2,1}}} \ln \left[\frac{\sqrt{\delta_{1,2}\delta_{2,1}}(\kappa_2 + \delta_{2,1}f_1) + \delta_{2,1}(\delta_{1,2}\delta_{2,1}f_1^2 + 2\kappa_2\delta_{1,2}f_1 + a_1)^{1/2}}{\delta_{1,2}\delta_{2,1}s_2(t_0^k) + a_2} \right],$$

where

$$a_1 = 2\delta_{1,2}\kappa_1 s_2(t_0^k) - \delta_{1,2}\delta_{2,1}s_1^2(t_0^k) - 2\kappa_2\delta_{1,2}s_1(t_0^k) + \kappa_1^2 + \delta_1^2 s_2^2(t_0^k) \tag{6.2.12}$$

$$a_2 = \delta_{2,1}\kappa_1 + \kappa_2\sqrt{\delta_{1,2}\delta_{2,1}} + \delta_{2,1}s_1(t_0^k)\sqrt{\delta_{1,2}\delta_{2,1}} \tag{6.2.13}$$

Here, t_0^k represents the starting time of a replacement cycle when component C_1 is replaced by a new component after the kth replacement. Recall that the degradation signal for a new component starts at 0. That is, $s_1(t_0^k) = 0$. Using this condition, $\mathbb{E}_k[T_1|f_1, f_2]$ can be further simplified as follows:

$$\mathbb{E}_k[T_1|f_1, f_2] \approx \frac{1}{\sqrt{\delta_{1,2}\delta_{2,1}}} \ln \left[1 + \frac{\delta_{2,1}\sqrt{\delta_{1,2}\delta_{2,1}}f_1}{\delta_{1,2}\delta_{2,1}s_2(t_0^k) + \delta_{2,1}\kappa_1 + \sqrt{\delta_{1,2}\delta_{2,1}}\kappa_2} \right]$$

However, $\lim_{k\to\infty} \mathbb{E}_k[T_1|f_1, f_2]$ does not generally exist because $s_2(t_0^k)$ is fluctuating between 0 and f_2. Hence, we consider the bounds of $\lim_{k\to\infty} \mathbb{E}_k[T_1|f_1, f_2]$ as follows:

$$L_1(f_1, f_2) \leq \lim_{k\to\infty} \mathbb{E}_k[T_1|f_1, f_2] \leq U_1(f_1) \tag{6.2.14}$$

where

$$L_1(f_1, f_2) = \frac{1}{\sqrt{\delta_{1,2}\delta_{2,1}}} \ln \left[1 + \frac{f_1}{f_2\sqrt{\delta_{1,2}\delta_{2,1}}/\delta_{2,1} + \kappa_1/\sqrt{\delta_{1,2}\delta_{2,1}} + \kappa_2/\delta_{2,1}} \right] \tag{6.2.15}$$

$$U_1(f_1) = \frac{1}{\sqrt{\delta_{1,2}\delta_{2,1}}} \ln \left[1 + \frac{f_1}{\kappa_1/\sqrt{\delta_{1,2}\delta_{2,1}} + \kappa_2/\delta_{2,1}} \right] \tag{6.2.16}$$

Let $N_i(t)$ represent the number of replacements of component C_i by time t. For large t, the value of $N_1(t)$ varies between:

$$\frac{t}{U_1(f_1)} \leq N_1(t) \leq \frac{t}{L_1(f_1, f_2)}.$$

Due to the symmetry in the DRI model, we have similar results for the component C_2. That is,

$$\frac{t}{U_2(f_2)} \leq N_2(t) \leq \frac{t}{L_2(f_2, f_1)},$$

where

$$L_2(f_2, f_1) = \frac{1}{\sqrt{\delta_{1,2}\delta_{2,1}}} \ln\left[1 + \frac{f_2}{f_1 \sqrt{\delta_{1,2}\delta_{2,1}}/\delta_{1,2} + \kappa_2/\sqrt{\delta_{1,2}\delta_{2,1}} + \kappa_1/\delta_{1,2}}\right] \quad (6.2.17)$$

$$U_2(f_2) = \frac{1}{\sqrt{\delta_{1,2}\delta_{2,1}}} \ln\left[1 + \frac{f_2}{\kappa_2/\sqrt{\delta_{1,2}\delta_{2,1}} + \kappa_1/\delta_{1,2}}\right] \quad (6.2.18)$$

Hence, the limiting average replacement cost, A_v, can be expressed as follows:

$$A_v = \lim_{t\to\infty}\left[e_1 \frac{N_1(t)}{t} + e_2 \frac{N_2(t)}{t}\right] \quad (6.2.19)$$

As a result, the upper and lower bounds of C_A can be found using the following expression

$$\frac{e_1}{U_1(f_1)} + \frac{e_2}{U_2(f_1)} \leq A_v \leq \frac{e_1}{L_1(f_1, f_2)} + \frac{e_2}{L_2(f_1, f_2)}.$$

Our goal is to choose f_1 and f_2 to minimize the upper bound of A_v. The optimization problem can be formulated as follows

$$\min_{f_1, f_2} \quad \frac{e_1}{L_1(f_1, f_2)} + \frac{e_2}{L_2(f_1, f_2)} \quad (6.2.20)$$

$$\text{s.t.} \quad 0 < f_i \leq d_i, \quad \text{for } i = 1, 2. \quad (6.2.21)$$

This optimization problem can be solved directly using mathematical software.

6.3 Estimating and Updating the DRI Model

In this section, we discuss how to estimate model parameters using historical degradation signals from an existing database of degradation signals. In particular, we present the maximal likelihood estimates (MLEs) of model parameters κ, σ^2, and Δ based on the historical degradation signals. We realizes that the each system and its components behaves differently when put to use in the field. Thus, we use signals from the components of each individual system to update this interactive

122

model based on the degradation characteristics of the components within each system. Specifically, we update the distributions of (κ, σ^2). The updated models are then used to estimate an updated residual life distributions for the components of each system as well as revised replacement times for the components.

6.3.1 Estimating Model Parameters Using Historical Signals

Suppose that between replacement times u_ℓ and $u_{\ell+1}$, degradation signals from a given system are monitored at discrete times $t_0, t_1, \ldots, t_q$ such that $u_\ell = t_0 < t_1 < \ldots < t_q < u_{\ell+1}$. Without loss of generality, we assume that $\epsilon_t = t_1 - t_0 = t_2 - t_1 = \ldots = t_q - t_{q-1}$. We let $s(t_m) = (s_1(t_m), s_2(t_m), \ldots, s_n(t_m))'$ be a vector of signals corresponding to the system components that are being monitored at time t_m, $m = 1, \ldots, q$. Thus, for $m = 1...q$ we have $s(t_0), s(t_1), \ldots, s(t_q)$.

Recall that the proposed degradation model described by Equation(6.1.2) is a continuous-time SDE model of $S(t)$, whereas, the degradation signals are usually monitored at discrete times. Linking a continuous-time model and discrete-time data is a challenging problem, and many researchers have explored how to estimate or approximate a 1-dimensional SDE model based on discrete-time data. These approximation methods include the discrete maximum likelihood (DML) method (cf. [43]), the local linearization method (cf. [97]), the generalized method of moments (cf. [25]), Monte Carlo Markov chain simulation, and others methods. Some of these methods become difficult to implement for parameter estimation in n-dimensional SDE systems due to the increased dimensionality. In this paper, we use the method of discrete maximum likelihood (DML) for parameter estimation because of its ease of implementation and speed. As shown by [43], the DML estimates converge to the exact MLE as the interval between two consecutive monitoring times, namely ϵ_t, converges to 0.

In a similar manner to what is used in the DML method, we approximate $S(t_m)$ as

$$S(t_m) = S(t_{m-1}) + [\kappa + \Delta s(t_{m-1})]\epsilon_t + B(t_m) - B(t_{m-1}). \qquad (6.3.1)$$

Note that $S(t_m) - S(t_{m-1})$'s are independent, each of which follows the distribution $S(t_m) - S(t_{m-1}) \sim MVN([\kappa + \Delta s(t_{m-1})]\epsilon_t, \epsilon_t^2 \Sigma)$, where $\Sigma = \text{diag}\{\sigma_1^2, \ldots, \sigma_n^2\}/\epsilon_t$. We denote the likelihood function of

(κ, Δ, Σ) by $f(\kappa, \Delta, \Sigma | s(t_1), \ldots, s(t_q))$, which is expressed as follows

$$f(\kappa, \Delta, \Sigma | s(t_1), \ldots, s(t_q))$$

$$= \prod_{m=1}^{q} \left[\frac{1}{2\pi^{n/2} |\Sigma|^{1/2}} \exp \left\{ -\frac{1}{2} [y_m - \kappa - \Delta s(t_{m-1})]^T \Sigma^{-1} [y_m - \kappa - \Delta s(t_{m-1})] \right\} \right], \qquad (6.3.2)$$

where $y_m = \frac{1}{\epsilon_t} [s(t_m) - s(t_{m-1})]$ for $m = 1, \ldots, q$. Proposition 6.3.1 below provides the expressions for the the MLEs of (κ, Δ, Σ).

Proposition 6.3.1. *Given the likelihood function described by Equation* (6.3.2), *the MLEs of* (κ, Δ, Σ) *are expressed as follows*

$$\hat{\Delta} = B \times A^{-1} \tag{6.3.3}$$

$$\hat{\kappa} = \frac{s(t_q) - s(t_0)}{t_q} - \frac{1}{q} \hat{\Delta} \sum_{m=1}^{q} s(t_{m-1}) \tag{6.3.4}$$

$$\hat{\Sigma} = \frac{1}{q} \sum_{m=1}^{q} [y_m - \hat{\kappa} - \hat{\Delta} s(t_{m-1})][y_m - \hat{\kappa} - \hat{\Delta} s(t_{m-1})]^T \tag{6.3.5}$$

where $A = (A_{.1}, A_{.2}, \ldots, A_{.n})$, $B = [B_{i,j}]_{i,j=1,\ldots,n}$, *and*

$$A_{.j} = \frac{1}{q} \left(\sum_{m=1}^{q} s(t_{m-1}) \right) \left(\sum_{m=1}^{q} s_j(t_{m-1}) \right) - \sum_{m=1}^{q} s(t_{m-1}) s_j(t_{m-1})$$

$$B_{i,j} = \frac{s_i(t_q) - s_i(t_0)}{t_q} \sum_{m=1}^{q} s_j(t_{m-1}) - \sum_{m=1}^{q} y_{m,i} s_j(t_{m-1})$$

Proof. Let $L = -\log f(\kappa, \Delta, \Sigma | s(t_1), \ldots, s(t_q))$ represent the negative log-likelihood function, then L can be expressed as follows:

$$L = \frac{nq}{2} \log(2\pi) + \frac{q}{2} \log |\Sigma| + \frac{1}{2} \sum_{m=1}^{q} [y_m - \kappa - \Delta s(t_{m-1})]^T \Sigma^{-1} [y_m - \kappa - \Delta s(t_{m-1})]$$

To obtain the MLEs of (κ, Δ, Σ), we find the values of (κ, Δ, Σ) that minimize L. In particular, we set the partial derivative of L with respect to theses parameters equal to 0 and solve for (κ, Δ, Σ) based on the following equations:

$$\frac{\partial L}{\partial \kappa} = 0 \tag{6.3.6}$$

$$\frac{\partial L}{\partial \Sigma^{-1}} = 0 \tag{6.3.7}$$

$$\frac{\partial L}{\partial \delta_{i,j}} = 0, \ i, j = 1, \ldots, n \tag{6.3.8}$$

124

Here, in Equation (6.3.7), we consider the partial derivative of L wrt Σ^{-1} instead of Σ for computational convenience. Note that there exist a $1-to-1$ mapping between Σ^{-1} and Σ. Hence, the MLE is preserved. In what follows, we solve Equations (6.3.6) – (6.3.8) for (κ, Δ, Σ).

- Equation (6.3.6) implies that $\sum_{m=1}^{q} [y_m - \kappa - \Delta s(t_{m-1})]^T \Sigma^{-1} = 0$. We use the fact that $\sum_{m=1}^{q} y_m = \frac{s(t_q)-s(t_0)}{\epsilon_t}$ and express κ as follows:

$$\kappa = \frac{s(t_q) - s(t_0)}{t_q} - \frac{1}{q}\Delta \sum_{m=1}^{q} s(t_{m-1}).\tag{6.3.9}$$

- Note that $[y_m - \kappa - \Delta s(t_{m-1})]^T \Sigma^{-1} [y_m - \kappa - \Delta s(t_{m-1})]$ is a scalar, which equals its trace. Thus,

$$[y_m - \kappa - \Delta s(t_{m-1})]^T \Sigma^{-1} [y_m - \kappa - \Delta s(t_{m-1})]$$

$$= Tr([y_m - \kappa - \Delta s(t_{m-1})]^T \Sigma^{-1} [y_m - \kappa - \Delta s(t_{m-1})])$$

$$= Tr(\Sigma^{-1} [y_m - \kappa - \Delta s(t_{m-1})][y_m - \kappa - \Delta s(t_{m-1})]^T)$$

Hence, in Equation (6.3.7),

$$\frac{\partial}{\partial \Sigma^{-1}} [y_m - \kappa - \Delta s(t_{m-1})]^T \Sigma^{-1} [y_m - \kappa - \Delta s(t_{m-1})] = [y_m - \kappa - \Delta s(t_{m-1})][y_m - \kappa - \Delta s(t_{m-1})]^T$$

Also, note that $\frac{\partial}{\partial \Sigma^{-1}} \log |\Sigma| = \Sigma$. Equation (6.3.7) can be re-written as

$$\frac{q}{2}\Sigma - \frac{1}{2} \sum_{m=1}^{q} [y_m - \kappa - \Delta s(t_{m-1})][y_m - \kappa - \Delta s(t_{m-1})]^T = 0$$

Hence, we express Σ as follows

$$\Sigma = \frac{1}{q} \sum_{m=1}^{q} [y_m - \kappa - \Delta s(t_{m-1})][y_m - \kappa - \Delta s(t_{m-1})]^T.\tag{6.3.10}$$

- To solve for $\delta_{i,j}$'s, we use the fact that $\Sigma = \text{diag}\{\sigma_1^2/\epsilon_t, \ldots, \sigma_n^2/\epsilon_t\}$ and re-write L as follows

$$L = C + \frac{1}{2} \sum_{m=1}^{q} \sum_{\ell=1}^{n} \frac{[y_{m,\ell} - \kappa_\ell - \Delta_{\ell \cdot} s(t_{m-1})]^2}{\sigma_\ell^2/\epsilon_t},$$

where $y_{m,\ell}$ is the ℓth element of y_m, $\Delta_{\ell \cdot}$ is the ℓth row of Δ, and C is a constant that does not contain $\delta_{i,j}$'s. Since for $\ell \neq i$,

$$\frac{\partial [y_{m,\ell} - \kappa_\ell - \Delta_{\ell \cdot} s(t_{m-1})]^2}{\partial \delta_{i,j}} = 0,$$

125

we can simplify the expression of $\frac{\partial L}{\partial \delta_{i,j}}$ as follows:

$$\frac{\partial L}{\partial \delta_{i,j}} = \frac{\partial}{\partial \delta_{i,j}} \left(\frac{1}{2} \sum_{m=1}^{q} \frac{[y_{m,i} - \kappa_i - \Delta_{i\cdot} s(t_{m-1})]^2}{\sigma_i^2/\epsilon_t} \right) = \frac{-\epsilon_t}{\sigma_i^2} \sum_{m=1}^{q} [y_{m,i} - \kappa_i - \Delta_{i\cdot} s(t_{m-1})] s_j(t_{m-1})$$

As a result, Equation (6.3.8) can be re-written as follows

$$\sum_{m=1}^{q} y_{m,i} s_j(t_{m-1}) - \kappa_i \sum_{m=1}^{q} s_j(t_{m-1}) - \Delta_{i\cdot} \left[\sum_{m=1}^{q} s(t_{m-1}) s_j(t_{m-1}) \right] = 0. \qquad (6.3.11)$$

Note that Equation (6.3.11) involves the term of κ_i's. We plug in the expression of κ_i using Equation (6.3.9). Based on equation (6.3.9), κ_i can be expressed as $\kappa_i = \frac{s_i(t_q) - s_i(t_0)}{t_q} - \frac{1}{q} \Delta_{i\cdot} \sum_{m=1}^{q} s(t_{m-1})$. Substitute κ_i in equation (6.3.11) and combine terms of $\Delta_{i\cdot}$, we have, for $i, j = 1, \ldots, n$,

$$\Delta_{i\cdot} \times A_{\cdot j} = B_{i,j}, \quad \text{where} \qquad (6.3.12)$$

$$A_{\cdot j} = \frac{1}{q} \left(\sum_{m=1}^{q} s(t_{m-1}) \right) \left(\sum_{m=1}^{q} s_j(t_{m-1}) \right) - \sum_{m=1}^{q} s(t_{m-1}) s_j(t_{m-1})$$

$$B_{i,j} = \frac{s_i(t_q) - s_i(t_0)}{t_q} \sum_{m=1}^{q} s_j(t_{m-1}) - \sum_{m=1}^{q} y_{m,i} s_j(t_{m-1})$$

The matrix form of Equation (6.3.12) can be expressed as

$$\Delta \times A = B,$$

where $A = (A_{\cdot 1}, A_{\cdot 2}, \ldots, A_{\cdot n})$ and $B = [B_{i,j}]_{i,j=1,\ldots,n}$. Therefore, Equations (6.3.6)–(6.3.8) are proved. $\qquad \square$

Equations (6.3.3)–(6.3.5) provide the MLE estimates of model parameters $(\kappa, \sigma^2, \Delta)$ based on the degradation signals between replacement times u_ℓ and $u_{\ell+1}$. We then use a two-stage method by [84] to synthesize the resulting estimates from N different replacement segments. Specifically, we denote the MLEs based on the degradation signals between u_ℓ and $u_{\ell+1}$ by $(\hat{\kappa}^\ell, \hat{\sigma}^{2,\ell}, \hat{\Delta}^\ell)$ for $\ell = 0, \ldots, N-1$. Recall that we assume Δ is fixed across all independent systems. Hence, we estimate Δ using the sample mean of Δ^ℓ's, i.e. $\hat{\Delta} = \frac{1}{N} \sum_{\ell=1}^{N} \hat{\Delta}^\ell$. With regard to κ and σ^2, which are assumed to be stochastic parameters that capture the inherent variability across various similar systems, we use $\hat{\kappa}^\ell$'s and $\hat{\sigma}^{2,\ell}$'s as the sampled data and fit a desired prior distributions for κ and σ^2, respectively. These prior distributions will be updated using real-time degradation signals of components of a system that is functioning in the field.

6.3.2 Updating the DRI Model Using Real-Time Degradation Signals

This section focuses on updating stochastic parameters κ and σ^2 using real-time degradation signals from the constituent components of a system functioning in the field. Specifically, we use the degradation signals that have been observed since the last replacement to update the distributions of (κ, σ^2). Specifically, we assume that we monitor real-time degradation signals of components from a fielded system at times $t_0^*, t_1^*, \ldots, t_k^*$ after the ℓth replacement, such that $U_\ell = u_\ell < t_0^* < t_1^* < \ldots < t_k^*$. Without loss of generality, we assume that $\epsilon_t^* = t_1^* - t_0^* = t_2^* - t_1^* = \ldots = t_k^* - t_{k-1}^*$. The observed signals $s(t_0^*), s(t_1^*), \ldots, s(t_k^*)$ are subsequently used update the next replacement time U_ℓ as well as the stochastic parameters, κ and σ^2.

6.3.2.1 Updating the distributions of κ and σ^2

Let $\mathcal{S}_k^* = (s(t_0^*), s(t_1^*), \ldots, s(t_k^*))$ represent the set of real-time signal observations. We estimate the posterior distributions of κ and σ^2 based on $\mathcal{S}_k^*$. We assume that the prior distribution of σ_i^2 follows an inverse Gamma distribution, i.e. $\sigma_i^2 \sim \Gamma^{-1}(\xi_i, \theta_i)$, where $\Gamma^{-1}(\xi, \theta)$ represents an inverse Gamma distribution with shape parameter ξ and scale parameter θ. Conditioning on σ_i^2, we assume that the independent degradation rate κ_i (the degradation rate of component C_i assuming that there is no component interactions) has a normal prior distribution $\kappa_i | \sigma_i^2 \sim \mathcal{N}(\mu_i, \tau_i \sigma_i^2)$ for $i = 1, \ldots, n$, where $N(\mu, \sigma^2)$ represents a normal distribution with mean μ and variance σ^2. These assumptions on the prior distributions facilitate the closed-form expressions for the posterior distributions of κ and σ^2. These two prior distributions are chosen for a few pragmatic reasons. First, the gamma distribution encompasses a number of important distributions (e.g., exponential, Erlang, and chi-square); second, the normal distribution is widely used to model a mixture of populations; third, such prior distributions yield a closed-form density function of the posterior distributions that is easy to use. Proposition 6.3.2 below summarizes some results in [13] and provides the updated distributions of the model parameters.

Proposition 6.3.2 (Berger, 1985)**.** *Assume that the prior distribution of σ_i^2 follows an inverse Gamma distribution $\Gamma^{-1}(\xi, \theta)$, and the prior distribution of $\kappa_i | \sigma_i^2$ follow a normal distribution $\mathcal{N}(\mu_i, \tau_i \sigma_i^2)$ for $i = 1, \ldots, n$. Given $\mathcal{S}_k^*$, the posterior distribution of σ_i^2 follows follows an inverse Gamma distribution, i.e., $\sigma_i^2 | \mathcal{S}_k^* \sim \Gamma^{-1}(\tilde{\xi}_i, \tilde{\theta}_i)$, and the posterior distribution of κ follows a $\mathcal{T}$ distribution, i.e.,*

$\kappa_i | S_k^* \sim \mathcal{T}\left(2\tilde{\xi}_i, \tilde{\mu}_i, \frac{\tilde{\tau}}{\tilde{\xi}_i \tilde{\theta}_i}\right)$ for $i = 1, \ldots, n$. The parameters of the posterior distributions are expressed as follows:

$$\tilde{\mu}_i = \frac{\mu_i + \epsilon_t^* \tau_i \sum_{m=1}^{k} x_{i,m}}{1 + k\tau_i \epsilon_t^*},$$

$$\tilde{\tau}_i = \frac{1}{k\epsilon_t^* + \tau_i^{-1}},$$

$$\tilde{\xi}_i = \xi_i + k/2,$$

$$\tilde{\theta}_i = \theta_i + \frac{\epsilon_t^*}{2} \sum_{m=1}^{k} (x_{i,m} - \bar{x}_i)^2 + \frac{k\epsilon_t^*(\bar{x}_i - \mu_i)^2}{2(1 + k\epsilon_t^* \tau_i)}.$$

where $x_{i,m} = \frac{s_i(t_m^*) - s_i(t_{m-1}^*)}{\epsilon_t^*} - \sum_{j=1}^{n} s_j(t_{m-1}^*) \delta_{j,i}$ and $\bar{x}_i = \frac{1}{k} \sum_{m=1}^{k} x_{i,m}$ for $m = 1, \ldots, k$.

Proof. By [13], the posterior probability density function (p.d.f.) of (σ_i^2, κ_i), denoted by $\pi_i(\kappa_i, \sigma_i^2 | S_k^*)$, is given by

$$\pi_i(\kappa_i, \sigma_i^2 | S_k^*) = \pi_{i,1}(\kappa_i | \sigma_i^2, S_k^*) \pi_{i,2}(\sigma_i^2 | S_k^*),$$

where $\pi_{i,1}(\kappa_i | \sigma_i^2, S_k^*)$ represents the p.d.f. of a normal distribution with mean $\tilde{\mu}_i$ and variance $\tilde{\tau}_i \sigma_i^2$, and $\pi_{i,2}(\sigma_i^2 | S_k^*)$ represents the p.d.f. of an inverse Gamma distribution with shape parameter $\tilde{\xi}_i$ and scale parameter $\tilde{\theta}_i$. Note that the p.d.f. of a random variable X, which follows $\mathcal{T}$ distribution $\mathcal{T}(\alpha, \mu, \gamma^2)$, is expressed as follows

$$f_{\mathcal{T}}(x) = \frac{\Gamma[(\alpha+1)/2]}{\gamma(\alpha\pi)^{1/2}\Gamma(\alpha/2)}\left(1 + \frac{(x-\mu)^2}{\alpha\gamma^2}\right)^{-(\alpha+1)/2}.$$

Hence, we integrate out σ_i^2 in the expression of the posterior joint probability density of κ_i and σ_i^2, namely $\pi_i(\kappa_i, \sigma_i^2 | S_k^*)$. The resulting pdf of κ_i is the pdf of a $\mathcal{T}$ distribution with $\kappa_i | S_k^* \sim \mathcal{T}\left(2\tilde{\xi}_i, \tilde{\mu}_i, \frac{\tilde{\tau}}{\tilde{\xi}_i \tilde{\theta}_i}\right)$. The details are omitted in this paper. $\square$

We let κ_i^* and σ_i^{*2} denote the posterior means of κ_i and σ_i^2, then κ_i^* and σ_i^{*2} can be estimated using the following expressions.

$$\kappa_i^* = \mathbb{E}(\kappa_i | S_k^*) = \tilde{\mu}_i, \quad \text{and} \quad \sigma_i^{*2} = \mathbb{E}(\sigma_i^2 | S_k^*) = \frac{\tilde{\theta}_i}{(\tilde{\xi}_i - 1)}. \tag{6.3.13}$$

In what follows, we use the updated values of κ_i^* and σ_i^{*2} to update the residual life distribution of each component C_i, $i = 1, \ldots, n$, and further update the distribution of the next replacement time $U_{\ell+1}$. The updating process can be performed each time new degradation signals are observed.

6.3.2.2 Updating the RLDs Using Real-Time Degradation Signals

The posterior distributions of κ and σ^2 are then used to computed posterior residual life distributions for the components of a fielded system that exhibit degradation interactions. Given that we have observed $s(t*_k)$, and our DRI model expressed in equation (6.1.2), the future path of the degradation signals after time t_k can be characterized by the following SDE system:

$$dS(t) = [\kappa^* + \hat{\Delta} \times S(t)]dt + dB^*(t), \quad \text{for } t > t_k^*, \tag{6.3.14}$$

$$S(t_k^*) = s(t_k^*),$$

where $\kappa^* = (\kappa_1^*, \ldots, \kappa_n^*)'$, $B^*(t) = (\sigma_1^* W_1(t), \ldots, \sigma_n^* W_n(t))'$, and $\hat{\Delta}$ represents the estimate value of $\hat{\Delta}$ based on the historical degradation signals.

If we let $S^*(t)$ denote the solution of the SDE system (6.3.14), by applying Proposition 6.1.1 we can express $S^*(t)$ as follows

$$S^*(t) = \exp[(t - t_k^*)\hat{\Delta}]s(t_k^*) + \int_0^{t-t_k^*} [(t - t_k^* - s)\hat{\Delta}]\kappa^* ds + \int_0^{t-t_k^*} [(t - t_k^* - s)\hat{\Delta}]dB^*(s), \tag{6.3.15}$$

where $\sigma^{*2} = (\sigma_1^{*2}, \ldots, \sigma_n^{*2})'$. The future evolution of $S^*(t)$ depends on the updated parameters (κ^*, σ^{*2}), which are the posterior means of (κ, σ^2) as shown in expression (6.3.13). Moreover, based on Proposition 6.1.2, $S^*(t)$ follows a multivariate normal distribution $MVN(\mu^*(t), \Sigma^*(t))$, where

$$\mu^*(t) = \exp[(t - t_k^*)\hat{\Delta}]s(t_k^*) + \int_0^{t-t_k^*} [(t - t_k^* - s)\hat{\Delta}]\kappa^* ds$$

$$\Sigma^*(t) = \int_0^t \exp[(t - t_k^* - s)\hat{\Delta}] \times \Sigma_0^* \times \exp[(t - t_k^* - s)\hat{\Delta}]^T ds,$$

where $\Sigma_0^* = \text{diag}\{\sigma_1^{*2}, \ldots, \sigma_n^{*2}\}$.

Therefore, the updated distribution of residual life of component C_i until the next replacement, namely R_i, is expressed as follows

$$\mathbb{P}(R_i < t - t_k | S_k^*) = \Phi\left(\frac{\mu^*(t)_{(i)} - d_i}{\sqrt{\Sigma^*(t)_{(i,i)}}} \right), \quad \text{for } t > t_k^*, \tag{6.3.16}$$

where $\mu^k(*)_{(i)}$ represents the ith element of $\mu^*(t)$, and $\Sigma^*(t)_{(i,i)}$ represents the $(i, i)^{th}$ element of $\Sigma^*(t)$. The updated distribution of the next replacement time $U_{\ell+1}$ can be computed as follows

$$\mathbb{P}(U_{\ell+1} > t + t_k^* | S_k^*) = \varphi_t^*(d), \quad \text{for } t > 0, \tag{6.3.17}$$

where $\varphi_t^*(\cdot)$ is the c.d.f. of a multivariate normal distribution with mean vector $\mu * (t)$ and covariance matrix $\Sigma^*(t)$.

6.4 Numerical Studies

In this section, we conduct a sequence of numerical studies and test our proposed approach for modeling continuous DRI among the constituent components of a given system using simulated signals. As a case in point, we focus on a hypothetical series system of three components that are interdependent. The system fails when any component fails. The degradation processes exhibit continuous DRI that are manifested in the behaviors of their degradation signals. In what follows, we present a procedure for simulating degradation signals of components with degradation processes that exhibit continuous DRIs. These signals are simulated until the entire system fails. We then use the simulated signals to test accuracy of the estimation procedure used to estimate the model parameters as well as the goodness of fit. In particular, we use the simulated signals to verify the assumptions on the prior distributions of model parameters and the signal noise by conducting the Kolmogorov-Smirnov test and the Shapiro-Wilk test, respectively. We also test accuracy of predicting the failure time of the system for different values of model parameters θ_i's and $\delta_{i,j}$'s, which characterize different levels of signal noise and component interactions. Recall that σ_i^2 is the diffusion parameter of the signal model and has a prior distribution that is assumed to be an inverse-Gamma distribution with shape parameter θ_i, and $\delta_{i,j}$ represents the magnitude of the DRI between components C_i and C_j, i.e., the infinitesimal change in the degradation rate of component C_j caused by its interaction with C_i. By choosing different values of θ_i's and $\delta_{i,j}$'s, we can test of prediction accuracy of the system failure time for various levels of signal noise and component DRI. (4) To highlight the capability of our model for capturing the effects of component interactions, we further compare our results with a benchmark model by [47], which adopts a similar modeling approach but does not take into account the effect of component DRI.

6.4.1 Signal Simulation

We focus on a series system of three constituent components and simulate degradation signals of the components until the system failure occurs. We use the baseline model parameters shown in Table 6.4.1 and simulate degradation signals via the following procedure.

Step B.1: Let $\epsilon_t = 0.1$ represent the time interval for discretization of the continuous DRI model. Note that smaller value of ϵ_t increases the accuracy of simulation and computation

cost.

Step B.2: Choose simulated values of σ_i^2 and κ_i from the following distributions: $\sigma_i^2 \sim \Gamma^{-1}(\xi_i, \theta_i)$ and $\kappa_i | \sigma_i^2 \sim \mathcal{N}(\mu_i, \tau_i \sigma_i^2)$ using the values defined in Table 6.4.1.

Step B.3: For $i = 1, 2, 3$, set $s_i(t_{m+1}) = s_i(t_m) + \sum_{j \neq i}^{n} \delta_{j,i} s_j(t_m) + z_i$, where $t_m = m\epsilon_t$ and $z_i \sim \mathcal{N}(0, \sigma_i^2 \epsilon_t)$. Repeat this step until $s_i(t_m) > d_i$ where d_i is the failure threshold for component C_i. The system failure time is denoted by L. We denote the actual failure time of the system by L.

Table 6.4.1: Baseline parameter values for the continuous model.

	Parameters	Component C_1	Component C_2	Component C_3
Failure threshold	d_i	10	10	10
Initial signal value	$s_i(0)$	0	1	0.8
Prior mean of κ_i	μ_i	0.02	0.06	0.08
Scale for prior variance of κ_i	τ_i	0.1	0.1	0.1
Prior shape parameter of σ_i^2	ξ_i	92	92	92
Prior scale parameter of σ_i^2	θ_i	9.1	9.1	9.1
DRI effects of Component C_1	$\delta_{1,i}$	0	0.05	0.08
DRI effects of Component C_2	$\delta_{2,i}$	0.06	0	0.09
DRI effects of Component C_3	$\delta_{3,i}$	0.08	0.06	0

Using the aforementioned simulation procedure, we generate degradation signals for components from 100 systems. The first 50 degradation signals are considered to represent a historical data set used to estimate the model parameters and test of the goodness of fit. The remaining 50 degradation signals are used to test real-time prediction of the RLDs.

6.4.2 Parameter Estimation and Goodness of Fit

Using degradation signals from each system, we obtain the MLEs of $(\kappa, \Delta, \sigma^2)$ using equations (6.3.3) – (6.3.5). The resulting estimates are used to fit the prior distributions of κ and σ^2 as discussed in Section 6.3.1. The estimated values of the model parameters based on the historical data set are summarized in Table 6.4.2. The hats on parameters represent the values estimated using the historical data set.

Table 6.4.2: Estimated values of baseline parameters.

Estimated parameters	Component C_1	Component C_2	Component C_3
$\hat{\mu}_i$	0.021	0.053	0.087
$\hat{\tau}_i$	0.087	0.157	0.152
$\hat{\xi}_i$	102.6	90.1	97.4
$\hat{\theta}_i$	12.45	11.71	10.34
$\hat{\delta}_{1,i}$	0.003	0.054	0.074
$\hat{\delta}_{2,i}$	0.066	0.001	0.092
$\hat{\delta}_{3,i}$	0.084	0.076	0.000

Table 6.4.3: P-values of the two-sample Kolmogorov-Smirnov test for prior distributions.

Parameters	(κ_1, σ_1^2)	(κ_2, σ_2^2)	(κ_3, σ_3^2)
P-Value	0.74	0.68	0.83

Table 6.4.4: P-values of the Shapiro-Wilk test for noise term.

Noise term	$B_1(t_{j+1}) - B_1(t_j)$	$B_2(t_{j+1}) - B_2(t_j)$	$B_3(t_{j+1}) - B_3(t_j)$
Range of p-Value	$[0.72, 0.81]$	$[0.86, 0.93]$	$[0.67, 0.84]$

With the estimated parameters, we test the goodness-of-fit of the prior distributions for $\sigma_i^2 \sim \Gamma^{-1}(\xi_i, \theta_i)$ and $\kappa_i | \sigma_i^2 \sim \mathcal{N}(\mu_i, \tau_i \sigma_i^2)$. In particular, we denote by $(\hat{\kappa}^\ell, \hat{\sigma}_i^{2,\ell})$ the MLEs of (κ, σ_i^2) based

on the historical degradation signals of components from the ℓth system. Our goal is to verify that the sample of $\{(\hat{\kappa}^\ell, \hat{\sigma}_i^{2,\ell}) : \ell = 1, \dots, 50\}$ satisfy the aforementioned assumptions of the prior distributions. To this end, we simulate a benchmark sample of (κ_i, σ_i^2) based on the model assumptions and compare the sample of $\{(\hat{\kappa}^\ell, \hat{\sigma}_i^{2,\ell}) : \ell = 1, \dots, 50\}$ with the benchmark sample using the two-sample Kolmogorov-Smirnov test. The p-values of the test are summarized in Table 6.4.3. The results show that there is no evidence to reject the model assumption on the prior distributions based on the historical data set.

We also test the model assumption that signal noise follows a Brownian motion process. To do this, we use the discretization procedure of the degradation signals of components from a given system in Equation (6.3.1), and examine the increments in the signal noise:

$$s(t_{j+1}) - s(t_j) - [\hat{\kappa} + \hat{\Delta} \times s(t_j)] = \boldsymbol{B}(t_{j+1}) - \boldsymbol{B}(t_j).$$

Recall that $\boldsymbol{B}(t_{j+1}) - \boldsymbol{B}(t_{j+1}) \sim MNV(\boldsymbol{0}, \boldsymbol{\Pi}_0(t_{j+1} - t_j))$, where $\boldsymbol{\Pi}_0 = \text{diag}\{\sigma_1^2, \dots, \sigma_n^2\}$. Hence, we verify the normality of $\{s_i(t_{j+1}) - s_i(t_j) : j = 0, \dots, k\}$ for $i = 1, 2, 3$ using the Shapiro-Wilk test. We apply the Shapiro-Wilk test to the historical degradation signals of components from each system. Table 6.4.4 summarizes the range of the resulting p-values of all signals in the historical data set. Based on the resulting values, we do not reject the assumption that increments in the noise term for each component are samples from a normal distribution.

6.4.3 Testing Prediction Accuracy of the RLD

To evaluate the performance of our proposed methodology, we simulate degradation signals of components observed from systems that are operating in the field and compare estimated system lifetime with the simulated system failure time L. In particular, we estimate the RLD of the system at the 30th, 60th, and 90th lifetime percentile of the system, i.e., $t_k^* = 0.3L, 0.6L, 0.9L$. We define $\hat{R}$ as the median estimate of the system residual life computed using Equation (6.3.16). Thus, the predicted system lifetime L is estimated as $t_k^* + \hat{R}$. Hence, the lifetime prediction error for a given system is computed by

$$e = \frac{|t_k^* + \hat{R} - L|}{L}. \tag{6.4.1}$$

Moreover, we investigate the prediction accuracy for various values of signal noise σ^2 and component interactions $\boldsymbol{\Delta}$. Specifically, we start with a baseline framework with parameter values

chosen according to Table 6.4.1 and conduct the simulation study for various model parameters based on the following series of tests:

(1) **Testing the effects of diffusion parameter σ^2**: For $m_1 = 0.1, 0.2, \ldots, 2.0$, we let $\theta_i = m_1 \times \theta_i^{\text{base}}$, $i = 1, \ldots, 3$, while holding other parameters fixed, where θ_i^{base}'s represent the baseline values listed in Table 6.4.1. Recall that $\mathbb{E}(\sigma_i^2) = \frac{\theta_i}{\xi-1}$. We test the prediction accuracy of the RLD when the prior mean of σ_i^2's equal $0.1, 0.2, \ldots, 1.9, 2.0$ times of the baseline value.

(2) **Testing the effects of interaction parameter Δ**: For $m_2 = 0.1, 0.2, \ldots, 2.0$, we let $\delta_{i,j} = m_2 \times \delta_{i,j}^{\text{base}}$ for $i = 1, \ldots, 3$ while holding other parameters fixed, where $\delta_{i,j}^{\text{base}}$'s represent the baseline values listed in Table 6.4.1.
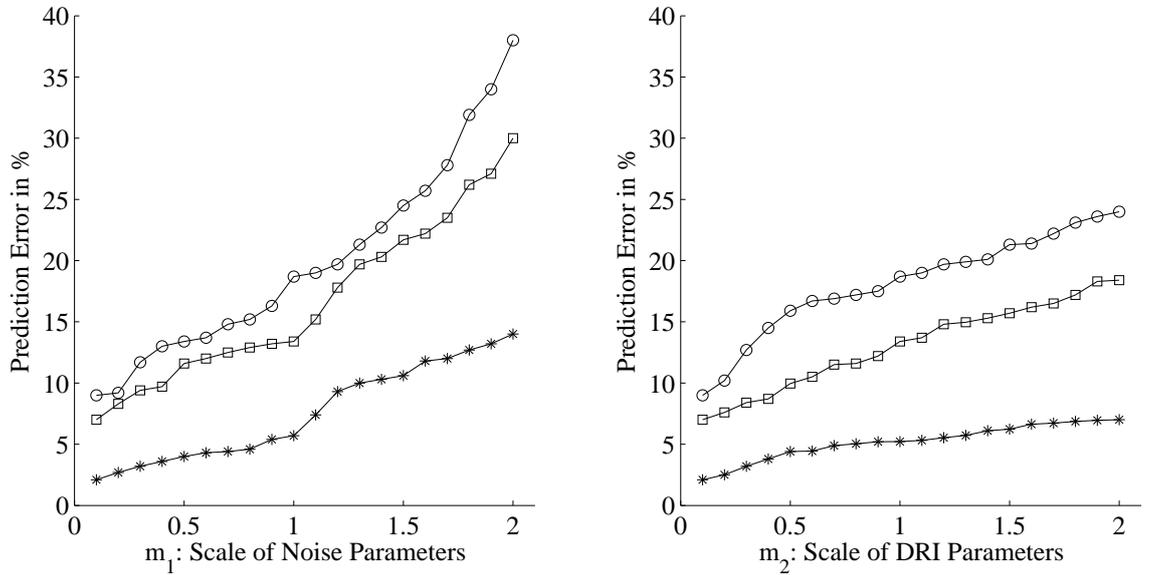
Figure 6.4.1: Prediction error for various values of parameters. "∘": 30th lifetime percentile; "□": 60th lifetime percentile; "∗": 90th lifetime percentile.

In these two sequences of simulation tests, m_1 and m_2 represent the scales of signal noises and component interactions, respectively. In other words, the amplitude of signal noise increases as m_1 increases, and the effect of component DRI becomes more evident when m_2 increases. For each simulation test, we simulate a sample of testing degradation signals of components from 100 systems using the procedure presented in Section 6.4.1 and compute the prediction error e for each

system. The average prediction error over all testing signals is summarized in Figure 6.4.1. The left plot in Figure 6.4.1 represents how the prediction accuracy of the system replacement time responds to the increase in signal noise (m_1); whereas, the right plot represents how the prediction accuracy responds to the increase in component DRI (m_2). For each plot, the horizontal axis represents the scale of noise and DRI parameters, and the vertical axis represents the prediction error in percentage. Within each plot, we present the prediction error at the $30th$ ($\circ$), $60th$ ($\square$), and $90th$ ($*$) lifetime percentiles of the system.

We observe from Figure 6.4.1 that: (1) the prediction error at a later lifetime percentile is lower than an early lifetime percentile. This can be attributed to the fact that incorporating more real-time information about the degradation process improves the accuracy of estimating the replacement time. (2) The prediction error of replacement time increases as either the signal noise or the magnitude of the DRI increases. However, by comparing the two plots in Figure 6.4.1, we notice that the prediction accuracy is less affected by the increase in the magnitude of DRI. This may be partly due to the ability of our proposed model to capture the effects of component interactions.

6.4.4 Comparing Prediction Accuracy with a Benchmark Model

We now compare the prediction errors of our proposed DRI model with a benchmark model presented in [47], which models the degradation signal of individual components without considering the effects of any form of degradation interactions. In particular, we study how the prediction accuracy of these two approaches differ for different values of model parameters, especially parameters that govern the level of interdependencies among the components, i.e., the magnitude of the DRI that takes place among components of a system. We also compute the corresponding prediction errors at the same lifetime percentiles. We focus on this specific model for the following reasons: (1) First of all, similar to the proposed approach in this paper, the model by [47] also utilizes real-time degradation signals to update the degradation model and compute corresponding posterior RLDs for fielded components. Thus, the difference between the prediction accuracy of these two approaches are not affected by different prediction times. (2) This benchmark model is similar in spirit to our proposed model in that it models the signal noise as a Brownian motion process, however unlike our modeling approach it does not account for any component interdependencies and degradation

135

interactions. Therefore, the comparison is efficient and fair in that any potential improvements in the prediction accuracy of our proposed approach can be attributed to the incorporation of component DRIs.

The model by [47] is presented as follows

$$S(t) = \phi + \theta \exp\left(\beta t + \epsilon(t) - \frac{\sigma_t^2}{2}\right). \tag{6.4.2}$$

[47] developed the expression for the RLD at time t_k^* for a single component, which is computed as

$$P(T \leq t) = \Phi\left(\frac{\tilde{\mu}(t + t_k^*) - d}{\sqrt{\tilde{\sigma}^2(t + t_k^*)}}\right), \tag{6.4.3}$$

where $\tilde{\mu}(t + t_k^*)$ and $\tilde{\sigma}^2(t + t_k^*)$ represent the posterior mean and variance of $S(t_k^* + t)$, respectively. d represents the failure threshold.

We apply Equation (6.4.3) to estimate the RLD of each component and thus the system replacement time. The prediction error is computed using Equation (6.4.1) for each system. The average prediction errors for different signal noise levels are presented in Figure 6.4.2, and the average prediction errors for different DRI magnitudes are presented in Figure 6.4.3. Similar to previous numerical study, the horizontal axes in both figures represent the scale of the parameter of interest, and the vertical axes represent the prediction error in percentage. The prediction error of our proposed approach is represented by "○", and that of the benchmark model is represented by "∗". The system lifetime is estimated at the 30*th*, 60*th*, and 90*th* lifetime percentiles.

We observe that (1) the increase in signal noise (m_1) has similar impacts on the prediction accuracy of both approaches. This is because as the signal noise increases the uncertainty in the future evolution increases. Thus, the prediction of system replacement time increases for both approaches. (2) The performances of our proposed approach and the benchmark model are similar when the effect of component DRI (m_2) is small. We believe this is because that when m_2 is very small, the DRI effects between components are minimal. In this case, the model by [47] becomes a special case of our proposed DRI model. (3) However, as the effect of component DRI increases, the performance of the benchmark model becomes significantly aggravated, whereas, that of our approach is less affected. This is mainly because the benchmark model does not take into account component interactions when predicting component lifetime distributions.
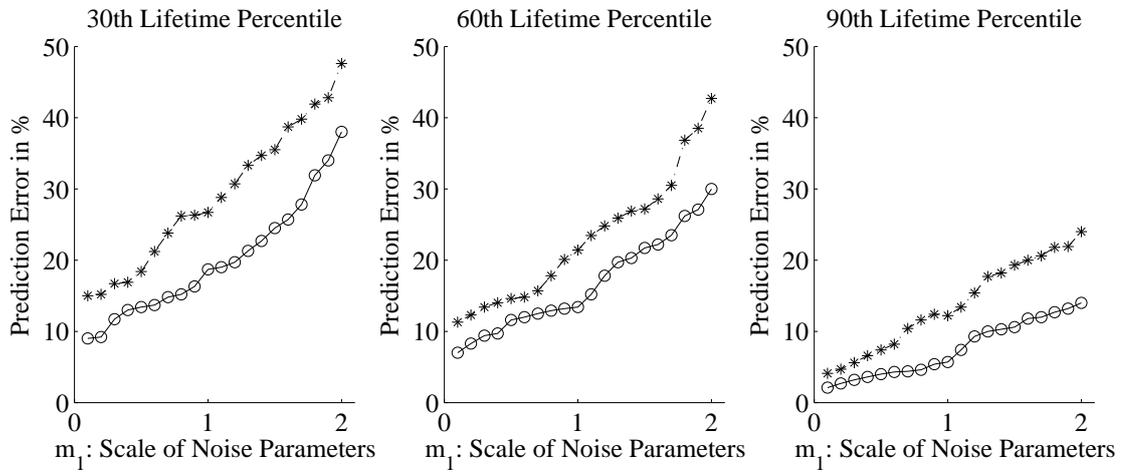
136

Figure 6.4.2: Prediction error compared with the benchmark model. "○": our proposed model; "∗": the benchmark model.
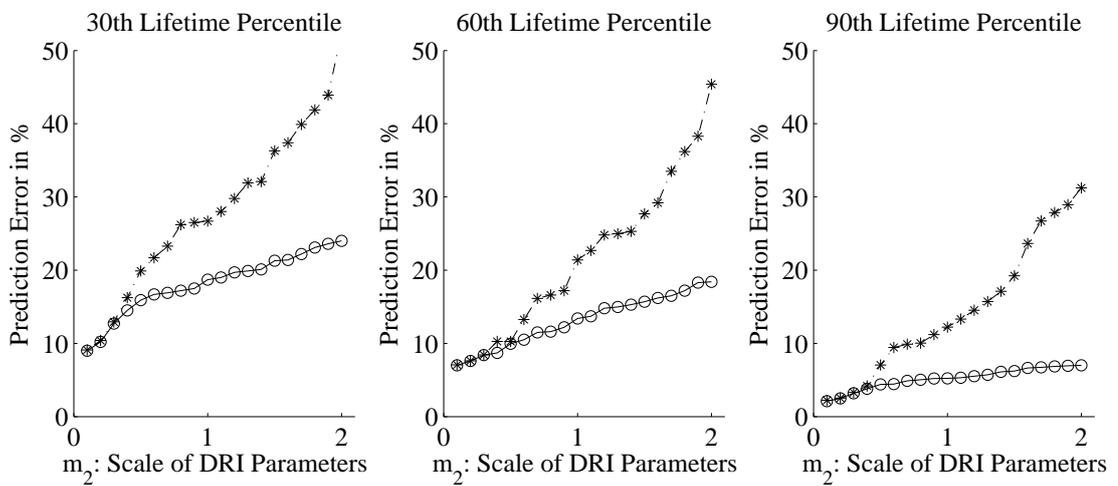

Figure 6.4.3: Prediction error compared with the benchmark model. "○": our proposed model; "∗": the benchmark model.

CHAPTER VII

CONCLUSIONS AND FUTURE WORK PLAN

7.1 Conclusions

We develop a sensor-based degradation framework for modeling the degradation signals of components in complex engineering systems. The main significance of our work is characterizing the effects of environmental profiles and the C2C interactions on the degradation signals. Our approach improves the prediction accuracy of component RLDs by incorporating the real-time observations of degradation signals and environmental conditions.

This dissertation starts with a stochastic degradation model that estimates and continuously updates the residual life distributions (RLD) of partially degraded components. Compared with the conventional degradation model, as described by [47], our model significantly improves the prediction accuracy of RLDs by using a first-passage time (FPT) approach. Specifically, we model the failure threshold as an absorbing barrier of the degradation signal. In this case, the probability of failure is equivalent to the crossing probability of the degradation signal to a crossing boundary. We develop the expressions of RLDs for a base case degradation model with an exponential functional form and investigate two types of engineering applications: (1) applications that have existing historical degradation signals (informative prior distribution); and (2) applications that have no prior information (non-informative prior distribution). We demonstrate that the model performs reasonably well in both cases, with the informative case outperforming the non-informative case. We validate our model using simulation studies and real-world vibration-based degradation signals from a rotating machinery application (rolling element thrust ball bearings). By comparing with [47], we demonstrate that our FPT approach improved about 20% of the prediction accuracy with real-time degradation signals from the component working in the field.

Subsequently, we propose a stochastic degradation modeling framework that computes the RLD of partially-degraded components operating under time-varying environmental or operating conditions. This framework uses historical and real-time signals related to the environmental conditions, as well as the underlying physical degradation process. In contrast to most existing models, we compute the components RLD in real time by utilizing the potential profile of future environmental conditions that the component is likely to experience. Degradation models for two types of environment processes were developed. The first model assumed that the environmental profile is

deterministic in nature while the second assumed that the environment evolves as a continuous-time Markov chain. It was demonstrated for the first model that our proposed framework improved the prediction accuracy when compared to similar models that do not include future environmental changes or shocks induced by environmental transitions. To further evaluate the performance of our approach, we conducted a series of validation experiments that generated empirical vibration-based degradation signals with time-varying loads and speeds. The experimental results show great promise for predicting the remaining useful lifetime of partially-degraded, critical components. For the second model, we demonstrated, via extensive simulation experiments, that our approach can be used to estimate the RLD if the environment has a moderate number of distinct states.

Furthermore, we present a stochastic methodology for modeling interactions among the degradation processes of interdependent components of a given system and uses such knowledge to predict their respective residual lifetimes. The proposed methodology is developed on the premise that degradation signals measured using sensors are directly correlated with the physical degradation process and any changes that occur due to degradation interactions manifest themselves in the behavior of the degradation signal. In contrast to most existing models, which either assume independent components or only investigate interactions caused by component failures, our framework captures the interactions among the underlying degradation processes of components that occur in continuous and discrete manners. For continuous component interactions, we developed an SDE-based degradation model and estimate the RLD with the aid of Itô calculus. For discrete component interaction, we developed a multi-state degradation model and assess the interaction mechanism using the techniques of change-point detection. Furthermore, our proposed framework uses historical and real-time signals related to the underlying physical degradation processes to estimate the RLDs of the constituent components. To evaluate the performance of our approach, we conducted a series of validation experiments that generated empirical vibration-based degradation signals with discrete and continuous component interactions. The experimental results show great promise for predicting the remaining useful lifetime of partially-degraded, critical components in a system with component interactions.

We would like to note that the degradation methodology presented in this dissertation is not only

140

limited to characterizing the interactions among the degradation processes of interdependent components and predicting their remaining lifetimes. Our methodology provides a formal framework for better understanding how the performance of a complex system is affected by its constituent components using a practical approach that relies on studying and modeling the behavior and evolution of degradation-based sensor signals. To further understand the behaviors of complex systems, additional developments are needed to model other types of component interactions, such as interactions that affect signal noise, or interactions that are dependent on the component type and/or degradation state.

7.2 Future Work

The future work includes extending the proposed stochastic degradation framework in two research tasks:

1. The first task is to extend the degradation models in Chapter 4 and Chapter 5 to construct a more general model that characterizes the health conditions of the constituent components in a network system. That includes modeling the degradation signals and estimating component residual lifetimes when the system is subject to time-varying environmental conditions and instant replacement. In addition, the model in Chapter 5 can be further applied to characterize the quality-reliability interactions in multi-state manufacturing systems.

2. In the second task, we will assess the network reliability using the simulation technique of cellular automata, which is efficient in updating the network structure using real-time information. This approach will be applied to maintain the reliability and the sustainability of the smart grids. We will investigate two reliability hazards in smart grid systems : the degradation of infrastructure and the volatile demands. The results of this research task will add to the limit literature that uses real-time pricing to balance demand and supply in smart grids. In addition, the incorporation of sensory data will provide insight on facilitating demand responses and management to mitigate net demand volatility.

7.2.1 Task 1 – Generalizing Time-Varying and Interactions Models

This task generalizes the degradation model in Chapter 5 to characterize the degradation signals of the constituent components in a network system, which are subject to time-varying environmental conditions and instant replacement. In addition, we will apply the stochastic model presented in Chapter 5 to model the interaction between tooling degradation and product quality in a multi-station manufacturing system with the goal of estimating failure due to the degradation of tools or the production of non-conforming products. This research task consists of the following three subtasks.

7.2.1.1 *Subtask 1.1 – Estimating the RLDs of Components With Instant Replacement.*

In this subtask, we will generalize the multi-component degradation model, as presented in Chapter 5, to estimate the RLDs of components in a multi-component engineering system when the failed components are replaced instantaneously. Specifically, we will investigate the scenario, in which the failed component is replaced with a new component and the time of replacement is ignored. The degradation model is generalized as follows

$$S_i(t) = \int_{\tau_i(t)}^{t} r_i(\kappa_i, \boldsymbol{h}(v)) \mathrm{d}v + B_i(t),$$

where $\tau_i(t)$ represents the latest replacement time for component i by t. After a component is replaced, its degradation signal transitions to state 0, and it affects other component by decreasing their degradation rates. Recall that the degradation model, as described in Chapter 5, focuses on characterizing the C2C interactions that increase the degradation rates of other components. The corresponding RLDs are estimated using the time-scale transforms by [37], which only accounts for increasing degradation rates for each degradation signal. In this task, we will investigate the degradation model, in which the C2C interactions can both increase or decrease the degradation rates of other components. We will generalize the time-scale transformation by [37] for estimating the RLDs using degradation signals, whose degradation rates may increase and decrease.

7.2.1.2 Subtask 1.2 – RLD Estimation with Component Interactions and Time-Varying Environmental Conditions

This subtask focuses on estimating the residual life distribution (RLD) of an engineering system, the constituent components of which are dependent and subject to the environmental profile of the entire system. We will incorporate our proposed models for time-varying environmental conditions and the multi-component system for characterizing the degradation signals of components in an n-component system. For $i = 1, \ldots, n$, we model the the degradation signal of component i as follows

$$S_i(t) = \int_{v=0}^{t} \left[\kappa_i(t) + \sum_{i' \neq i} h_{i',i}(v) \delta_{i',i} \right] dv + B_i(t). \tag{7.2.1}$$

Component interactions on the degradation rates are captured by $h_{i',i}(v)$'s and $\delta_{i',i}$'s, as described in Chapter 5. We will investigate the effect of operational/environmental conditions on the natural degradation rates of each components. That is, we assume that

$$\kappa_i(t) = \theta(t) + \varphi_i(t),$$

where $\theta(t)$ captures the environmental profile of the entire system, and $\varphi_i(t)$ captures the environmental condition that is specific to each component.

We will incorporate the effects of the operational conditions on the degradation processes of components. The environmental/operational conditions generally consists of two parts: (1) the environmental condition common to all components and (2) the operational condition specific to each component. We assume that the independent degradation rate of each component depends on the common environment. This also captures the dependence among the constituent components of an engineering system. For example, as the system is subject to shocks, the degradation rates of all components are affected. Within an engineering system, the operational condition applied to each individual component may be different, and each component may be subject to different future operational profile. $\varphi_i(t)$'s capture such operational conditions that are specific to each component.

We will investigate how to estimate the RLD of each component for various functional forms of environmental conditions $\theta(t)$ and $\varphi_i(t)$, including the piecewise constant function, linear function, and others. The techniques of time-scale transformations can be applied. For example, when $\theta_i(t)$ and $\varphi_(t)$ are both piecewise constant functions and $X_i(t)$ evolves according to a Brownian motion

process, the RLD of component i follows an inverse Gaussian distribution under the time-scale transform define by

$$\xi_i(t) = \int_{v=0}^{t} \left[\theta(t) + \varphi_i(t) + \sum_{i' \neq i} h_{i'}(v) \delta_{i',i} \right] dv.$$

In this case, the lifetime distribution of component i follows an inverse Gaussian distribution under the time-scale transformation $\xi_i(t)$. That is,

$$\mathbb{P}(R_{0,i} < t) = IG(\xi(t); d_i, \sigma_i^2).$$

The RLDs can be computed using similar time-scale transforms that depend on real-time degradation signals.

7.2.1.3   Subtask 1.3 – Application: Modeling the Quality-Reliability Interactions in Multi-Station Manufacturing Systems.

This subtask is a joint work with Ms. Li Hao and Professor Jan Shi. In this subtask, we examine the failures of multi-stage engineering systems, in which the degradation of tools and the quality of products affect each other. Most papers in the related literature focus on the impact of tooling degradation on the quality of products. Very few (cf. [26]) have considered the effects of product quality on the degradation of tools in a multi-station manufacturing system. We will investigate two failure modes in such engineering systems : the production of non-conforming units or the failure of tools.

We will investigate a system with m stations and n tools, in which the product performance of station i at time t is measure by $Y_j(t)$ for $j = 1, \ldots, m$. In the same spirit of [26], we characterize $Y_j(t)$ using the response model in robust parameter design, which is expressed as follow

$$Y_j(t) = \eta_j + \boldsymbol{\alpha}'_j \times \boldsymbol{S}(t) + \boldsymbol{\beta}'_j \times z_t + \boldsymbol{S}(t)' \times \boldsymbol{\Gamma}_j \times z_t, \tag{7.2.2}$$

where $\boldsymbol{S}(t)$ represents the degradation states of tools, and z_t represents the main effect of noise with $\mathbb{E}(z_t)$ and $\text{cov}(z_t)$ independent of the time index. This model can be obtained based on specific physical process models when the physical knowledge is available or using the techniques of design of experiments.

In the same spirit of [26], we define the quality index of products from station j, denoted by q_j, as the variation of $Y_j(t)$ from its target value. To this end, we denote the target value of the product

quality characteristic (PQC) by γ_j for $j = 1, \ldots, m$, where

$$\gamma_j = \mathbb{E}(Y_j(t)|S(t) = 0) = \eta_j + \boldsymbol{\beta}'_j \times \mathbb{E}(z_t). \tag{7.2.3}$$

Using Equation (7.2.3), we expresss quality index q_j as follows

$$q_j(t|S(t)) = \mathbb{E}((Y_j(t) - \gamma_j)^2|S(t)). \tag{7.2.4}$$

By [26], q_j can be further simplified as follows

$$q_j(t|S(t)) = S(t)' \times \boldsymbol{B_j} \times S(t) + d_j, \text{ where} \tag{7.2.5}$$

$$\boldsymbol{B_j} = \boldsymbol{\Gamma}_j \times \text{cov}(z_t) \times \boldsymbol{\Gamma}'_j + (\boldsymbol{\alpha}_j + \boldsymbol{\Gamma}_j \times \mathbb{E}(z_t)) \times (\boldsymbol{\alpha}_j + \boldsymbol{\Gamma}_j \times \mathbb{E}(z_t))'$$

$$d_j = \boldsymbol{\beta}'_j \times \text{cov}(z_t) \times \boldsymbol{\beta}_j.$$

We consider the degradation signals of the tools, which are characterized by the following model

$$S(t_{k+1}) - S(t_k) = \boldsymbol{r}(S(\boldsymbol{t_k}))(t_{k+1} - t_k) + \boldsymbol{\epsilon}_k,$$

where $\boldsymbol{r}(S(\boldsymbol{t_k}))$ the degradation rate of tools and $\boldsymbol{\epsilon}(t)$ represents the noise part of the degradation signals. As a result, the tooling degradation is driven by both of the natural degradation process of tools and the effects of PQC from upstream stations. In particular, we assume that the degradation rates of the tools are affected by the deviation of the product quality and express the degradation rates in the following form

$$\boldsymbol{r}(S(t_k)) = \boldsymbol{\kappa} + \boldsymbol{C} \times \boldsymbol{\theta}(t), \tag{7.2.6}$$

where $\boldsymbol{\kappa}$ represents the natural rate of tooling degradation, and $\boldsymbol{C}$ characterizes the effects product quality on tooling degradation. Here, $\boldsymbol{\theta}(t) = (\theta_1(t), \ldots, \theta_m(t))'$ represents the deviation of the PQC from its target value derived from the performance model. $\theta_j(t)$ can be expressed as follows

$$\theta_j(t) = \mathbb{E}(Y_j(t) - \gamma_j|S(t)) = \boldsymbol{\alpha}'_j \times S(t) + S(t)' \times \boldsymbol{\Gamma}_j \times \mathbb{E}(z_t) = (\boldsymbol{\alpha}_j + \boldsymbol{\Gamma}_j \times \mathbb{E}(z_t))' \times S(t). \tag{7.2.7}$$

Hence, $\boldsymbol{\theta}(t) = \boldsymbol{D} \times S(t)$, where

$$\boldsymbol{D} = [(\boldsymbol{\alpha}_1 + \boldsymbol{\Gamma}_1 \times \mathbb{E}(z_t)), \ldots, (\boldsymbol{\alpha}_m + \boldsymbol{\Gamma}_m \times \mathbb{E}(z_t))]'$$

Eventually, we rewrite the differential form of the degradation model as follows

$$d S(t) = [\boldsymbol{\kappa} + \boldsymbol{\Delta} \times S(t)] \, dt + \boldsymbol{\Sigma} \times dW(t), \tag{7.2.8}$$

145

where $\Delta = C \times D$. $W(t) = (W_1(t), \ldots, W_n(t))'$, where $W_i(t)$'s characterize the noise of the degradation signals, which evolves according to Brownian motion processes. $\Sigma = \text{diag}\{\sigma_1^2, \ldots, \sigma_n^2\}$ characterizes the amplitude of noise in the degradation signals. We assume that failures occur as degradation signals $S(t)$ or quality indices $q(t)$ cross pre-specified thresholds. This requires accurate estimation of the future distributions of $S(t)$ and $q(t)$, which can be achieved by applying the SDE techniques, proposed in Chapter 5.

7.2.2   Task 2 – Scalability to General Network Systems

In this task, we will utilize the stochastic model for individual components from the previous task to assess the RLDs of network systems, which are subject to time-varying operational conditions and component interactions. The structures of network systems can generally be divided into two categories : non-complex network systems and complex network systems. The non-complex systems are referred to the systems, which can be reduced to series and/or paralleled systems. Whereas, complex systems are referred to engineering systems, in which such decomposition is not available. For small and non-complex systems, the reliability estimate can be obtained with the aid of system structure functions. For large non-complex and complex systems — systems with more than 10 constituent components according to [55] — the system structure function is very difficult to compute. According to [127], the exact closed-form reliability expression for such systems is extremely difficult, if possible. Therefore, various approximation techniques and simulation techniques have been developed to assess the reliability of large and complex network systems. In what follows, we will investigate the simulation technique based on cellular automata (CA) and its application to the reliability maintenance of smart grid systems.

7.2.2.1   Subtask 2.1 – Evaluating System Reliability Using a CA-Based Simulation Technique

This subtask is a joint work with Mr. Murat Yildirim. The assessment or even the approximation of network reliability requires ascertaining the connectivity of a set of sources to a set of demands in the network. Generally, it is equivalent to finding the minimum cut set or the minimum path set of the network. These approaches lead to NP-hard problems, which require cumbersome and mathematically intensive methods of solution. More importantly, in many real-world applications, the connectivity of the network changes due to component failures. In such cases, the conventional

algorithms requires re-evaluating the network connectivity and thus reliability from scratch.

In this subtask, we will utilize the Monte Carlo simulation technique along with the algorithm of cellular automata to estimate and update the network reliability with real-time information. The first application of cellular automata in network reliability estimation is presented in [105, 106]. In these two papers, the authors use CA to estimate the network reliability when the constituent nodes have static failure probability. We will simulate degradation signals based on the stochastic model developed in the previous research task to characterize network system subject to time-varying operational conditions and component interactions. When one constituent component fails, the CA algorithm will be applied to examine the connectivity of the network. Once the connection between the sources and the demands fails, the system fails. An advantage of our approach is that it can be efficiently used to incorporate the connectivity change of nodes in the real-time information.

7.2.2.2 *Subtask 2.2: Application – Improving the Reliability and Sustainability of Smart Grids.*

The advent of alternative and renewable energy (for example, wind, solar, etc.) coupled with increased interconnectivity of traditional power networks requires sophisticated monitoring and control systems that allow these complex systems to function efficiently. This has given rise to what is, today, referred to as "smart grids". At the heart of the efficient operation of a smart grid is a set of tools that ensure the highest levels of reliability and sustainability. In this subtask, we will use stochastic methodologies to develop prognostic models that can be used to predict grid degradation and quantify the likelihood of a failure event.

Smart grids aggregate various resources, including the networks of multiple generation companies and renewable resources (solar, wind, and others). The aggregation of resources, induces significant volatility in the net demand of smart grids, which aggravates the network reliability. Therefore, it is very important to model and predict the demand profiles of smart grids, and adjust the price in real time to maintain the network reliability. Sensory demand data from customers will be to processed to enhance the efficiency of data transmission and analysis. In particular, the technique of wavelet analysis will be applied for de-noising and feature extraction. The loss of data information can be quantified based on wavelet coefficients of data noise. The resulting processed data will be used to model the demand profiles based on non-homogeneous Poisson processes. Each

147

demand profile can be compounded by two non-homogeneous Poisson processes : one for regular demands, and the other for rare events with peak demands. This model will be updated based on sensory demand data in real time. Given the model of demand profiles, the future demands can be predicted in finite horizons. The resulting demand estimates will be further used to facilitate decision making on real-time pricing. Specifically, the price can be adjusted at each decision epoch, based on dynamic programming, to address economics of the network and enhance network reliability.

The results of this research task will add to the limit literature that uses real-time pricing to balance demand and supply in smart grids. In addition, the incorporation of sensory data will provide insight on facilitating demand responses and management to mitigate net demand volatility.

REFERENCES

[1] AALEN, O. and GJESSING, H., "Understanding the shape of the hazard rate: a process point of view," *Statistical Science*, vol. 16, no. 1, pp. 1–14, 2001.

[2] ABDEL-HAMEED, M. and PROSCHAN, F., "Nonstationary shock models," *Stochastic Processes and their Applications*, vol. 1, no. 4, pp. 383–404, 1973.

[3] ALBIN, S. and CHAO, S., "Preventive replacement in systems with dependent components," *IEEE Transactions on Reliability*, vol. 41, no. 2, pp. 230–238, 1992.

[4] ARMSTRONG, M., "Joint reliability-importance of components," *IEEE Transactions on Reliability*, vol. 44, no. 3, pp. 408–412, 1995.

[5] BAI, J. and PERRON, P., "Computation and analysis of multiple structural change models," *Journal of Applied Econometrics*, vol. 18, no. 1, pp. 1–22, 2003.

[6] BANJEVIC, D. and JARDINE, A., "Calculation of reliability function and remaining useful life for a markov failure time process," *IMA Journal of Management Mathematics*, vol. 17, no. 2, p. 115, 2006.

[7] BANJEVIC, D., JARDINE, A., MAKIS, V., and ENNIS, M., "A control-limit policy and software for condition-based maintenance optimization," *INFOR-OTTAWA-*, vol. 39, no. 1, pp. 32–50, 2001.

[8] BARAUD, Y., GIRAUD, C., and HUET, S., "Gaussian model selection with an unknown variance," *The Annals of Statistics*, vol. 37, no. 2, pp. 630–672, 2009.

[9] BARLOW, R. and PROSCHAN, F., "Statistical theory of reliability and life testing," *Holt, Rinehart and Winston, New York*, 1975.

[10] BARLOW, R. and WU, A., "Coherent systems with multi-state components," *Mathematics of Operations Research*, pp. 275–281, 1978.

[11] BARROS, A., BERENGUER, C., and GRALL, A., "A maintenance policy for two-unit parallel systems based on imperfect monitoring information," *Reliability Engineering & System Safety*, vol. 91, no. 2, pp. 131–136, 2006.

[12] BAZOVSKY, I., *Reliability theory and practice*. Dover Pubns, 2004.

[13] BERGER, J., *Statistical decision theory and Bayesian analysis*. Springer, 1985.

[14] BHATTACHARYA, D. and SAMANIEGO, F., "Estimating component characteristics from system failure-time data," *Naval Research Logistics (NRL)*, vol. 57, no. 4, pp. 380–389, 2010.

[15] BIAN, L. and GEBRAEEL, N., "Stochastic framework for partially degradation systems with continuous component degradation-rate-interactions," *Submitted to Naval Research Logistics*, 2013.

[16] BIAN, L. and GEBRAEEL, N., "Stochastic modeling and real-time prognostics for multi-component systems with degradation-rate-interactions," *Submitted to IIE Transactions, 2nd Round Review*, 2013.

[17] BIAN, L., GEBRAEEL, N., and KHAROUFEH, J., "Real-time estimation of component residual life distribution in dynamic environments with unknown future loading profiles," *Submitted to IIE Transactions*, 2013.

[18] BIAN, L. and GEBRAEEL, N., "A stochastic methodology for prognostics under time-varying environmental future profiles," in *Proceedings of the 2011 Conference on Intelligent Data Understanding*, 2011.

[19] BIAN, L. and GEBRAEEL, N., "Computing and updating the first-passage time distribution for randomly evolving degradation signals," *IIE Transactions*, vol. 44, no. 11, pp. 974–987, 2012.

[20] BIAN, L. and GEBRAEEL, N., "Stochastic methodology for prognostics under continuously varying environmental profiles," *Statistical Analysis and Data Mining*, 2012. in press, DOI: 10.1002/sam.11154.

[21] BILLINGSLEY, P., "Statistical methods in markov chains," *The Annals of Mathematical Statistics*, vol. 32, no. 1, pp. 12–40, 1961.

[22] BIRNBAUM, Z., ESARY, J., and SAUNDERS, S., "Multi-component systems and structures and their reliability," *Technometrics*, pp. 55–77, 1961.

[23] BOUTI, A. and AIT KADI, D., "A state-of-the-art review of fmea/fmeca," *International Journal of reliability, quality and safety engineering*, vol. 1, no. 4, pp. 515–543, 1994.

[24] CHA, J. and MI, J., "Study of a stochastic failure model in a random environment," *Journal of applied probability*, vol. 44, no. 1, pp. 151–163, 2007.

[25] CHAN, K., KAROLYI, G., LONGSTAFF, F., and SANDERS, A., "An empirical comparison of alternative models of the short-term interest rate," *Journal of Finance*, pp. 1209–1227, 1992.

[26] CHEN, Y. and JIN, J., "Quality-reliability chain modeling for system-reliability analysis of complex manufacturing processes," *Reliability, IEEE Transactions on*, vol. 54, no. 3, pp. 475–488, 2005.

[27] CHRYSSAPHINOU, O., LIMNIOS, N., and MALEFAKI, S., "Multi-state reliability systems under discrete time semi-markovian hypothesis," *Reliability, IEEE Transactions on*, vol. 60, no. 1, pp. 80–87, 2011.

[28] ÇINLAR, E., *Markov additive processes. II*, vol. 24. Springer, 1972.

[29] ÇINLAR, E., "Shock and wear models and markov additive processes," *Theory and Application of Reliability: with Emphasis on Bayesian and Nonparametric Methods*, pp. 193–214, 1977.

[30] Cox, D., "Regression models and life-tables," *Journal of the Royal Statistical Society. Series B (Methodological)*, vol. 34, no. 2, pp. 187–220, 1972.

[31] Cox, D. and MILLER, H., *The theory of stochastic processes*. Chapman and Hall, 1995.

[32] CROWDER, M. and KIMBER, A., *Statistical analysis of reliability data*. Chapman & Hall/CRC, 1994.

[33] DANIELS, H., "Approximating the first crossing-time density for a curved boundary," *Bernoulli*, vol. 2, no. 2, pp. 133–143, 1996.

[34] DE GRUTTOLA, V. and TU, X., "Modelling progression of cd4-lymphocyte count and its relationship to survival time," *Biometrics*, vol. 50, no. 4, pp. 1003–1014, 1994.

[35] DEKKER, R., WILDEMAN, R., and VAN DER DUYN SCHOUTEN, F., "A review of multi-component maintenance models with economic dependence," *Mathematical Methods of Operations Research*, vol. 45, no. 3, pp. 411–435, 1997.

[36] DOBSON, I., CARRERAS, B., and NEWMAN, D., "A loading-dependent model of probabilistic cascading failure," *Probability in the Engineering and Informational Sciences*, vol. 19, no. 1, pp. 15–32, 2005.

[37] DOKSUM, K. and HÓYLAND, A., "Models for variable-stress accelerated life testing experiments based on wiener processes and the inverse gaussian distribution," *Technometrics*, vol. 34, no. 1, pp. 74–82, 1992.

[38] EBRAHIMI, N., "The mean function of a repairable system that is subjected to an imperfect repair policy," *IIE Transactions*, vol. 41, no. 1, pp. 57–64, 2009.

[39] ELSAYED, A., "Reliability engineering," 1996.

[40] ESARY, J. and MARSHALL, A., "Shock models and wear processes," *The Annals of Probability*, vol. 1, no. 4, pp. 627–649, 1973.

[41] FAUCETT, C. and THOMAS, D., "Simultaneously modelling censored survival data and repeatedly measured covariates: a gibbs sampling approach," *Statistics in Medicine*, vol. 15, no. 15, pp. 1663–1685, 1996.

[42] FELDMAN, R., "Optimal replacement with semi-markov shock models," *Journal of Applied Probability*, vol. 13, no. 1, pp. 108–117, 1976.

[43] FLORENS-ZMIROU, D., "Approximate discrete-time schemes for statistics of diffusion processes," *Statistics*, vol. 20, pp. 547–557, 1989.

[44] FREUND, J., "A bivariate extension of the exponential distribution," *Journal of the American Statistical Association*, pp. 971–977, 1961.

[45] GAMERMAN, D., "Dynamic bayesian models for survival data," *Applied Statistics*, vol. 40, no. 1, pp. 63–79, 1991.

[46] GEBRAEEL, N., "Sensory-updated residual life distributions for components with exponential degradation patterns," *Automation Science and Engineering, IEEE Transactions on*, vol. 3, no. 4, pp. 382–393, 2006.

[47] GEBRAEEL, N., LAWLEY, M., LI, R., and RYAN, J., "Residual-life distributions from component degradation signals: A bayesian approach," *IIE Transactions*, vol. 37, no. 6, pp. 543–557, 2005.

[48] GEBRAEEL, N. and PAN, J., "Prognostic degradation models for computing and updating residual life distributions in a time-varying environment," *Reliability, IEEE Transactions on*, vol. 57, no. 4, pp. 539–550, 2008.

[49] GHASEMI, A., YACOUT, S., and OUALI, M., "Evaluating the reliability function and the mean residual life for equipment with unobservable states," *Reliability, IEEE Transactions on*, vol. 59, no. 1, pp. 45–54, 2010.

[50] GORJIAN, N., MA, L., MITTINTY, M., YARLAGADDA, P., and SUN, Y., "A review on degradation models in reliability analysis," in *Proceedings of the 4th World Conference on Engineering Asset Management, Athens, Greek*, pp. 28–38, Athens, Greek, 2009.

[51] HARRIS, T., KOTZALAS, M., and EBRARY, I., *Rolling bearing analysis*. Wiley, 1984.

[52] HOLLANDER, M. and PEÑA, E., "Dynamic reliability models with conditional proportional hazards," *Lifetime Data Analysis*, vol. 1, no. 4, pp. 377–401, 1995.

[53] HØYLAND, A. and RAUSAND, M., *System reliability theory: models and statistical methods*, vol. 518. Wiley, 1994.

[54] HUDSON, J. and KAPUR, K., "Reliability bounds for multistate systems with multistate components," *Operations Research*, pp. 153–160, 1985.

[55] HWANG, C., TILLMAN, F., and LEE, M., "System-reliability evaluation techniques for complex/large systems: A review," *Reliability, IEEE Transactions on*, vol. 30, no. 5, pp. 416–423, 1981.

[56] IGAKI, N., SUMITA, U., and KOWADA, M., "Analysis of markov renewal shock models," *Journal of Applied Probability*, vol. 32, no. 3, pp. 821–831, 1995.

[57] JARDINE, A., BANJEVIC, D., and MAKIS, V., "Optimal replacement policy and the structure of software for condition-based maintenance," *Journal of Quality in Maintenance Engineering*, vol. 3, no. 2, pp. 109–119, 1997.

[58] JENSEN, P. and BELLMORE, M., "An algorithm to determine the reliability of a complex system," *Reliability, IEEE Transactions on*, vol. 18, no. 4, pp. 169–174, 1969.

[59] JOHANSSON, J. and HASSEL, H., "An approach for modelling interdependent infrastructures in the context of vulnerability analysis," *Reliability Engineering & System Safety*, vol. 95, no. 12, pp. 1335–1344, 2010.

[60] KAPUR, K. and LAMBERSON, L., "Reliability in engineering design," *New York, John Wiley and Sons, Inc., 1977. 605 p.*, vol. 1, 1977.

[61] KARATZAS, I. and SHREVE, S., *Brownian motion and stochastic calculus*, vol. 113. Springer Verlag, 1991.

[62] KHAROUFEH, J., "Explicit results for wear processes in a markovian environment," *Operations Research Letters*, vol. 31, no. 3, pp. 237–244, 2003.

[63] KHAROUFEH, J. and COX, S., "Stochastic models for degradation-based reliability," *IIE Transactions*, vol. 37, no. 6, pp. 533–542, 2005.

[64] KHAROUFEH, J., FINKELSTEIN, D., and MIXON, D., "Availability of periodically inspected systems with markovian wear and shocks," *Journal of Applied Probability*, vol. 43, no. 2, pp. 303–317, 2006.

[65] KHAROUFEH, J. and MIXON, D., "On a markov-modulated shock and wear process.," *Naval Research Logistics*, vol. 56, no. 6, pp. 563–576, 2009.

[66] KHAROUFEH, J., SOLO, C., and ULUKUS, M., "Semi-markov models for degradation-based reliability," *IIE Transactions*, vol. 42, no. 8, pp. 599–612, 2010.

[67] KIM, Y., CASE, K., and GHARE, P., "A method for computing complex system reliability," *Reliability, IEEE Transactions on*, vol. 21, no. 4, pp. 215–219, 1972.

[68] KVAM, P. and PEÑA, E., "Estimating load-sharing properties in a dynamic reliability system," *Journal of the American Statistical Association*, vol. 100, no. 469, pp. 262–272, 2005.

[69] LAVIELLE, M. and LEBARBIER, E., "An application of mcmc methods for the multiple change-points problem," *Signal Processing*, vol. 81, no. 1, pp. 39–53, 2001.

[70] LAWLESS, J. and CROWDER, M., "Covariates and random effects in a gamma process model with application to degradation and failure," *Lifetime Data Analysis*, vol. 10, no. 3, pp. 213–227, 2004.

[71] LAWLESS, J. and LAWLESS, J., "Statistical models and methods for lifetime data," 1982.

[72] LEBARBIER, E., "Detecting multiple change-points in the mean of gaussian process by model selection," *Signal processing*, vol. 85, no. 4, pp. 717–736, 2005.

[73] LEE, M.-L. T. and WHITMORE, G. A., "Proportional hazards and threshold regression: their theoretical and practical connections," *LIFETIME DATA ANALYSIS*, vol. 16, pp. 196–214, APR 2010. Missouri Workshop on Methods for Life History Data Analysis, Columbia, MO, OCT 16-18, 2008.

[74] LEE, M., DEGRUTTOLA, V., and SCHOENFELD, D., "A model for markers and latent health status," *Journal of the Royal Statistical Society. Series B (Statistical Methodology)*, vol. 62, no. 4, pp. 747–762, 2000.

[75] LEE, M., WHITMORE, G., LADEN, F., HART, J., and GARSHICK, E., "Assessing lung cancer risk in railroad workers using a first hitting time regression model," *Environmetrics*, vol. 15, no. 5, pp. 501–512, 2004.

[76] LEE, M., WHITMORE, G., and ROSNER, B., "Threshold regression for survival data with time-varying covariates," *Statistics in medicine*, vol. 29, no. 7-8, pp. 896–905, 2010.

[77] LEE, W., GROSH, D., TILLMAN, F., and LIE, C., "Fault tree analysis, methods, and application: A review," *Reliability, IEEE Transactions on*, vol. 34, no. 3, pp. 194–203, 1985.

[78] LEMOINE, A. and WENOCUR, M., "A note on shot-noise and reliability modeling," *Operations Research*, vol. 34, no. 2, pp. 320–323, 1986.

[79] LI, J., COIT, D., and ELSAYED, E., "Reliability modeling of a series system with correlated or dependent component degradation processes," in *2011 International Conference on Quality, Reliability, Risk, Maintenance, and Safety Engineering*, pp. 388–393, IEEE, 2011.

[80] LIAO, C. and TSENG, S., "Optimal design for step-stress accelerated degradation tests," *Reliability, IEEE Transactions on*, vol. 55, no. 1, pp. 59–66, 2006.

[81] LIAO, H. and ELSAYED, E., "Reliability inference for field conditions from accelerated degradation testing," *Naval Research Logistics*, vol. 53, no. 6, pp. 576–587, 2006.

[82] LIAO, H., ZHAO, W., and GUO, H., "Predicting remaining useful life of an individual unit using proportional hazards model and logistic regression model," in *Reliability and Maintainability Symposium, 2006. RAMS'06. Annual*, pp. 127–132, IEEE, 2006.

[83] LISNIANSKI, A. and LEVITIN, G., *Multi-state system reliability: assessment, optimization and applications*, vol. 6. World Scientific Pub Co Inc, 2003.

[84] LU, C. and MEEKER, W., "Using degradation measures to estimate a time-to-failure distribution," *Technometrics*, vol. 35, no. 2, pp. 161–174, 1993.

[85] LU, S., LU, H., and KOLARIK, W., "Multivariate performance reliability prediction in real-time," *Reliability Engineering & System Safety*, vol. 72, no. 1, pp. 39–45, 2001.

[86] MARSHALL, A. and OLKIN, I., "A multivariate exponential distribution," *Journal of the American Statistical Association*, pp. 30–44, 1967.

[87] MARSHALL, A. and OLKIN, I., "Families of multivariate distributions," *Journal of the American Statistical Association*, pp. 834–841, 1988.

[88] McCOOL, J., "Testing for dependency of failure times in life testing," *Technometriics*, vol. 48, pp. 41–48, 2006.

[89] MEEKER, W. and ESCOBAR, L., *Statistical methods for reliability data*. Wiley Hoboken, NJ, 1998.

[90] MOUSTAFA, M., "Reliability analysis of k-out-of-n systems with dependent failures and imperfect coverage," *Reliability Engineering & System Safety*, vol. 58, no. 1, pp. 15–17, 1997.

[91] MURTHY, D. and NGUYEN, D., "Study of a multi-component system with failure interaction," *European journal of operational research*, vol. 21, no. 3, pp. 330–338, 1985.

[92] MURTHY, D. and WILSON, R., "Parameter estimation in multi–component systems with failure interaction," *Applied stochastic models and data analysis*, vol. 10, no. 1, pp. 47–60, 1994.

[93] MYERS, L., "Survival functions induced by stochastic covariate processes," *Journal of Applied Probability*, vol. 18, no. 2, pp. 523–529, 1981.

[94] NELSON, W., *Accelerated testing: statistical models, test plans and data analyses*. Wiley Online Library, 1990.

[95] NICOLAI, R. and DEKKER, R., "Optimal maintenance of multi-component systems: a review," *Complex System Maintenance Handbook*, pp. 263–286, 2008.

[96] ONAR, A. and PADGETT, W., "Inverse gaussian accelerated test models based on cumulative damage," *Journal of Statistical Computation and Simulation*, vol. 66, no. 3, pp. 233–247, 2000.

[97] OZAKI, T., "Local gaussian modelling of stochastic dynamical systems in the analysis of nonlinear random vibrations," *Journal of Applied Probability*, pp. 241–255, 1986.

[98] PAN, Z. and BALAKRISHNAN, N., "Reliability modeling of degradation of products with multiple performance characteristics based on gamma processes," *Reliability Engineering & System Safety*, vol. 96, no. 8, pp. 949–957, 2011.

[99] PARK, C. and PADGETT, W., "Accelerated degradation models for failure based on geometric brownian motion and gamma processes," *Lifetime Data Analysis*, vol. 11, no. 4, pp. 511–527, 2005.

[100] PARK, C. and PADGETT, W., "New cumulative damage models for failure using stochastic processes as initial damage," *Reliability, IEEE Transactions on*, vol. 54, no. 3, pp. 530–540, 2005.

[101] PARK, C. and PADGETT, W., "Stochastic degradation models with several accelerating variables," *Reliability, IEEE Transactions on*, vol. 55, no. 2, pp. 379–390, 2006.

[102] PETTIT, L. and YOUNG, K., "Bayesian analysis for inverse gaussian lifetime data with measures of degradation," *Journal of Statistical Computation and Simulation*, vol. 63, no. 3, pp. 217–234, 1999.

[103] PIJNENBURG, M., "Additive hazards models in repairable systems reliability," *Reliability Engineering & System Safety*, vol. 31, no. 3, pp. 369–390, 1991.

[104] ROBINSON, M. and CROWDER, M., "Bayesian methods for a growth-curve degradation model with repeated measures," *Lifetime Data Analysis*, vol. 6, no. 4, pp. 357–374, 2000.

[105] Rocco S, C. and ZIO, E., "Solving advanced network reliability problems by means of cellular automata and monte carlo sampling," *Reliability Engineering & System Safety*, vol. 89, no. 2, pp. 219–226, 2005.

[106] Rocco S, C. and ZIO, E., "Solving advanced network reliability problems by means of cellular automata and monte carlo sampling," *Reliability Engineering & System Safety*, vol. 89, no. 2, pp. 219–226, 2005.

[107] Ross, S., "A model in which component failure rates depend on the working set," *Naval research logistics quarterly*, vol. 31, no. 2, pp. 297–300, 1984.

[108] SARI, J., *Multivariate degradation modeling and its application to reliability testing*. PhD thesis, 2007.

[109] SCARF, P. and DEARA, M., "Block replacement policies for a two-component system with failure dependence," *Naval Research Logistics (NRL)*, vol. 50, no. 1, pp. 70–87, 2003.

[110] SCHOTTL, A., "A reliability model of a system with dependent components," *IEEE Transactions on Reliability*, vol. 45, no. 2, pp. 267–271, 1996.

[111] SCHWARZ, G., "Estimating the dimension of a model," *The annals of statistics*, pp. 461–464, 1978.

[112] SHAKED, M. and SHANTHIKUMAR, J., "On the first failure time of dependent multicomponent reliability systems," *Mathematics of operations research*, pp. 50–64, 1988.

[113] SHAO, Y. and NEZU, K., "Prognosis of remaining bearing life using neural networks," *Proceedings of the Institution of Mechanical Engineers, Part I: Journal of Systems and Control Engineering*, vol. 214, no. 3, pp. 217–230, 2000.

[114] SHEU, S. and LIOU, C., "Optimal replacement of a k-out-of-n system subject to shocks," *Microelectronics Reliability*, vol. 32, no. 5, pp. 649–655, 1992.

[115] SHINSTINE, D., AHMED, I., and LANSEY, K., "Reliability/availability analysis of municipal water distribution networks: Case studies," *Journal of Water Resources Planning and Management*, vol. 128, p. 140, 2002.

[116] SI, X., WANG, W., HU, C., and ZHOU, D., "Remaining useful life estimation-a review on the statistical data driven approaches," *European Journal of Operational Research*, 2010.

[117] SIEGMUND, D., "Boundary crossing probabilities and statistical applications," *The Annals of Statistics*, vol. 14, no. 2, pp. 361–404, 1986.

[118] SINGPURWALLA, N., "Survival in dynamic environments," *Statistical Science*, vol. 10, no. 1, pp. 86–103, 1995.

[119] SUN, Y., MA, L., MATHEW, J., WANG, W., and ZHANG, S., "Mechanical systems hazard estimation using condition monitoring," *Mechanical systems and signal processing*, vol. 20, no. 5, pp. 1189–1201, 2006.

[120] SUN, Y., MA, L., MATHEW, J., and ZHANG, S., "An analytical model for interactive failures," *Reliability Engineering & System Safety*, vol. 91, no. 5, pp. 495–504, 2006.

[121] TIAN, Z. and LIAO, H., "Condition based maintenance optimization for multi-component systems using proportional hazards model," *Reliability Engineering & System Safety*, 2011.

[122] TSE, P. and ATHERTON, D., "Prediction of machine deterioration using vibration based fault trends and recurrent neural networks," *Journal of Vibration and Acoustics*, vol. 121, p. 355, 1999.

[123] TSENG, S., BALAKRISHNAN, N., and TSAI, C., "Optimal step-stress accelerated degradation test plan for gamma degradation processes," *Reliability, IEEE Transactions on*, vol. 58, no. 4, pp. 611–618, 2009.

[124] TSENG, S. and PENG, C., "Optimal burn-in policy by using an integrated wiener process," *IIE Transactions*, vol. 36, no. 12, pp. 1161–1170, 2004.

[125] VAN NOORTWIJK, J., "A survey of the application of gamma processes in maintenance," *Reliability Engineering & System Safety*, vol. 94, no. 1, pp. 2–21, 2009.

[126] VLOK, P., WNEK, M., and ZYGMUNT, M., "Utilising statistical residual life estimates of bearings to quantify the influence of preventive maintenance actions," *Mechanical systems and signal processing*, vol. 18, no. 4, pp. 833–847, 2004.

[127] WANG, H. and PHAM, H., "Survey of reliability and availability evaluation of complex networks using monte carlo techniques," *Microelectronics and reliability*, vol. 37, no. 2, pp. 187–209, 1997.

[128] WANG, L. and POTZELBERGER, K., "Boundary crossing probability for brownian motion and general boundaries," *Journal of Applied Probability*, vol. 34, no. 1, pp. 54–65, 1997.

[129] WANG, P. and VACHTSEVANOS, G., "Fault prognostics using dynamic wavelet neural networks," *Artificial Intelligence for Engineering Design, Analysis and Manufacturing*, vol. 15, no. 4, pp. 349–365, 2001.

[130] Wang, S., Hong, L., Chen, X., Zhang, J., and Yan, Y., "Review of interdependent infrastructure systems vulnerability analysis," in *Intelligent Control and Information Processing (ICICIP), 2011 2nd International Conference on*, vol. 1, pp. 446–451, IEEE, 2011.

[131] Wang, W., "An adaptive predictor for dynamic system forecasting," *Mechanical Systems and Signal Processing*, vol. 21, no. 2, pp. 809–823, 2007.

[132] Wang, W., Golnaraghi, M., and Ismail, F., "Prognosis of machine health condition using neuro-fuzzy systems," *Mechanical Systems and Signal Processing*, vol. 18, no. 4, pp. 813–831, 2004.

[133] Wang, X., "Wiener processes with random effects for degradation data," *Journal of Multivariate Analysis*, vol. 101, no. 2, pp. 340–351, 2010.

[134] Wang, X., Guo, B., and Cheng, Z., "Residual life estimation based on bivariate wiener degradation process with time-scale transformations," *Journal of Statistical Computation and Simulation*, no. ahead-of-print, pp. 1–19, 2012.

[135] Wang, Y. and Pham, H., "Modeling the dependent competing risks with multiple degradation processes and random shock using time-varying copulas," *IEEE Transactions on Reliability*, vol. 61, no. 1, pp. 13–22, 2012.

[136] Wang, Y. and Taylor, J., "Jointly modeling longitudinal and event time data with application to acquired immunodeficiency syndrome," *Journal of the American Statistical Association*, vol. 96, no. 455, pp. 895–905, 2001.

[137] Whitmore, G. and Schenkelberg, F., "Modelling accelerated degradation data using wiener diffusion with a time scale transformation," *Lifetime Data Analysis*, vol. 3, no. 1, pp. 27–45, 1997.

[138] Wulfsohn, M. and Tsiatis, A., "A joint model for survival and longitudinal data measured with error," *Biometrics*, vol. 53, no. 1, pp. 330–339, 1997.

[139] Xie, M. and Lai, C., "Reliability analysis using an additive weibull model with bathtub-shaped failure rate function," *Reliability Engineering & System Safety*, vol. 52, no. 1, pp. 87–93, 1996.

[140] Xu, D. and Zhao, W., "Reliability prediction using multivariate degradation data," in *Proceedings of Annual Reliability and Maintainability Symposium*, pp. 337–341, IEEE, 2005.

[141] Xu, Z., Ji, Y., and Zhou, D., "A new real-time reliability prediction method for dynamic systems based on on-line fault prediction," *IEEE Transactions on Reliability*, vol. 58, no. 3, pp. 523–538, 2009.

[142] Xue, J. and Yang, K., "Dynamic reliability analysis of coherent multistate systems," *Reliability, IEEE Transactions on*, vol. 44, no. 4, pp. 683–688, 1995.

[143] Yam, R., Tse, P., Li, L., and Tu, P., "Intelligent predictive decision support system for condition-based maintenance," *The International Journal of Advanced Manufacturing Technology*, vol. 17, no. 5, pp. 383–391, 2001.

[144] Yao, Y., "Estimating the number of change-points via schwarz'criterion," *Statistics & Probability Letters*, vol. 6, no. 3, pp. 181–189, 1988.

[145] You, M., Li, L., Meng, G., and Ni, J., "Two-zone proportional hazard model for equipment remaining useful life prediction," *Journal of Manufacturing Science and Engineering*, vol. 132, p. 041008, 2010.

[146] Zequeira, R. and Bérenguer, C., "On the inspection policy of a two-component parallel system with failure interaction," *Reliability Engineering & System Safety*, vol. 88, no. 1, pp. 99–107, 2005.

[147] Zhao, X., Fouladirad, M., Bérenguer, C., and Bordes, L., "Condition-based inspection/replacement policies for non-monotone deteriorating systems with environmental covariates," *Reliability Engineering & System Safety*, vol. 95, no. 8, pp. 921–934, 2010.

[148] Zhou, J., Pan, Z., and Sun, Q., "Bivariate degradation modeling based on gamma process," in *Proceedings of the World Congress on Engineering 2010 Vol III, WCE 2010*, 2010.